UNIVERSITY OF CAPE TOWN
DIVISION OF BIOMEDICAL ENGINEERING
DEPARTMENT OF HUMAN BIOLOGY
FACULTY OF HEALTH SCIENCES

MASTERS IN MEDICAL SCIENCES (BIOMEDICAL ENGINEERING)

DESIGN AND *IN VITRO* VERIFICATION OF A STRESS RADIOGRAPHY DEVICE TOWARDS IT'S SUITABILITY FOR MULTI-LIGAMENT LAXITY MEASUREMENTS

MINOR DISSERTATION

Submitted to

THE UNIVERSITY OF CAPE TOWN

In partial fulfilment of the requirements for the degree

AUTHOR:
Giancarlo Beukes

SUPERVISOR:
Dr Sudesh SIvarasu

26 September 2017

Declaration

I, Giancarlo Beukes, hereby declare that the work on which this dissertation is based is my original work (except where acknowledgements indicate otherwise) and that neither the whole work nor any part of it has been, is being, or is to be submitted for another degree in this or any other university.
I empower the university to reproduce for the purpose of research either the whole or any portion of the contents in any manner whatsoever.

Signature: Signed by candidate

Date: 26 September 2017

Abstract

The human knee is a hinge joint, primarily facilitating locomotion. Knee joint instability, due to ligament injuries, is a result of direct or indirect trauma, non-anatomical stresses during pivoting movements about the knee, imbalanced landing during jumping and rapid deceleration during high intensity locomotion. Biomechanical indications of an unstable knee joint include decreased joint integrity, hyperlaxity, abrupt locking and catching combined with clicking noises during locomotion. Approximately, two hundred and fifty thousand ACL injuries occur in the United States of America annually. Current diagnostic procedures are subjective according to the clinician's experience. This potentially leads to misdiagnosis of the injury and improper treatment. Non-invasive diagnostic techniques make use of manual methods, MRI and laxity measurement devices (e.g. arthrometers and stress radiography devices). Laxity measurement devices (the focus of this study) determine ligament health by measuring their elasticity and stiffness. Directional tibial and fibular bone translation is induced by applying an external load to the joint. The bone translation is measured in relation to the load applied, which denotes ligament laxity.

The Laxmeter is a novel, cost effective and radiolucent multi-ligament laxity measurement stress radiography device. This device facilitates the measurement of MCL and LCL laxity at multiple degrees of knee joint flexion, however, it lacks the essential means to perform the laxity measurement technique. The current study aims to redesign the Laxmeter to perform ACL, PCL, MCL and LCL laxity measurement procedures at multiple fixed degrees of knee joint flexion. The *in vitro* functional verification of the device was limited to (according to scope) a single cadaver trial; to validate functionality, structural integrity, usability as well as demonstrate the Laxmeter concept prior to a prospective full clinical trial.

The redesigned Laxmeter Prototype consists of a load applicator capable of applying a 250N load to various aspects of the proximal lower leg, to induce bone translation for laxity measurements. The load applicator is designed to integrate with the ergonomic patient support structure, the later potentially improving reproducibility and accuracy of the laxity measurement results.

The cadaver trial demonstrated the device's capability of measuring the laxity of the ACL, MCL and LCL at predetermined knee flexion angles. To measure the ligament laxity, equal loads were applied to both proximal lower limbs independently. The bilateral average displacement of the tibia with respect to the femur for each ligament was noted. In the case of the ACL, the Laxmeter measured an average laxity of 3.07mm at 30° knee flexion and a load of 150N. The average laxities for the MCL and LCL at 30° knee flexion and 150N were 1.11mm and 2.02mm. The trial yielded preclinical results that were comparable with existing clinical and healthy cadaver based studies (using similar techniques), and suggests that the Laxmeter is capable of measuring the laxity of the ACL, MCL and LCL at various degrees of knee flexion. PCL laxity measurements could not be performed due to compromised structural integrity, which was essential to make the Laxmeter portable and lightweight.

Future recommendations for the device include rotational ankle fixation; improved overall limb fixation; improved structural integrity to allow for PCL laxity measurements as well as further preclinical (functional) verification procedures prior to a full clinical trial.

Acknowledgements

I would like to express my utmost gratitude to the following people:

My parents, Mr Jerry Beukes and Mrs Berdine Beukes, for their support, motivation and love. I am forever indebted to you both and am truly grateful for the opportunity you have given me. You always said that, “The first degree is for the parents and the second degree is for you”; but for all you have done, I dedicate this to you both.

My supervisor, Dr Sudesh Sivarasu, for the assistance, mentorship and all the opportunities that I have been given during this course. You have given me far more than a Biomedical Engineering Degree and for that I will always be grateful.

My siblings, Abrille Beukes and Storm Beukes, for their support and assistance through this degree.

My friends and colleagues, Ameen Bardien and Yasheen Brijlal, for their assistance with the electronics system of this study.

My colleagues: Roopam Dey, Elizabeth Kruse, Jerry Sam, Gokul Nair, Cara Mills, Albert Opiyo, Safa Naraghi, Edmund Wessels, Alastair During, Rosslee Guess, Scott Bruton and the rest of the Medical Devices and Orthopaedics team for their friendship, guidance and assistance.

Ziana Louw for her moral support and encouragement throughout the process and always pushing me to keep going.

Mpho Katjiuongua, Sina Parastaran and Rooha Rowhani for their friendship, motivation and support throughout this degree.

The German Academic Exchange Service (DAAD) for sponsoring this research.

The National Research Fund (NRF) for sponsoring this research.

List of Abbreviations

2.d.p.	Two Decimal Places
3.s.f.	Three Significant Figures
3D	Three-Dimensional
ACL	Anterior Cruciate Ligament
ADC	Analogue to Digital Converter
ADL	Activities of Daily Living
ALL	Anterolateral Ligament
AMA	American Medical Association
AP	Anteroposterior
CAD	Computer-assisted design
CFRP	Carbon fibre Reinforced Plastics
DAAD	German Academic Exchange Service
E.g.	Example
FEM	Finite Element Modelling
FHS	Faculty of Health Sciences
FMEA	Failure Modes and Effects Analysis
FSP	Force-Sensing Pad
GNRB	Genourob
HREC	Human Research Ethics Committee
IEEE	Institute of Electrical and Electronics Engineering
IKDC	International Knee Documentation Committee
JLM	Joint Locking Mechanism
LAS	Load Application System
LCL	Lateral Collateral Ligament
LLSP	Lower Leg Support Panel
LODOX	Low Dosage X-ray
MCL	Medial Collateral Ligament
ML	Mediolateral
MRI	Magnetic Resonance Imaging
NRF	National Research Fund
PCL	Posterior Cruciate Ligament
POT	Variable Resistor
PSS	Patient Support Structure
PSU	Power Supply Unit
PTC	Posterior Tibial Cortex
RAM	Random Access Memory
RPN	Risk Priority Number
SF	Safety Factor
UCT	University of Cape Town
ULSP	Upper Leg Support Panel
USA	United States of America
ZAR	South African Rand

Symbols

δ	FSP deflection
$\sum$	Summation of a range of values
σ_b	Bearing stress experienced by the LLSP
σ_t	Tensile stress experienced by the LLSP
μC	Microcontroller
A_b	Bearing Area on LLSP
A_t	Tensile area on LLSP
b	Cross-sectional width of the FSP
D	LAS fixation bolt diameter (10mm)
E	Elastic Modulus
F_{AF}	Force due to ankle fixation
F_h	Reaction force at heel
F_k	Force experienced by the knee joint
F_W	Weight of the lower leg
H	Cross-sectional height of the FSP
I	Moment of Inertia
l	Length of the FSPs
M_k	Moment about the knee joint
M_h	Moment about the heel
N	Number of LAS fixation bolts in a row
N_f	Ultimate tensile load of a ligament (Load at failure)
N_t	Maximum load for ligament laxity measurement procedures
P	250N load applied to the proximal lower leg
SF	Safety Factor
SF_{bm}	Safety Factor concerning the bearing on the LLSP
SF_{tm}	Safety Factor concerning the tension on the LLSP
$S_{y\text{-Plexiglas}\,®}$	Yield strength of Plexiglas®
t	LLSP thickness (8mm)
t_s	Width of the Lateral LAS Support Structure (90mm)

Contents

List of Figures

List of Tables

1 Introduction

1.1 Background to Study

The knee joint is one of the largest and most complex joints in the human body; consisting of various structures such as the femur, tibia, patella, synovial fluid, ligaments, and meniscus. One of the primary functions of the joint is ambulation, and as such, the joint is susceptible to many injuries. Knee joint instability or injury due to ligament impairment (e.g. sprain, partial tear and complete rupture) may result from strenuous physical activities, such as sports, strenuous physical exercise, or occupational hazard. Further causes of knee joint ligamentous injuries because of weakened joint stability are due to genetic makeup and medical conditions such as osteoarthritis (Collette et al. 2012). The four major ligaments of the knee joint in consideration are the anterior cruciate ligament (ACL), the posterior cruciate ligament (PCL), the medial collateral ligament (MCL) and the lateral collateral ligament (LCL). Exposing the joint to excessive valgus and varus loading, pivotal movements, direct or indirect trauma as well as combined loading may cause the ligamentous sprain as well as partial and complete ligament ruptures (Kakarlapudi and Bickerstaff 2001).

A common ligamentous knee injury in the United States of America (USA) would be that of the ACL. Approximately 250,000 cases of ACL injuries are recorded annually in the USA, which translates to about 1 in 1275.6 persons (Souryal 2015). However, a more recent study estimated the number of injuries to be lower with 1 in 3500 persons sustaining ACL injuries in the USA annually (Freidberg 2016). Estimates indicate that approximately 1 case of ACL injury per 3333.3 persons is recorded annually in the United Kingdom (UK) (Bollen 2000). ACL injury occurrences in New Zealand would exceed those previously stated as studies have recorded approximately 11.84 injuries (ACL surgeries + non-surgical injuries) per 1000 persons annually, which equals 1 in 84.5 persons (Gianotti et al. 2009). These countries can be considered active nations due to their participation in major sports events and general physical activities.

This study focuses primarily on the South African context. Although there is limited information regarding the incidence of ligamentous knee injuries in South Africa, a correlation can be made between the incidence rate and how active the population is. The above-mentioned countries are comparable to South Africa due to their rugby culture (New Zealand and the UK), their passion for football (the UK and the US), their love for cricket (New Zealand and the UK) and all other outdoor and indoor sports, athletics and recreational activity participation. South Africa hosts the Cape Argus as well as the Comrades Marathon annually and features in several international sports competitions including the cricket, soccer and rugby world cups (Pennington 2014; Morgan 2015). The country boasts some of the top athletes in the world, which compete at the Olympic and Commonwealth Games (SASCOC 2016). On a more day-to-day outlook, a significant number of South Africans enjoy hiking, swimming, running, training, casual sports and surfing only to mention a few (Pennington 2014). The population of this country and that of the world is becoming increasingly more active and health conscious, which causes the increased risk of sustaining a ligamentous knee injury.

1.2 Clinical Problem Description

The clinical problem is a knee joint injury as a result of multiple sprained, partially torn or ruptured ligaments. The injury results from damage to any one, or a combination, of the four major ligaments in the knee joint. The primary function of the ligaments within the joint is to provide stability, allowing for six degrees of freedom (DOFs) as indicated in Table 1.1 (Muller 1996). Damage to the ligaments leads to compromised knee joint integrity. Hyperflexion and hyperextension as well as excessive valgus and varus deformation of the knee joint, beyond the range of motion indicated in Table 1.1, leads to ligamentous knee joint injury.

Table 1.1: Six DOFs for the knee joint and movement limitations (Table credit: (Muller 1996; MayoClinic 2017))

DOF	*Movement type*	*Movement limitations*
Extension - Flexion	Rotation	From 5° – 0° – 135°
Exorotation - Endorotation	Rotation	25°/15° – 0° – 10°/15°
Varus - Valgus Rotation	Rotation	A few degrees
Anterior - Posterior	Translation	3mm – 0 – 5mm
Medio - lateral	Translation	A few degrees
Compression - Distraction	Translation	A few degrees

In addition, symptoms of knee joint injury include the following (Levy 2016; MayoClinic 2017):

- Profound pain
- Effusion and stiffness
- Snapping or popping sound
- Inability to naturally support weight and antalgic gait (walk awkwardly to avoid pain)

When a patient exhibits the mentioned symptoms, a diagnosis of the knee joint instability injury must be performed. Diagnosis is carried out by measuring the laxity (elasticity or stiffness) of the ligaments within the joint by performing various physical laxity measurement tests manually. The procedure involves fixating the patient's upper leg as well as distal lower leg, flexing the knee to a specified angle and manually applying a load to the anterior, posterior, medial and lateral aspects of the proximal lower leg (Bickley and Prabhu 2003; Lubowitz et al. 2008). These procedures include the Lachman test (ACL diagnosis), Anterior (ACL diagnosis) and Posterior (PCL diagnosis) Drawer Tests as well as the Adduction (LCL diagnosis) and Abduction (MCL diagnosis) Stress Tests (Bickley and Prabhu 2003). While conducting these tests, it is important to examine both knees and compare the tibial translation with respect to the femur. Figure 1.1 shows the prevalence of ligament injuries in the UK and illustrates the dominating incidence rates of ACL (in particular) and MCL injuries (Bollen 2000).

As a result of the clinician's judgment, manual laxity measurement results have been found to produce unreliable results (Tsai et al. 2008). Devices have been developed to more accurately and consistently diagnose a ligamentous injury. These devices, known as laxity measurement devices, are subdivided into two main categories namely arthrometers and stress radiography devices. Arthrometers provide digital measurements of the tibial translation whereas stress radiography devices provide radiographic measurements of tibial translation. Other diagnostic tools include arthroscopy (an invasive and costly procedure) and various imaging techniques (some of which are exorbitant) such as Magnetic Resonance Imaging (MRI), Ultrasound, and Computerised Tomography (Fanelli et al. 1994; Timmerman et al. 1994).

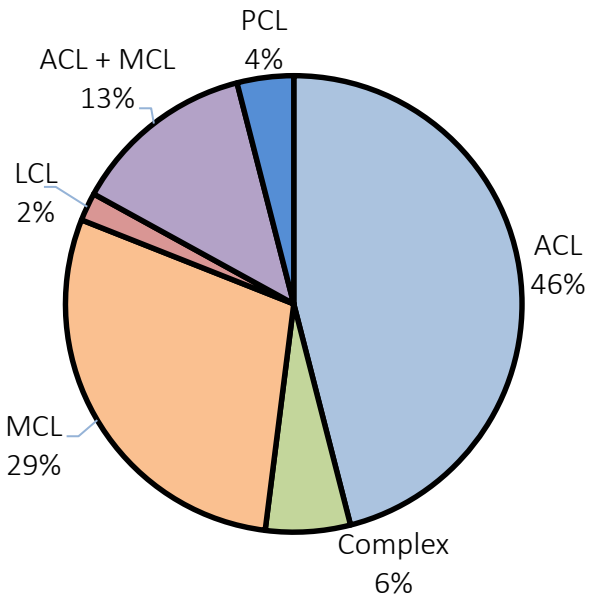

Figure 1.1: Classification of 500 ligamentous knee injuries in the UK (image credit: (Bollen 2000))

The image illustrates the distribution of the ligamentous knee joint injuries in the UK. The dominant occurrence of the ACL and MCL instabilities are shown by the large areas of the chart.

Treatment options for ligamentous injuries include pain inhibition, reducing joint supporting loads, rehabilitation therapy, knee supporting device or brace, and ligament reconstruction. The treatment options translate into both temporary (pain inhibition, reducing joint supporting loads and supportive devices) and permanent (rehabilitation therapy and ligament reconstruction) solutions. The more permanent solutions are the more efficient option, but the costliest as well. The current study focuses on the diagnostic aspect of the treatment process and therefore, no further detail is discussed regarding treatment methods and rehabilitation processes.

1.3 Problem Significance

The study concentrates specifically on the diagnosis of knee joint instability due to ligamentous injury i.e. sprain, partial tear or complete rupture. A non-invasive means of determining the instability is by bone distraction or translation, which denotes the ligament's laxity i.e. the elasticity or stiffness of the ligaments. The diagnosis of a partial or complete ligament tear carried out by a clinician (physiotherapist or orthopaedic surgeon) is entirely subjective, particularly with partial ligament tears (Bouguennec et al. 2015). Several devices are available, capable of determining the laxity (by means of induced bone translation) of either the ACL in isolation, the cruciate ligaments in conjunction, the collateral ligaments in combination or all four major ligaments with limitations. These limitations include non-ergonomic patient positioning and excessive radiation exposure to the radiographic assistant. There is no direct means of determining the laxity of ligaments, therefore, this indirect approach by bone translation and distraction, has been adopted as the common practise. The results of laxity measurement device tests aid the clinician in making more informed decisions regarding the diagnosis and prognosis of the injury.

The study focuses on developing a multi-ligament laxity measurement stress radiography device. Therefore, the results obtained from this study will be compared to previous studies that make use of stress radiography devices (e.g. the Telos™ Stress Device) and arthrometers (e.g. the KT-1000™ and Genourob (GNRB®)) for further validation. The Telos™ Stress Device can determine the laxity of the ACL, PCL, MCL and LCL and other ligaments in the ankle, elbow and shoulder joints (Scheuba 2009). The device is widely used to assess the state of knee joint instability as a result of ligament damage. The results from this technique have been found to have acceptable reliability in ACL, PCL, MCL and LCL injury diagnosis, however, inconsistencies were found when comparing stress radiography (as a technique) to other laxity measurement techniques (James et al. 2014). The Telos™ Stress Device, as well as existing arthrometers (the KT-1000™ and Genourob), have several limitations; which include non-ergonomic patient positioning, the need for a radiographic assistant during testing, restricted to measuring only cruciate or collateral ligament laxities and the devices produce unreliable results when compared to the GNRB®.

1.4 Research Approach

The study comprises of both a design component and a preclinical (functional) verification component. The design component focuses on a frugal yet innovative approach to engineering design. The preclinical component followed the procedures of a true experimental design. A single random cadaver specimen and a single test method was used to functionally verify the efficacy (functionality, structural integrity and usability) of this device, as an overall knee joint laxity measurement stress radiography device prior to a full clinical trial.

1.5 Hypothesis

Knee instability as a result of ligament rupture is a common injury amongst active populations. Laxity measurement devices can provide physicians with detailed information regarding the severity of knee joint ligament injuries. Existing devices including the Laxmeter Prototype One have several functional limitations. The solutions to the functional constraints can be based on proving the validity of these hypotheses:

1. A laxity measurement stress radiography device that allows for and induces anteroposterior (AP) and mediolateral (ML) lower leg translation for measuring the laxity of the ACL, PCL, MCL and LCL at various flexion-extension angles will improve the physician's overall assessment of the knee injury.

2. Providing anatomical support and creating the ideal patient position during laxity measurement tests as well as fixating the patient's pelvis will improve the reproducibility and accuracy of the laxity measurement test results.

1.6 Study Aim

Design and experimentally validate the function of a novel multi-ligament laxity measurement stress radiography device (the Laxmeter) that reliably and accurately measures the laxity of the ACL, PCL, MCL and LCL at multiple fixed degrees of flexion.

1.7 Research Objectives

1. Redesign the Laxmeter Prototype One, to accommodate multi-ligament laxity measurements at multiple fixed degrees of knee joint flexion.
2. Design and develop an electromechanical linear load applicator with a loading range 0 - 250N.
3. Redesign the Laxmeter to allow for convenient packaging, storage, portability and straightforward setup.
4. Perform pilot experimental verification procedures by means of *in vitro* Cadaver validation for the suitability of the device aimed at multi-ligament laxity measurements.

1.8 Key Project Parameters

The issue regarding improved diagnosis of knee joint instability injuries due to ligament damage is prevalent in South Africa and the rest of the world. From a socio-economic standpoint, the project aims to develop an affordable laxity measurement stress radiography device, which successfully addresses the needs of both the clinicians and patients. The study incorporates these key parameters into the design: effectivity, practicality, ergonomics, portability, aesthetic appeal, test reproducibility, functionality and affordability.

The design parameters are:

1. Develop a linear Load Application System (LAS) which includes:
    i. A mechanical component (LAS support structure) to support the load applicator and allow for anteroposterior (AP) as well as mediolateral (ML) directional load application.
    ii. An electronic component to apply the 25N incremental load (0-250N) to the lower leg.
2. Redesign the existing mechanical system (patient support structure(PSS)) to feature:
    i. A more lightweight structure (inclusive of material considerations).
    ii. AP and ML tibial translation.
    iii. Storability and packaging.
3. Design a systems integration adaptor to amalgamate the LAS and the PSS.
4. Investigate materials for systems manufacture of the Prototype and final product.
5. Provide future iteration recommendations.

The preclinical parameters were:

1. Determine the efficacy of the Laxmeter as a non-invasive diagnostic tool for multi-ligament laxity measurements at multiple fixed degrees of flexion based on a cadaver pilot study.

1.9 Scope of the Study

The study was focused on and limited to developing a stress radiography device capable of determining the laxity of all four major ligaments of the knee joint at multiple fixed degrees of joint flexion. This is an investigation of a proof of concept and potentially a minimum viable product. The scope focuses on describing the function and efficacy of a working Prototype by conducting a single cadaver functional verification pilot study.

1.10 Dissertation Overview

This thesis document describes the design, preclinical and research methodologies of the study highlighted in Figure 1.2. **Chapter 2 (The Literature Review)** describes the anatomy, clinical problem, technical problem and provides justification for the need of a low-cost solution. **Chapter 3 (Design Methodology)** outlines the approach to design, the components and concepts that developed as well as the manufacturing processes followed to produce a functioning Prototype. **Chapter 4 (Design Outcomes)** details the design considerations of the Laxmeter Prototype developed for experimental trials. **Chapter 5 (Experimental Methodology)** provides a detailed description of the experimental validation procedure, through a cadaver trial, to prove the Laxmeter's efficacy. **Chapter 6 (Experimental Outcomes)** describes the results obtained through the preclinical cadaver trials and the results of a global laxity measurement device comparative study. **Chapter 7 (The Discussion)** summarises the performance and efficacy of the Laxmeter, based on the experimental validation results. Finally, **Chapter 8 (The Conclusion)** concludes the study and discusses the Outcome Measures met by this study, the limitations of the study and provides suggested recommendations for future iterations/ work.

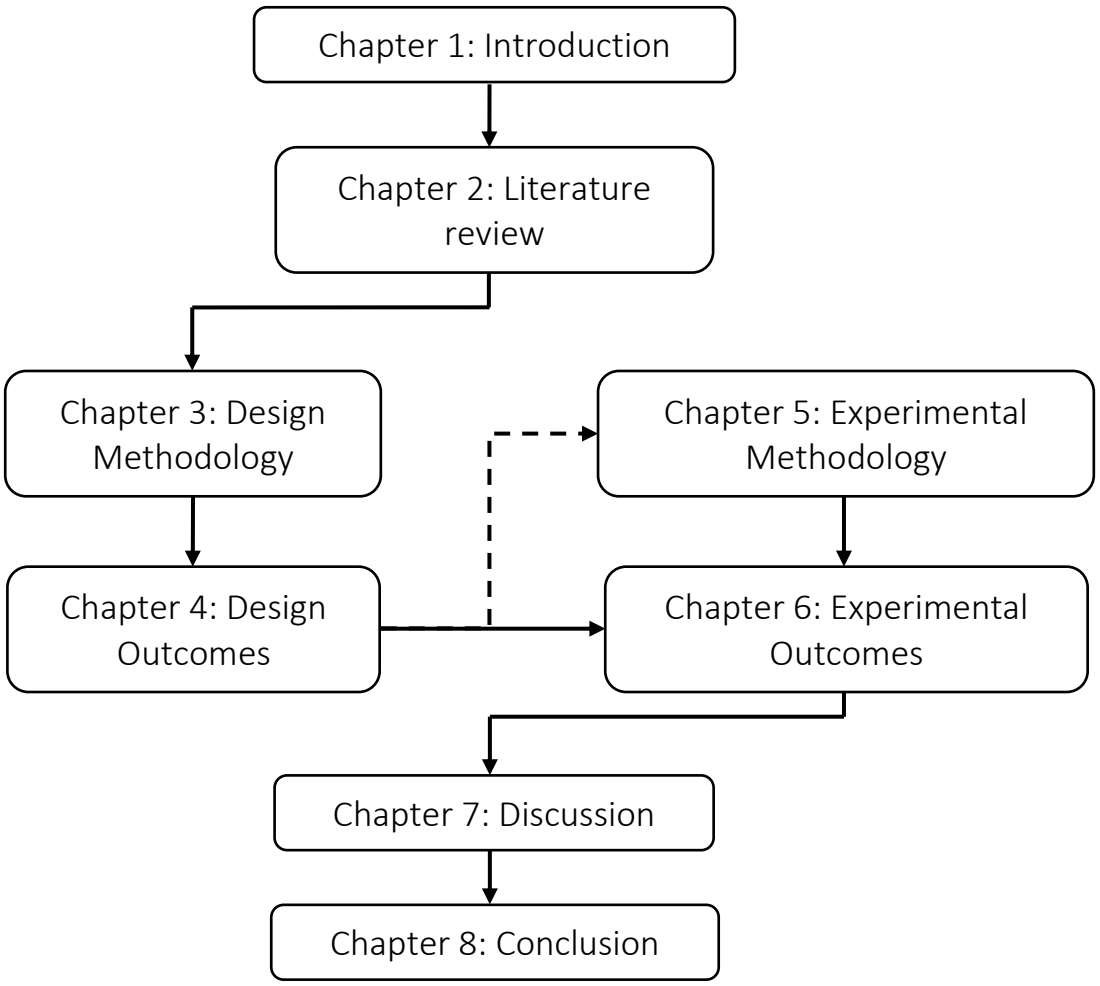

Figure 1.2: Chapter organisation flow chart.

2 Literature Review

2.1 The Knee Joint

2.1.1 Introduction to Joint Anatomy

The knee joint (as illustrated in Figure 2.1) is the point of articulation between the femur and tibia; the tibia and fibula as well as the femur and patella. The joint comprises soft tissue structures including ligaments, menisci and synovial fluid. The knee joint is one of the most heavily loaded joints in the human body, and is associated with osteoarthrosis as well as the elevated risk of injury (Bendjaballah et al. 1997). A small degree of rotation of the femur relative to the tibia is allowed by the knee joint (Gilroy et al. 2008; Drake et al. 2014). Its stability is maintained by the shape of the femoral and tibial condyles, the profile of the meniscus and the four major ligaments that surround the joint cavity (Gilroy 2008; Drake et al. 2014). The four major ligaments of the knee joint (as shown in Figure 2.1) include the ACL, the PCL, the MCL and the LCL. The fifth ligament that forms part of the knee joint known as the anterolateral ligament (ALL), is hypothesised to stabilise internal tibial rotation at flexion angles greater than 35° (Claes et al. 2013; Parsons et al. 2015). However, anterior tibial translation is primarily withstood by the ACL and ML translation is primarily withstood by the collateral ligaments. Therefore, the ALL has not been considered as a primary/ major knee joint stabilising ligament.

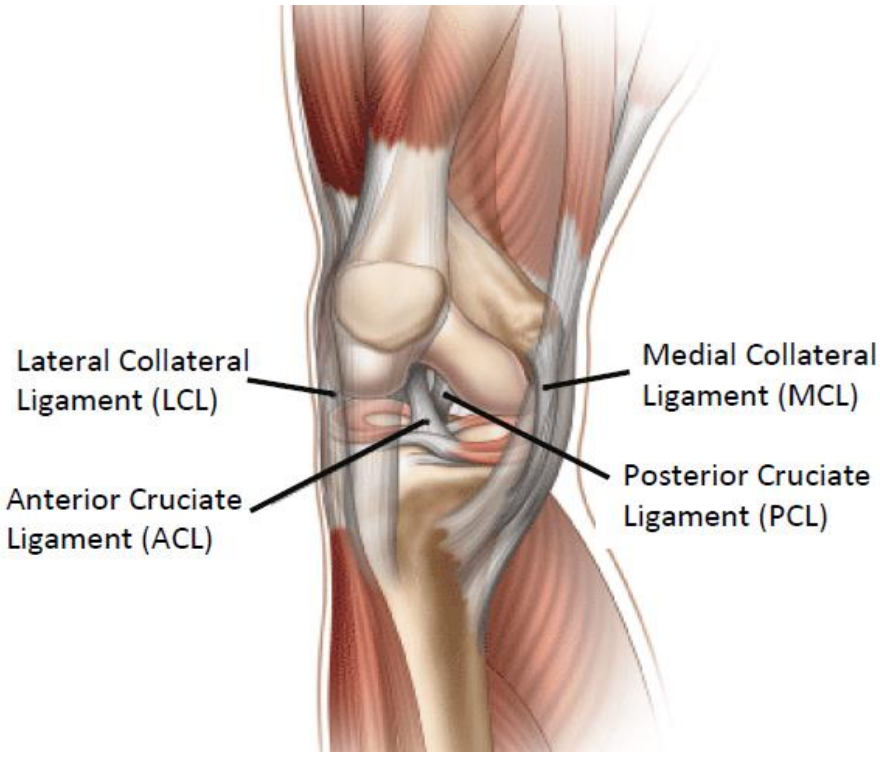

Figure 2.1: Anatomy of the knee joint highlighting the positions of the ACL, PCL, MCL and LCL (image credit: (MendMyKnee 2017)).

A typical healthy knee joint allows for 130 - 150° of flexion and 5 - 10° of hyperextension (Roach and Miles 1991). At a certain degree of flexion, the cruciate ligaments will be tauter than the collateral ligaments. During full extension of the knee joint, the collateral ligaments will be tauter than the cruciate ligaments (Brantigan and Voshell 1941). The aim of ligament laxity measurement results would be to provide physicians with a more detailed assessment regarding the health of these ligaments and the severity of the lesions. The aim is accomplished by conducting the laxity measurement tests at a particular degree of flexion to evaluate a specific ligament's laxity.

2.1.2 Ligaments

2.1.2.1 Function

The primary function of the ligaments is to provide stability to the knee joint throughout the entire range of motion (Pena et al. 2006; Ascani et al. 2015). Each ligament provides stability by restraining the motion of the knee in more than one degree of freedom (Pena et al. 2006; Ascani et al. 2015). The overall stability of the joint depends on the contribution of all ligaments during movement (Pena et al. 2006). The ACL and PCL stabilise the joint during flexion, whereas all four ligaments stabilise the joint during extension (as indicated in Table 2.1) (Brantigan and Voshell 1941). Understanding the role of each ligament in restraining and stabilising the joint, allows for a more accurate diagnosis and assessment of necessary surgical or non-surgical procedures (Pena et al. 2006). Table 2.1 summarises the function of each ligament and the state of each ligament during knee joint flexion and extension.

Table 2.1: The function and state of the four major knee joint ligaments during flexion and extension (information credit: (Woon and Hughes 2015)).

Ligaments	*Flexion*	*Extension*	*Function*
ACL	Taut (Anteromedial bundle of the ligament)	Taut (Posterolateral bundle of the ligament)	Prevention of anterior tibial translation on the femur
PCL	Taut (Anterolateral bundle of the ligament)	Taut (Posteromedial bundle of the ligament)	Prevention of posterior tibial translation and posterolateral tibial rotation on the femur
MCL	Relaxed	Taut	Provides valgus angulation restraint and prevents axial rotation
LCL	Relaxed	Taut	Supports varus angulation restraint and prevents axial rotation

2.1.2.2 Knee Joint and Ligament Biomechanics

The biomechanics of the knee joint can be analysed using a Load-Elongation (as illustrated in Figure 2.2 for an ACL) or a Stress-Strain curve. When the ligamentous tissue is subjected to a constant strain rate, the load required to stretch the ligament beyond the tissue's elastic limit (peak of the curve) to its rupture point (beyond the peak of the curve) can be plotted against its elongation. This relation allows for determining the elongation limit of a ligament, which has been calculated in previous studies (Hefzy 1984; Woo et al. 1999).

According to previous studies, the maximum load a ligament (ACL) can withstand before failing due to rupture is approximately 370N with an approximate elongation of 7.7mm (Takeda et al. 1994; Woo et al. 1999). These values depend on the collagen fibre composition, orientation of the fibres, and the collagen interaction with ground substance (Woo et al. 1999). It is essential that the load applied, for the diagnosis of a sprained ligament, should not exceed the elastic limit of the ligament. A safety factor (SF) should be incorporated to account for human variation in ligament laxity.

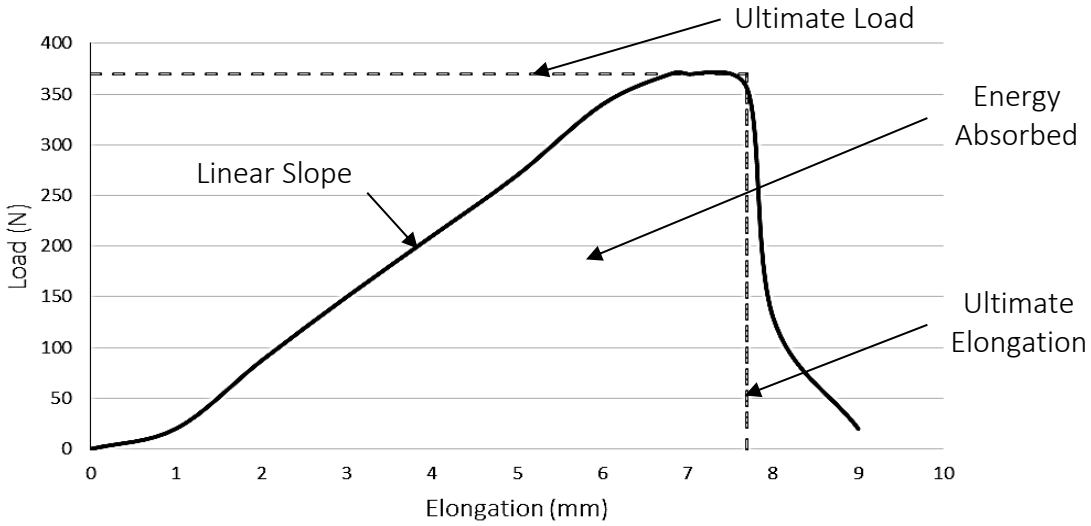

Figure 2.2: Load-Elongation curve for ligaments (Image credit: (Takeda et al. 1994; Woo et al. 1999)).

The image illustrates the degree of ligament lengthening as a result of load applied. The exponential decline in the curve indicates the point of ligament failure.

Incorporating an SF of 1.5 and considering the ligamentous elastic limit (shown in Figure 2.2), the maximum safe value to which the ligaments may be loaded (N_t) during a laxity measurement test can be determined. The maximum translational load applied to the proximal lower leg, according to existing laxity measurement studies, may be calculated and verified as shown in Eq. (2.1) (Boyer et al. 2004; Robert et al. 2009; Beldame and S. Mouchel 2012; Collette et al. 2012; Leferve et al. 2014).

$$SF = \frac{Load\ (N_f)\ at\ failure}{Load\ (N_t)\ for\ testing} \tag{2.1}$$

$$SF = \frac{N_f}{N_t}$$

$$N_t = \frac{N_f}{SF}$$

$$N_t = \frac{370N}{1.5}$$

$$N_t = 246.67\ (2.d.p) \approx 250N$$

2.2 Clinical Presentation and Evaluation

2.2.1 Injury Description

Efficient functioning of the knee joint results from compact bone structures and flexible but strong muscular attributes (Medsport 2011). In addition, smooth and secure ligamentous and cartilaginous structures contribute to the functioning of a healthy knee joint. Compromised joint function results from an imbalance/ disruption of one or more of these internal structures.

Injuries experienced by the knee joint are common amongst athletes, hard-labourers, and active people. Compromised knee joint integrity due to ligamentous sprain, partial tear or complete rupture are common injuries associated with the knee joint and account for approximately 40% of all knee injuries (AposTherapy 2015). An injury to the ACL, which is a common knee ligament injury, results from the posterior translation of the femur on the tibia. Injury to the PCL occurs from the anterior translation of the femur relative to the tibia. In addition, both cruciate ligaments stabilise the joint in rotation as well. Injury to the MCL (which is a common collateral ligament injury) results from valgus deformation of the knee joint. Varus deformation of the knee joint results from injury to the LCL. Compound injuries occur where more than one ligament has been injured. Therefore, damage to the four major ligaments of the knee joint leads to an inability to support significant load on the joint due to the induced instability (Kakarlapudi and Bickerstaff 2001; Bise 2016).

2.2.2 Causes

Illness, effects of ageing, previous and current occupation, lifestyle, medical history, level of physical activity, and natural bodily compensation for a damaged bodily structure all potentially lead to compromised knee joint integrity. Direct and indirect trauma are two of the leading causes of knee joint instability, as a result of damaged ligaments (Kakarlapudi and Bickerstaff 2001). In addition, pivotal movements in sports, jumping and rapid deceleration are more frequent causes of knee joint ligament injuries (Kakarlapudi and Bickerstaff 2001). The mechanical symptoms of an injury of this nature include catching, locking, hyperlaxity, clicking, and decreased integrity of the knee joint (Kakarlapudi and Bickerstaff 2001). From a biomechanics perspective, any form of excessive exertion on the joint, loading the ligaments beyond the elastic limit, would cause ligament failure and joint instability.

Valgus and varus stresses, leading to valgus and varus deformation of the joint, are a primary cause of compromised knee joint integrity because of damage to the associated ligaments (Bendjaballah et al. 1997). The affected person would thus be unable to support any substantial load on the joint. The injury would limit the individual's ability to carry out normal activities of daily life (ADLs). In some cases, this form of injury could jeopardise the affected person's ability to work, depending on their occupation. A non-invasive and efficient means of diagnosing a compromised joint would reduce recovery time and ensure the most appropriate treatment option is selected.

2.2.3 Symptoms and Consequences of Knee Ligament Injuries

The degree of the ligament injury and the implemented treatment method largely affects the injury's impact on a patient's day-to-day life. The overall result of a ligamentous knee injury is the instability of the joint. With compromised joint integrity, the results range according to severity.

A sprained ligament would lead to a mild degree of pain. The likelihood of the patient bearing their body weight is reasonably high. The joint would be slightly unstable and supporting significant weight would be detrimental to the rehabilitation process. However, with implementing appropriate treatment methods the injury can be overcome and in most cases, the patient would continue with their ADLs.

A partial tear in one or more of the four major ligaments in the knee joint, results in joint instability, potentially leading to the inability to support one's body weight. The likelihood of causing further damage to the injured ligaments during ambulation will be high. Therefore, it would be advised to remain inactive and consider appropriate treatment options. The injury could potentially impact one's ability to carry out ADLs, including work.

Finally, a complete ligament rupture would result in total inability to support any load on the joint and immense pain. The patient would be inactive and incapable of carrying out any locomotive activity. A summarised comparison of the injury types and their consequences are indicated in Table 2.2.

Table 2.2: Comparison of ligament injuries and their consequences.

Ligament injury	*Degree of pain*	*Possibility of bearing body weight*	*Stability of joint*	*Treatment method*
Sprain	Mild	High	Stable	Rest, Rehabilitation
Partial tear	Medium	None	Unstable	Rehabilitation
Complete rupture	Immense	None	Highly unstable	Surgery & Rehabilitation

Grading systems exist to assist with evaluating the severity of knee joint instability. A modified version of the Lysholm Knee Scoring Scale (Tegner and Lysholm Scoring scale as indicated in Table 2.3) may be used to evaluate the severity of the injury as it is considered an acceptable rating scale (Lysholm and Tegner 2009). The scale assesses the patient's symptoms post-surgery when carrying out ADLs (Tegner and Lysholm 1985). However, the scale assists in understanding the symptoms during ADL, and is therefore, applicable to pre-surgery cases as an initial diagnosis questionnaire. This rating system is discreet whereby a healthy patient would score 100 points. Using the scale and allocating a score to the injury may provide a better understanding of what the injured person is physically capable of and the social impact of the injury.

Table 2.3: A summarised adaptation of the Tegner and Lysholm Knee Scoring Scale (Image credit: (Lysholm and Tegner 2009)).

Clinical presentation	*Maximum Score*
Limp	5
Support	5
Locking	15
Instability	25
Pain	25
Swelling	10
Stair-climbing	10
Squatting	5
Total	100

The table indicates a summarised adaptation of the Tegner and Lysholm Knee Scoring Scale. A higher score for each clinical presentation would indicate a healthier patient, however, a lower score would indicate a severely injured patient with these symptoms: constant limping, inability to bear weight, frequently experiencing a locked joint, instability with every step taken, experiencing a constantly painfully swollen joint and is incapable of climbing stairs or squatting.

According to Tegner et al., 1985, a patient with less than 64 points would be unable to carry out ADLs. A patient with a score of 65-83 points would have a 66.66% chance of being able to carry out ADLs, however, unable to play sport or participate in strenuous exercise. A patient with a score of 84 and above would have a 92% percent chance of being capable of carrying out ADLs. However, sports activities would be challenging. Considering these values, Table 2.4 provides an interpretation of where a sprain, partial tear, and complete rupture would rate according to The Tegner and Lysholm Scale.

Phisitkul et al. (2006) describes the Hughston classification scale, which categorises the laxity of knee joint ligament injuries (Grade 1+, 2+, 3+). The scale is primarily focused on MCL laxity measurements, however, it is assumed that the scale may be utilised for LCL laxity, since it is similar to the American Medical Association (AMA) classification scale. Laxity classification is based on absolute joint separation. Grades 1+, 2+ and 3+ correlate with a bone separation distance of 3-5mm (0-5mm according to AMA), 6-10mm, and more than 10mm. Grade 1+, Grade 2+ and Grade 3+ laxity ratings are typical associated with ligamentous sprain/ tenderness, a partial tear and a complete thickness rupture.

Table 2.4: Score evaluation of a sprain, partial tear, and complete rupture according to the "The Tegner and Lysholm Knee Scoring Scale."

Injury severity	*Ligament*	*Score (100)*	*Ability to carry out ADLs (100%)*
Healthy	All	91 - 100	100
Sprain		84 - 90	95.3
Partial tear	ACL, PCL*, MCL, LCL	65 - 83	66.6
Complete rupture		<= 64	0

The table indicates the Tegner and Lysholm score evaluations of the degrees of laxity measurement injuries. However, and injured PCL might not affect a patient's ability to carry out ADL (*).

Although compromised knee joint integrity can severely limit one's ability to carry out ADLs, injuries of this nature heal and full recoveries are possible with modern medicine. An accurate diagnosis and prognosis would be necessary to determine the most appropriate treatment method for the injury. Accurate diagnosis and prognosis might avoid the costly implications of misdiagnosis or time-consuming diagnosis, which would require interventions such as arthroscopic surgery and MRI scans. Arthroscopic surgeries and MRI scans are expensive options in improved diagnosis methodologies.

The clinical consequences of knee joint ligament injuries when left untreated include cartilage breakdown, joint degradation and advancing degeneration i.e. osteoarthritis. Ligament damage leads to subchondral bone destruction resulting in cartilage breakdown, bone to bone joint articulation and ultimately knee joint replacements (Bailey and Mansell 1997).

2.2.4 Treatment Methods

The treatments available, depending on the severity of the injury, include pain inhibition, decreasing the load supported by the joint, rehabilitation therapy, use of a knee brace, and ligament reconstruction. Patients would most likely make use of pain medication to temporarily relieve the pain caused by the injury. However, this could cause further damage to the ligaments if no other treatment option is considered. The use of crutches and walking sticks alleviate the pain experienced during ambulation and allow the joint structures time to heal. Physiotherapy presents a relatively long-term treatment option that would involve stability and strength exercises. Patients with instability symptoms as a result of complete ligament rupture, participating in sports and manual labour could undergo surgical treatment to replace the damaged ligaments with a tendinous graft (OrthoInfo 2009). Laxity measurement devices, aid the physicians' decisions regarding the most appropriate treatment method by accurately quantifying ligament laxity injuries.

2.2.5 South African Relevance

The need for joint health diagnostic tools in South Africa would largely depend on the activity level of the population. According to Pennington (2014), one in every five adults in South Africa exercise at least once a month or are part of a health club (i.e. gymnasium or place of exercise). South Africa hosts the Cape Argus (the largest individually timed race in the world) and the Comrades Marathon (one of the most attended ultra-marathons in the world) (Pennington 2014; Morgan 2015). Many South Africans enjoy running, hiking up the Drakensberg Mountains and Table Mountain, surfing and other physical activities. The country has a large mining industry and a large manual labour workforce in the construction, mining and automotive industries. People who participate in active exercise, sports, manual labour, and training would be at risk of injuring any of the four major ligaments of the knee joint and thereby compromise the joint's integrity. Statistical information regarding the number of injuries in South Africa is limited. However, activity levels of the South African population indicate the potential prevalence of knee joint ligament injuries within the country's context.

2.3 Laxity

2.3.1 Introduction to Laxity

Ligament laxity is the loosening or lack of tautness of a ligament (FarlexInc. 2017; Merriam-Webster 2017). The loosening of the ligament results from loading the ligamentous tissue, whereby injury occurs when loading is beyond its elastic limit. Hypermobility and pain are common symptoms of a ligamentous laxity related injury. There are no direct means of determining the laxity of a ligament, however, an indirect method is practiced in knee injury diagnostics. Knee joint ligament laxity is determined using an adaptation of joint distraction i.e. separating the femur from the tibia and fibula at a joint surface by application of a known load. The distraction/ translation occurs parallel (ACL and PCL procedures) and perpendicular (MCL and PCL procedures) to the joint surface plane. Figure 2.3 illustrates the planar bone translation when measuring PCL ligament laxity.

Figure 2.3: Example of parallel planar bone distraction/ translation - process used to determine ligamentous laxity (image credit: (Savarese et al. 2011)).

2.3.2 Methods of Measurement

The laxity of the four major ligaments in the knee joint is determined by applying a load to various aspects of the proximal lower leg. The distal lower leg would be secured, allowing the tibia and fibula to pivot about the ankle joint. The direction of the applied load would depend on the required ligament laxity measurement. In addition, the state of the ligament at a specified degree of knee flexion (as indicated in Table 2.5) needs consideration during laxity measurement testing.

For example, the ACL laxity measurement would be performed while the joint is in flexion i.e. 30° or 90° (from full extension). At full extension, all four ligaments are taut, therefore, to eliminate the collateral ligaments from affecting the laxity results, the joint would be flexed. Anterior translation of the tibia with respect to the femur will yield an ACL laxity measurement result. Table 2.5 summarises the laxity measurement methodology.

Table 2.5: Load direction, lower leg translation and knee flexion angle for ligament laxity measurements (Information credit: (Bickley and Prabhu 2003; Lubowitz et al. 2008)).

Ligament	*Lower leg translation direction*	*Proximal lower leg surface to which load is applied*	*Knee flexion from full extension (0°)*
ACL	Anteriorly	Posterior	30° and 90°
PCL	Posteriorly	Anterior	30° and 90°
MCL	Medially	Lateral	0° and 30°
LCL	Laterally	Medial	0° and 30°

2.3.3 Existing Devices

Due to the variability in the rate at which the load is manually applied to the tibia and the magnitude and direction of the load, laxity measurement devices have been developed (Branch et al. 2010). Laxity measurement devices help to quantify the tibial translation during laxity measurement examinations (Leferve et al. 2014). These devices assist in the diagnosis and prognosis of ligamentous injuries associated with the knee joint.

Several devices exist capable of measuring the laxity of the knee joint ligaments i.e. arthrometers and stress radiography devices. Arthrometers provide digital laxity measurements whereas stress radiography devices make use of radiographic imaging techniques. The KT-1000™ (Figure 2.4) and Genourob (GNRB®) (Figure 2.5) arthrometers, and the Telos™ Stress (Radiography) Device (Figure 2.6), are the standard device techniques used for measuring the laxity of the ligaments associated with the knee joint (Leferve et al. 2014). A critical mention for this study would be the University of Cape Town's (UCT's) own Laxmeter (Figure 2.7) – an existing novel low-cost stress radiography device (Sivarasu and Patnaik 2014a; Sivarasu and Patnaik 2014b; Beukes et al. 2017).

The KT-1000™ (Figure 2.4) arthrometer was developed by Dale Daniel in the 1980's to quantify the diagnosis of ACL tears (LaPrade 2017). The device measures the laxity of the ACL primarily and the PCL as a secondary function. This is done by applying a load to the posterior and anterior aspects of the proximal tibia and measuring the AP translation of the tibia about the femur. The patient is placed in a supine position with their thighs resting on an 110mm high bolster to maintain 25-30° knee flexion (Collette et al. 2012). The patient's heels are placed on a positioning cup to maintain a symmetrical 15° external rotation of the lower limb according to the Lachman test instructions (Bickley and Prabhu 2003; Lubowitz et al. 2008). The device secures the lower limb with two Velcro® straps. Upon completing a calibration process, the examiner then applies the load using a force-sensing handle located on the device. The device will produce an audio tone as a result of applying 67N, 89N and 134N loads at which translation is displayed on a dial and manually recorded (Collette et al. 2012). The KT-2000™ exists, however, researchers make use of the KT-1000™ in the more recent laxity measurement studies. The KT-2000™ comprises of the same components as the KT-1000™, with the addition of graphic display of tibial translation on the X axis and load applied on the Y-axis (Lin et al. 2011; Collette et al. 2012).

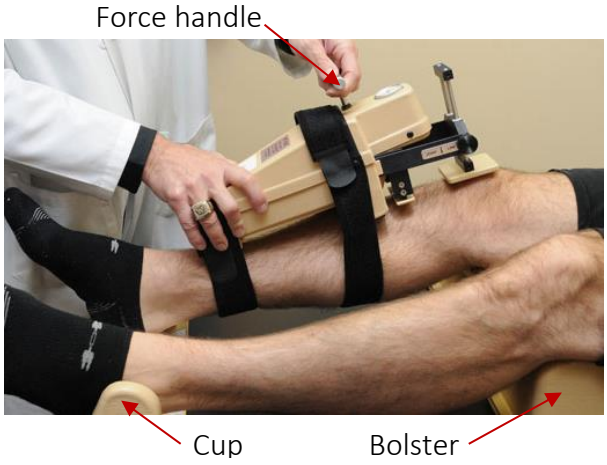

Figure 2.4: KT-1000™ (Image credit: (LaPrade 2017)).

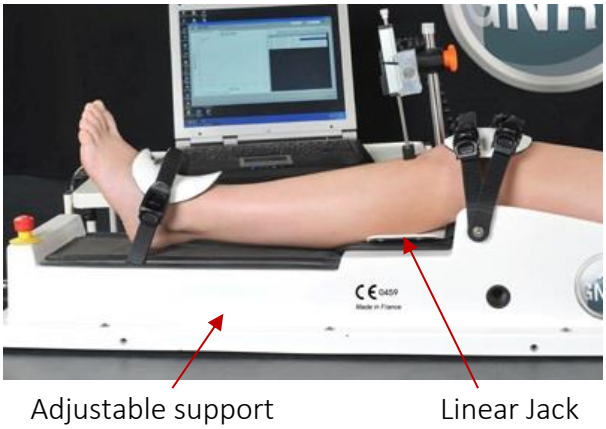

Figure 2.5: GNRB® (Image credit: (UCORS 2011)).

The GNRB® (Figure 2.5) arthrometer system measures ACL laxity. The device requires the patient to lie on a standard examination table in a supine position. Both knees are tested for comparative purposes, with the healthy knee undergoing the laxity testing process first (Robert et al. 2009; Collette et al. 2012). The knee is placed on an adjustable support and fixed in a 0° rotation and 20° knee flexion position. Electrodes are placed on the hamstring compartment of the upper leg to monitor and control muscle relaxation (Robert et al. 2009; Collette et al. 2012). The absence of hamstring muscle contraction during load application improves the reliability of the test results (Lin et al. 2011). Once the supports have been fitted to the patient, the testing procedure can commence. A linear jack is used to apply a gradually increasing load, as specified by the examiner, at a rate of 11mm/s (Collette et al. 2012). The device can apply loads of 67, 89, 134, 150 and 250N to the posterior aspect of the proximal tibia (Robert et al. 2009; Beldame and S. Mouchel 2012; Collette et al. 2012). Translation of the tibia with respect to the patella is recorded with a displacement transducer (Robert et al. 2009; Collette et al. 2012).

The Telos™ Stress Device (Figure 2.6) allows for an overall examination of the knee joint's laxity. The patient is placed in either a supinated position for MCL and LCL tests or in a lateral (sideways) position for ACL and PCL laxity tests. The lower limb is secured by means of two counter supports. Afterwards, the knee flexion angle is adjusted accordingly (Scheuba 2009). The knee joint angle of flexion required for MCL and LCL laxity tests would be between 15° and 30°. The knee joint angle of flexion for ACL and PCL laxity measurements would be between 10° and 20°. Once the limb is in position, a pressure device is used to apply a load of either 150 or 250N to the proximal tibia. A stress radiograph (X-ray image) of the joint position would then be taken at the applied load (Leferve et al. 2014). Staubli & Jakob (1991) described a commonly used method of measuring the AP tibial translation from stress radiographs (Leferve et al. 2014).

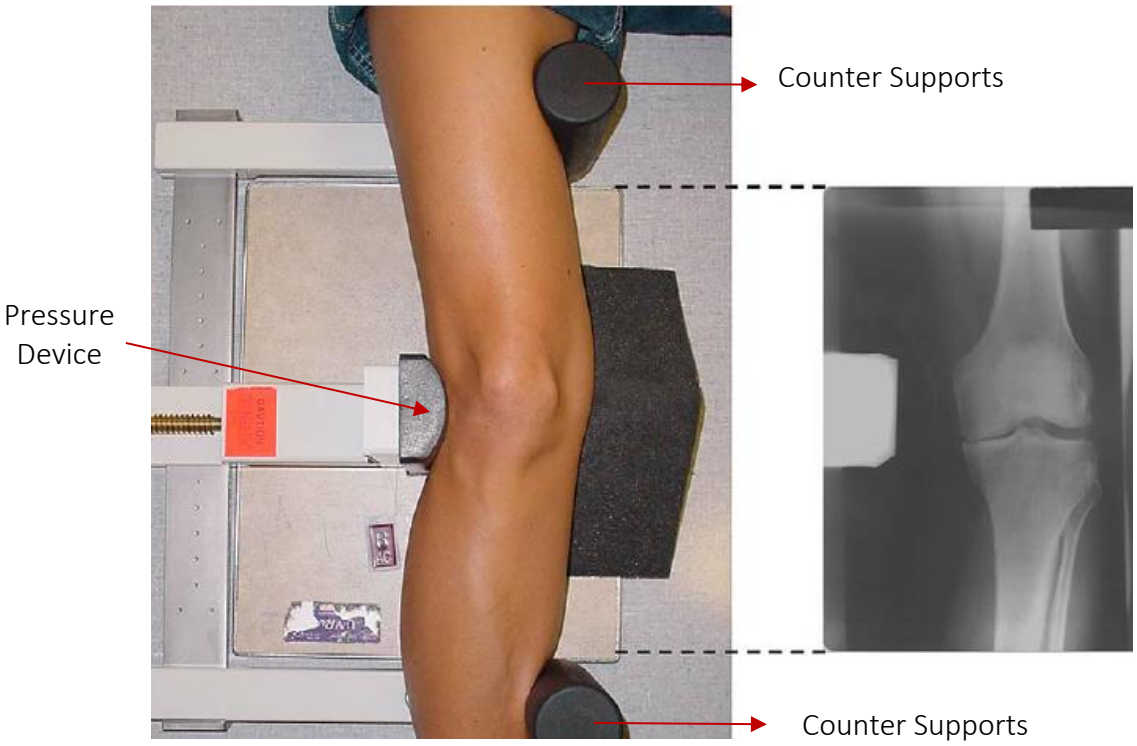

Figure 2.6: Telos™ Stress Device (Image credit:(Lewek et al. 2004)).

The Laxmeter – stress radiography device (as illustrated in Figure 2.7) was developed to facilitate the measurement of knee joint ligament laxity at various angles of joint flexion (Sivarasu and Patnaik 2014a; Sivarasu and Patnaik 2014b). The entire device is constructed of radiolucent material so as not to create interference with the X-ray images. The patient is placed in a supine position on top of the Laxmeter structure. The hip joint is initially flexed to a 90° angle, allowing the patient to rest their lower leg on the horizontal panel. The device places the patient in the ideal position for all knee joint laxity measurement tests. The Laxmeter has a knee flexion adjustment mechanism, which locks into place to fix the angle of flexion. The process of determining the valgus and varus stresses experienced by the knee joint is aided by the Laxmeter. The device substitutes an X-ray table, which could be further developed, enabling the assessment of knee joint ligament laxity (Sivarasu and Patnaik 2014b). The device soley consists of a large and unfeasible patient support structure. A load application system is required to induce bone distraction for stress radiography laxity measurements procedures.

Figure 2.7: UCT's Laxmeter - A novel, low-cost stress radiography device (Image credit: (Sivarasu and Patnaik 2014b)).

The diagnosis of compromised joint integrity due to ligament damage and the decision to reconstruct the ligaments could be made more reliably with the results obtained with the various laxity measurement devices. The results would potentially improve the clinician's understanding of the severity of the injury.

2.3.4 Limitations

2.3.4.1 Introduction to Limitations

Laxity measurement devices have been tested and the results compared with one another in various studies, particularly for ACL ligament laxity examinations (Robert et al. 2009; Beldame and S. Mouchel 2012; Collette et al. 2012; Leferve et al. 2014; Vauhnik et al. 2014; Sivarasu and Patnaik 2014b). Although these devices assist in improving the clinician's diagnosis by quantifying the tibial translation, they aren't without limitation. The KT-1000™, the GNRB®, the Telos™ Stress Device and the Laxmeter all have their limitations. These limitations, as highlighted according to Sivarasu & Patnaik (2014b) are:

- Affordability
- Performance i.e. Accuracy, reliability and reproducibility
- Patient ergonomics
- Occupational hazards
- Functionality related to ligament laxity
- Inability to perform bilateral imaging of knee joints at various flexion angles
- Ease of storage

2.3.4.2 Affordability

Existing laxity measurement devices come with a large Capital acquirement cost. According to MEDmetric (2011), the cost of a KT-1000™ and a KT-2000™ would be approximately US$4300 (ZAR 57281.10) and US$8470 (ZAR 112853.27) (Converter 2017). A quotation request from Genourob indicated a price tag of approximately €11000, which converts to US$ 11784 and ZAR 157000 (Converter 2017). Existing information concerning the cost of the GNRB® arthrometer is unavailable. However, the features of the device imply a rather large price tag, potentially exceeding that of the KT-1000™. Information regarding the cost of the Telos™ Stress Devices is limited, however, Leferve et al. (2014) referred to the device as expensive when compared to the KT-1000™. The Laxmeter structural frame was manufactured and assembled in 2014 for US$430 (ZAR 4500), which would be a tenth of the KT-1000™ in US dollars (Sivarasu and Patnaik 2014b). Table 2.6 provides a summary and cost comparison of the above-mentioned laxity measurement devices.

Table 2.6: Cost comparison of existing laxity measurement devices (Information credit: (MEDmetric 2011; Leferve et al. 2014; Sivarasu and Patnaik 2014b; Converter 2017)).

Device name	*Type*	*Cost*
KT-1000™	Arthrometer	US$4300 (ZAR 57281.10)
KT-2000™	Arthrometer	US$8470 (ZAR 112853.27)
GNRB®	Arthrometer	US$11784 (ZAR 156851.56)
Telos™	Stress radiography device	More than the KT-1000™
Laxmeter	Stress radiography device	US$430 (ZAR 4500 in 2014)

2.3.4.3 Performance

As mentioned, several studies have been performed comparing existing laxity measurement devices, focussing on ACL injury diagnosis. Accuracy, reliability and reproducibility of results can be considered as overall device performance.

Research suggests that the KT-1000™ produces relatively inaccurate and unreliable results when compared to the GNRB® (FORSTER et al. 1989; Wiertsema et al. 2008; Collette et al. 2012). In addition, the accuracy of the KT-1000™ is operator dependent (Leferve et al. 2014). The KT-1000™ has been found to demonstrate subordinate reproducibility of laxity measurement results compared to the GNRB®, potentially due to inaccurate replication of lower limb external rotation and exact angle of knee flexion (Robert et al. 2009; Bouguennec et al. 2015). Evaluation consisted of comparing two examiners (experienced and novice considerations) using one device to test one knee, one examiner using both devices on one knee and one examiner using one device on both knees. Significance was determined by means of the F-test. Furthermore, in comparative studies between the KT-1000™ and the Telos™ Stress Device, the Telos™ produced better reliability than the KT-1000™ (Jardin et al. 1999; Margheritini et al. 2003). The studies compared the results of device specific experienced operators diagnosing the same patient population. Therefore, it can be deduced that the KT-1000™ arthrometer is less reliable than the Telos™ Stress Device and the GNRB® arthrometers. Existing research indicates that the GNRB® arthrometer performs as well if not better than the Telos™ Stress Device (Beldame and S. Mouchel 2012; Leferve et al. 2014; Bouguennec et al. 2015). In the case of the Laxmeter, no comparative studies have been done to date. Therefore, it can be deduced that the GNRB® arthrometer has the best overall performance of stress radiography devices regarding accuracy, reliability and reproducibility of measurement tests.

2.3.4.4 Patient Ergonomics

Patient ergonomics is a major concern regarding laxity measurement device limitations. This limitation is particular to the Telos™ Stress Device. In the case of ACL and PCL injuries, the patient is oriented in a highly non-ergonomic position (Sivarasu and Patnaik 2014b). Patient position during ACL laxity measurement tests is illustrated in Figure 2.8. In addition, the inner or outer rotation of the tibia would need to be manually positioned by the examiner during testing, thereby increasing patient discomfort (Scheuba 2009). Cruciate ligament laxity measurement tests require a change of orientation of either the patient or the Telos™ Stress Device.

Figure 2.8: Non-ergonomic patient position during Telos™ ACL and PCL laxity measurement testing (Image credit: (Beldame and S. Mouchel 2012)).

2.3.4.5 Occupational Hazard

Consideration towards the health and safety of the examiner carrying out a laxity measurement test is crucial. With stress radiography, the radiation due to the chosen image modality poses a threat. The Telos™ Stress Device makes use of X-rays to capture tibial translation. During cruciate ligament laxity measurements, the examiner manually maintaining the inner and outer rotation of the tibia would be indirectly exposed to X-ray radiation (Scheuba 2009; Sivarasu and Patnaik 2014a).

2.3.4.6 Functionality Related to Ligament Laxity

Laxity measurement devices can perform the Lachman as well as the Anterior Drawer Tests to measure the laxity of the ACL and the Posterior Drawer Test to measure the laxity of the PCL. The KT-1000™ measures the laxity of the ACL (primarily) and the PCL, whereas the GNRB® is limited to measuring the laxity of only the ACL ligament (Lin et al. 2011). Certain laxity measurement devices can perform the Adduction and Abduction stress tests used to measure the laxity of the LCL and MCL. The Telos™ Stress Device can potentially measure the laxity of all four major ligaments of the knee joint (Scheuba 2009). Table 2.7 indicates the functional capabilities of the various laxity measurement devices. The above-mentioned ligament measuring techniques performed by the laxity measurement devices are described in Section 2.3.5 Measurement Techniques.

Table 2.7: Laxity measurement technique capabilities and limitations of existing laxity measurement devices and techniques. X represents inability to carry out the test, '✓' represents ability to perform the test with reduced reliability, '✓*' represents ability to conduct the test with ergonomically awkward positions, '✓†' represents allowance for test but inability to functionally perform the test and '✓✓' represents full ability to carry out the test.

Existing Devices	*Lachman Test (ACL)*	*Anterior Drawer Test (ACL)*	*Posterior Drawer Test (PCL)*	*Adduction Stress Test (LCL)*	*Abduction Stress Test (MCL)*	*Various degrees of flexion*	*Stress Radiography (radiation)*
KT-1000™	✓	✓✓	✓✓	X	X	X	X
GNRB®	✓✓	✓✓	X	X	X	X	X
Telos™ Stress Device	X	✓	✓	✓✓	✓✓	✓*	✓✓
Laxmeter 1.0	X	X	X	✓†	✓†	✓✓	✓✓

2.3.4.7 Bilateral Imaging at Various Flexion Angles

The commercially available Telos™ Stress Device focuses on unilateral laxity measurement imaging. The Laxmeter, however, aims to address this limitation. It allows for bilateral imaging of the both knee joints at specific flexion angles, simultaneously (Sivarasu and Patnaik 2014b).

2.3.4.8 Ease of Storage

The KT-1000™, GNRB® and Telos™ Stress Device are compact laxity measurement devices. However, the Laxmeter attempts to create the ideal laxity measurement test setup, utilising ideal patient positioning during testing (Sivarasu and Patnaik 2014a; Sivarasu and Patnaik 2014b). The device is structurally sound and large enough to carry the weight of an average person resting both lower limbs on the horizontal panel (as illustrated in Figure 2.9). Due to its size and weight, the Laxmeter presents a challenge regarding transportation and storage.

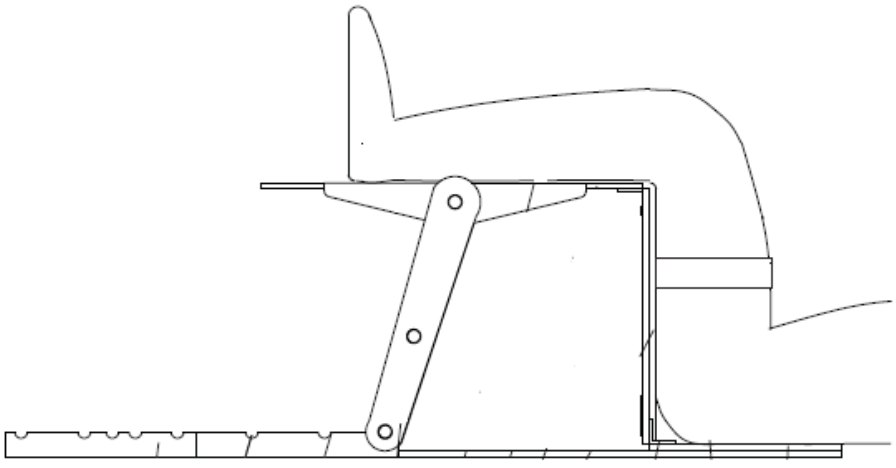

Figure 2.9: Position of patient on the Laxmeter (Image credit: (Sivarasu and Patnaik 2014b)).

2.3.5 Measurement Techniques

2.3.5.1 Introduction

Laxity measurement devices, which focus on quantifying tibial translation during laxity measurement tests, provide digital, analogue or radiographic measurement results. Alternative laxity measurement technique results include Arthroscopy real time visual imagery and MRI images.

2.3.5.2 Digital and Analogue Types

The KT-1000™ provides analogue measurement results. The translation of the tibia is read off the dial on the anterior surface of the device (as illustrated in Figure 2.10) and manually recorded at the sound of each audio tone (as described in Section 2.3.3 Existing Devices). The KT-2000 however, provides digital tibial translation (shown in Figure 2.11) results through graphical representation. The GNRB® takes digital result output one step further. The results obtained from GNRB® laxity measurement tests are presented in the form of digital output (including automated translation results interpretation i.e. pathologic or healthy) and graphical interpretation displayed as a Force-Displacement curve (as illustrated in Figure 2.12).

Figure 2.10: KT-1000™ output.

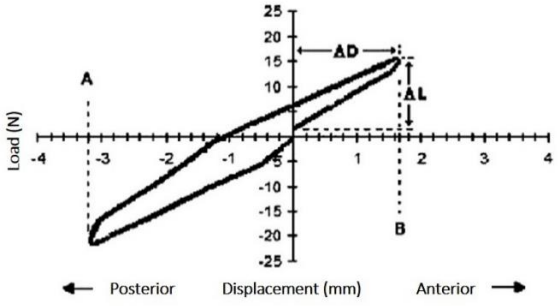

Figure 2.11: KT-2000TM output (Image credit: (Kupper et al. 2007)).

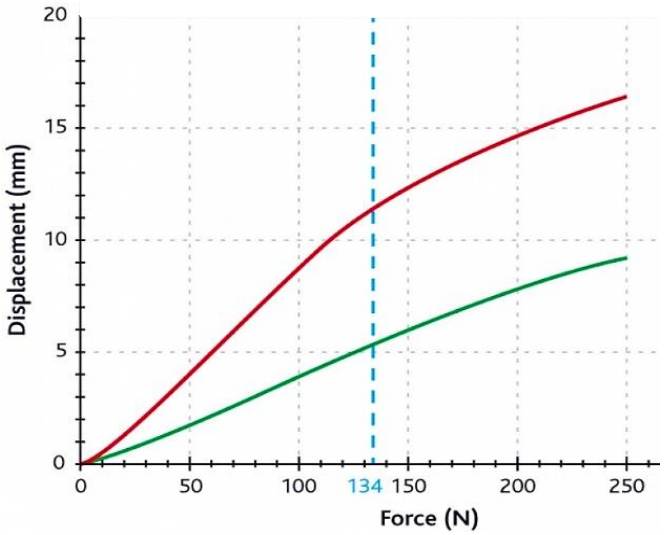

Figure 2.12: GNRB® graphical and digital output (Image credit: (Genourob 2017)).

2.3.5.3 Radiography

Stress radiography devices, such as the Telos™ Stress Device, make use of X-ray imaging modalities to capture the translation of the tibia (as illustrated in Figure 2.13). The measurement data is processed through manually measuring the tibial translation on the image, using tracing paper and a graduate ruler with 0.5mm precision (Beldame and S. Mouchel 2012). A technique which refers to specific bone landmarks is used to measure the translation of the tibia (Jacobsen 1976; Beldame and S. Mouchel 2012). The data analyst would measure the translation about the medial plateau (for ACL laxity measurements) and posterior cortex to minimise measurement errors at the lateral compartment and thereby improve measurement result reliability (Staubli and Jakob 1991; Beldame and S. Mouchel 2012).

Figure 2.13: Telos™ Stress Device radiograph with landmarks (image credit: (Beldame and S. Mouchel 2012)).

2.3.5.4 Magnetic Resonance Imaging, Arthroscopy and Clinical Examinations

MRI has been reported as a diagnostic technique for ACL tears (Thomas et al. 2007). The technique is reported to be a preferred alternative to arthroscopy (surgery involving the insertion of an arthroscope into the joint) due to the invasiveness and risks of arthroscopic surgery (Crawford et al. 2007). However, in comparative studies to clinical examinations, the MRI diagnostic results (a more expensive alternative) presented no significant difference in accuracy for diagnosing ACL tears (Rose and Gold 1996; Kocabey et al. 2004; Thomas et al. 2007). Kocabey et al. (2004) recommended the use of MRI in more complicated and unclear diagnostic cases. According to Crane (2017), the cost of a knee MRI scan in a South African Government Hospital is approximately R3824 (comparable to the cost of arthroscopic surgery – R4860) and according to News24 (2014), a knee MRI scan in the private health sector costs approximately R8800. In the case of clinical examinations, the standard physiotherapist consultation fee in South Africa of R500 - R700 would be the cost implication involved (Kincaid 2017; PhysioPRO 2017).

2.4 Materials and Manufacturing

2.4.1 Material Considerations

This study includes the design and development a of laxity measurement device. The study considered the following locally (Cape Town, South Africa) available materials:

- Acrylic
- Cast Nylon
- Ertalyte

Acrylic (Plexiglas®) is an affordable and rigid polymer, with a high impact resistance and tensile strength (Gartech 2014). In addition, the material is recyclable and has exceptional light transmission properties.

Cast Nylon is cost effective with a high tensile and compressive strength and a high impact resistance (Gartech 2014). The material has a favourable wear resistance and higher rigidity compared to extruded Nylon 6. However, the material is hydroscopic and will alter its mechanical properties due to moisture absorption.

Ertalyte® (polyethylene terephthalate) is a material with high strength and rigidity as well as desirable wear resistance properties (Gartech 2014). The material has excellent strain resistance and is suitable for high precision mechanical parts sustaining heavy loads (Quadrant 2017).

2.4.2 Manufacturing Considerations

This study made use of the resources provided by UCT. Three-dimensional (3D) printing is rapidly becoming a popular manufacturing technique. Models are produced by layering and fusing materials to produce a 3D object (Ventola 2014). Integration between the printer and computer-assisted design (CAD) software results in a convenient and cost effective, rapid prototyping system (Berman et al. 2012). Additional manufacturing techniques considered for this study was workshop machining. Milling, turning, drilling and band saw work are generalised methods of manufacturing large scale models. Laser cutting is a manufacturing technique used to cut specific shapes out of plastic or acrylic sheets. The use of this machining process in the industry is increasing due to the improved quality of the product and finish quality (Choudhury and Shirley 2010).

2.5 Summary

Knee joint injuries due to ligament damage are a widespread problem in South Africa and the rest of the world. These injuries are diagnosed by determining the laxity (elasticity and stiffness) of the ligaments within the joint. Laxity is determined by immobilising the femur as well as the distal tibia and inducing proximal lower leg translation. The direction of the translation depends on which ligament has been injured and the amount of translation determines the diagnosis. Laxity measurement devices can effectively assist the clinician in diagnosing a knee joint ligamentous injury by quantifying tibial translation results. However, existing devices (including the Laxmeter) have limitations regarding device capabilities, accuracy and reliability. An affordable, lightweight and functional laxity measurement stress radiography device capable of effectively measuring the laxity of all four major ligaments of the knee joint at multiple DOFs, and addressing the limitations of existing laxity measurement devices would be the benchmark in affordable ligament injury diagnostics. The device would be a valuable assistive tool for the developing world, in need of an affordable means of diagnosing ligamentous injuries associated with the knee joint.

3 Design Methodology

3.1 Overview

This section investigates the design and functionality of a novel, radiolucent and low-cost stress radiography device aimed at non-invasive diagnosis of ligamentous knee injuries. The intended function of the device is to measure the laxity of the four major ligaments of the knee joint at multiple degrees of knee flexion using bone distraction and translation techniques. The device assists the clinician in assessing the severity of a knee joint ligamentous injury and making a more informed and accurate diagnosis.

Existing devices are unable to measure the laxity of the ACL, PCL, MCL and LCL without complications affecting patient comfort, reproducibility and overexposure to radiation. In addition, certain devices are limited to measure the laxity of only one or two ligaments. The Laxmeter considers the limitations of existing devices and attempts to address these limitations; incorporating patient ergonomics, test reproducibility and fixation of the patient's pelvis. These factors make the device novel. The device measures ligament laxity at nine defined knee joint flexion angles to provide a more informed diagnosis. Figure 3.1 illustrates an LCL example of the knee joint ligamentous injuries that the Laxmeter would potentially diagnose.

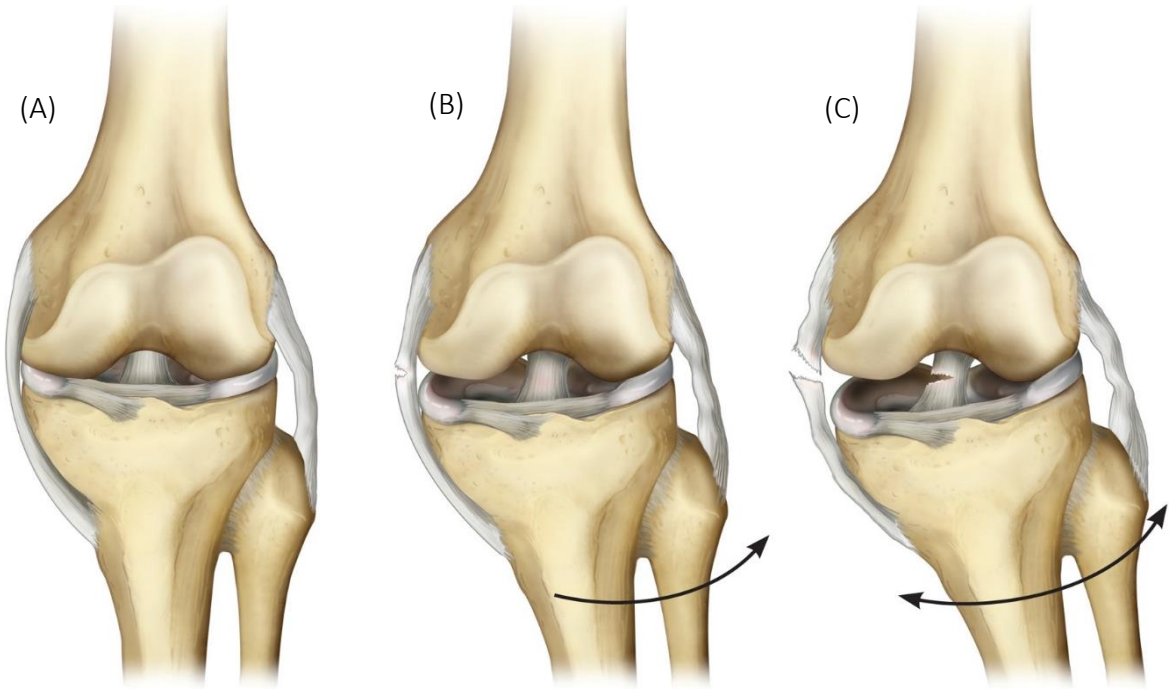

Figure 3.1: Levels of knee joint (LCL) ligamentous injuries: A) Sprained, B) Partially torn and C) Complete rupture of LCL and partial tear of ACL (Image credit: (Kneesafe 2015)).

This chapter is divided into three major Sections i.e. I] Electronic design, II] Mechanical design and III] Systems Integration. Figure 3.2 illustrates a methodology flowchart providing a highlighted overview of the design methodology.

3.2 Flow Chart

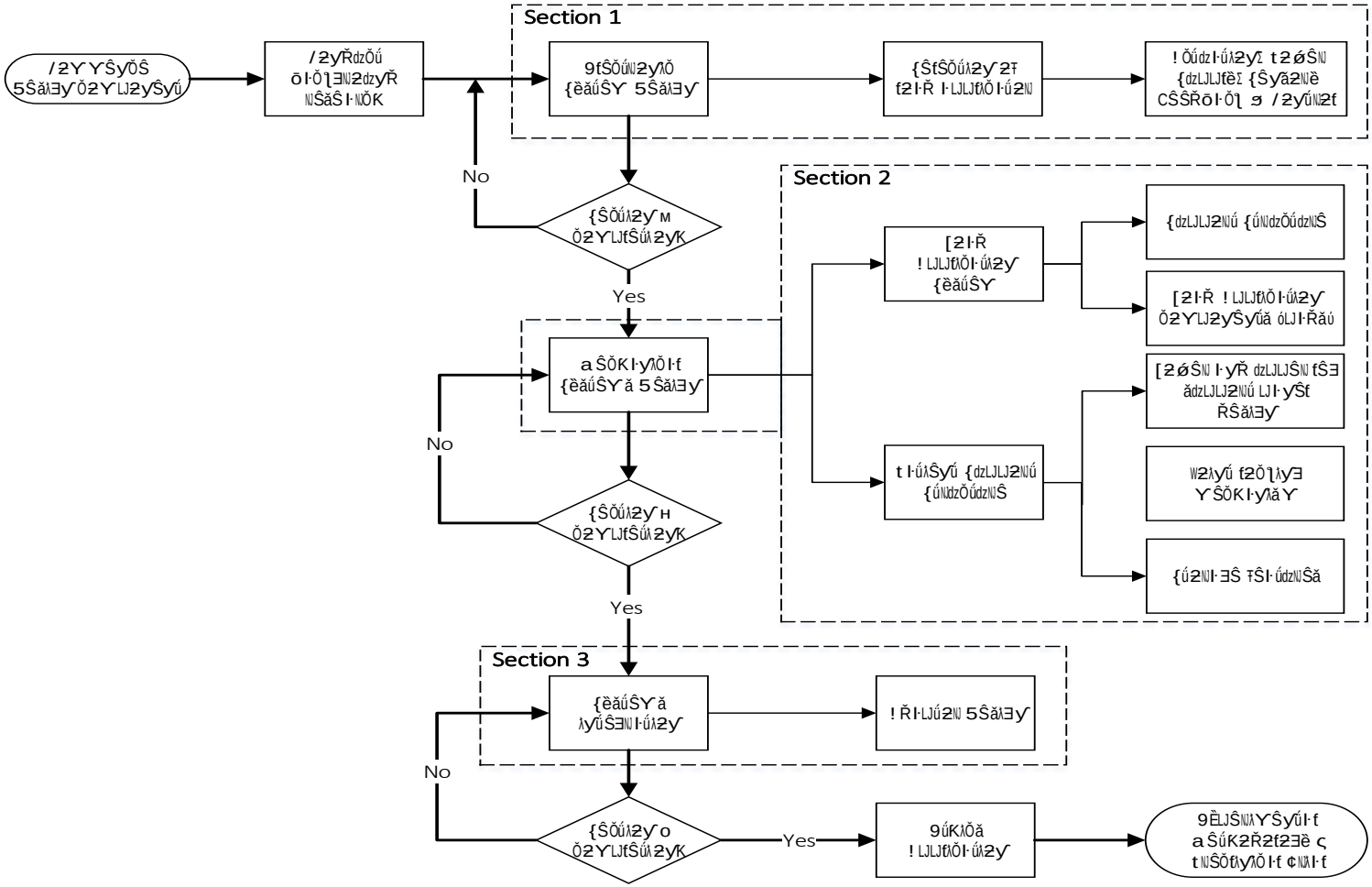

Figure 3.2: Flow Chart indicating the Design Methodology pathway.

3.3 Design Considerations

The framework of the existing Laxmeter Prototype One was designed to address the limitations of the current laxity measurement devices. However, the initial Prototype consisted of only the PSS and required further development (including the addition of the LAS). The aim of this study is to develop the Laxmeter to achieve multi-ligament laxity measurements by implementing the design objectives – Section 1.7 Research Objectives.

The design specifications for this study were identified according to the research objectives. The specifications were informed by the variability of patient requirements, clinical partner's input, material selection, patient ergonomics and Prototype One limitations. The design specifications were deduced according to the research objectives and are stated as follows:

I. Electromechanical LAS
    a. Electronic system requirements/ specifications
        i. Capable of applying a maximum pushing and pulling load of 250N.
        ii. Applying the load in increments of 25N (within a ±5N accuracy).
        iii. Pausing for approximately 30 seconds at every increment (for data collection purposes).

    b. Mechanical system requirements/ specifications
        i. Support the weight of the electronics system and the 250N load as well as the resulting reaction forces.
        ii. Account for human variation in lower leg diameter i.e. up to the 95th percentile.
        iii. Account for the future modifications of the PSS to integrate with the LAS.

II. PSS design requirements
    a. Allow AP and ML translation of the proximal lower leg.
    b. Make adequate design modifications for systems integration with the LAS mechanical system.
    c. Integrate a bone translation tracking system.
    d. Storability, portability and foldability, which enables quick and easy setup.

III. Integration design
    a. The design of an adaptor system to accomplish overall device assembly.

The Laxmeter is an assembly of two primary systems, the electromechanical LAS and the mechanical PSS, and their respective subsystems, shown in Figure 3.3. Each system would work in synergy to ensure that the Laxmeter functions efficiently and optimally. The subsystem approach enabled the design to more effectively meet the functional needs that were identified for the Laxmeter.

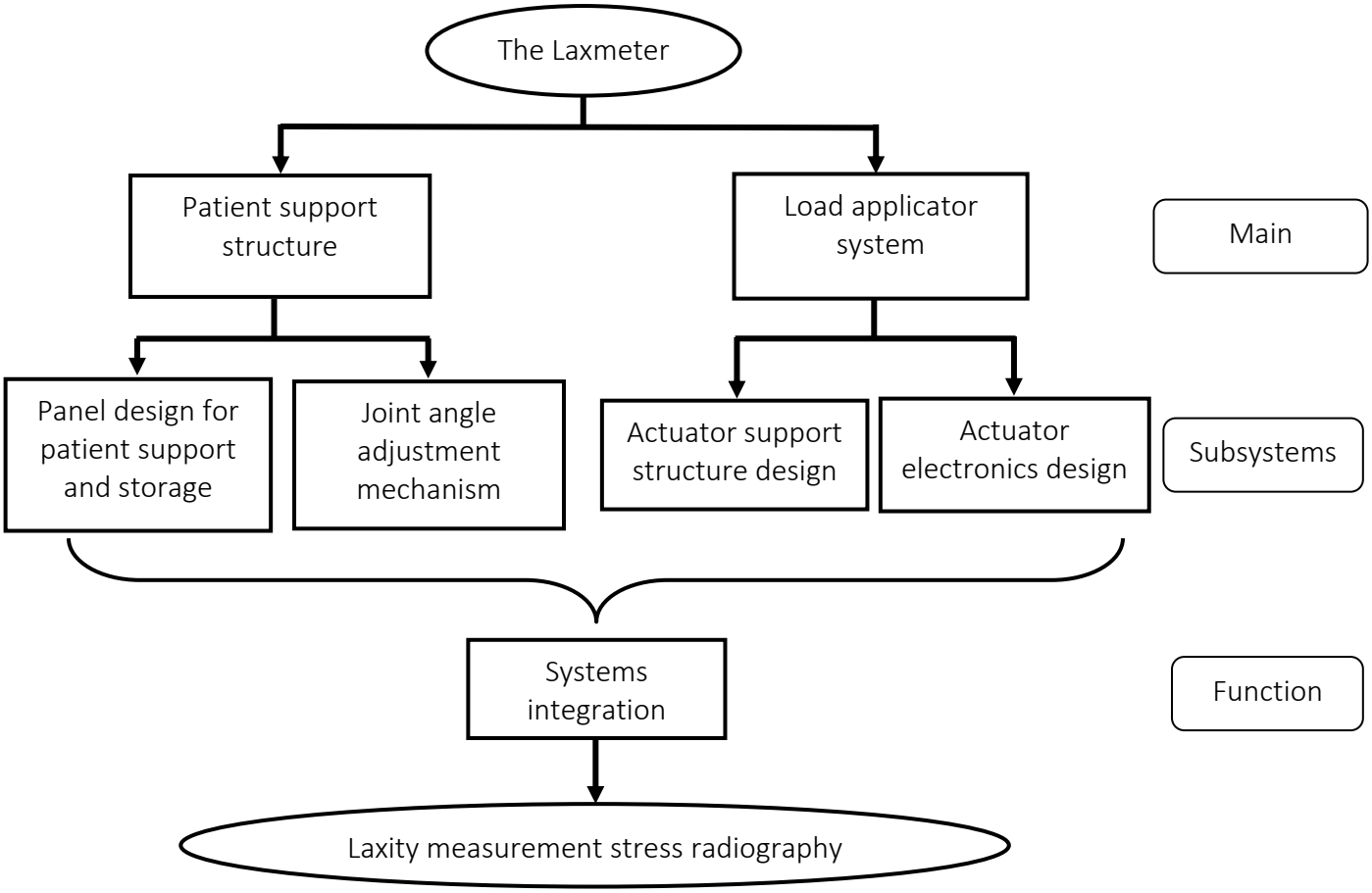

Figure 3.3: Design schematic of the Laxmeter design process.

Section I: Electronic System Design

The study requires an efficiently functioning electronics system for inducing accurate translation. The electronic system has specific requirements to ensure that the system functions efficiently and produces accurate readings. The electronic system controls the linear load actuator by means of a user interface. This section describes how the electronic system design considerations and requirements were achieved.

3.4 Actuation

The study requires a motorised actuation system designed to apply the required load to the proximal lower leg, to induce tibial translation. There are various actuation systems available, including pneumatic, hydraulic, electric and mechanical actuators, with the ability to produce linear, rotary and oscillating motions. The hydraulic and pneumatic actuators make use of fluids to induce a mechanical action. Electric actuators are powered by motors, thereby generating mechanical motion by converting electrical energy to torque. Mechanical actuators convert rotary motion to linear motion. The actuation required for this study would have the following primary requirements:

- Apply a maximum load of 250N (as specified in Section 2.1.2.2 Knee Joint and Ligament Biomechanics).
- Apply the load in increments of 25N (with an accuracy of ±5N).
- Lock at each increment for radiographic image capturing purposes.
- Induce tibial translation in a specified direction (AP and ML).

Secondary requirements would include affordability and compact systems configuration, allowing for portability. The actuator should be available locally, ensuring no delays in delivery of the product and readily available technical support (i.e. repair and replacement).

3.5 Power Supply

The power supply for this study would primarily depend on the requirements of the actuator selected. The power source required to supply the electronic system would need to meet the following considerations:

- Supply the appropriate voltage and current to all the electronic components i.e. the actuator, microcontroller (µC), driver and circuit operations.
- Mains power is suitable for the electromechanical system as it is readily available in the required clinical setting due to the use of a radiographic imaging modality (X-ray machine). This implies that the device would not need a portable power supply.

3.6 Sensory Feedback

The sensory feedback aspect of this study is one of the most crucial components of the electronic system. A set of load sensors is required to measure the load applied to the proximal lower leg. There are several existing sensors and electronic components capable of measuring the applied load; however, a cost-effective solution was selected for this study. The load sensors would be required to accurately measure loads (within a predetermined threshold) of up to 250N. The sensors would measure the load applied, presented on a visual display and recorded in relation to the amount of lower limb translation. Figure 3.4 illustrates the logic map of the load application process followed by this study.

The process of load application, as measured by the sensors and indicated by the visual display, will cease at a maximum load of 250N. Thereafter, the load will be removed from the participant's limb. Higher sensor accuracy, would ensure more reliable laxity measurement test results. An approximate degree of error may be included to account for sensor limiting factors such as noise, drift, hysteresis, repeatability and linearity error. In addition, application specific factors including the material considerations, the area of contact and the need for a robust design affects the accuracy of the sensors. A large factor that would require consideration, is the heat generated when applying the load, which would cause the sensor to drift, reducing the accuracy of the reading.

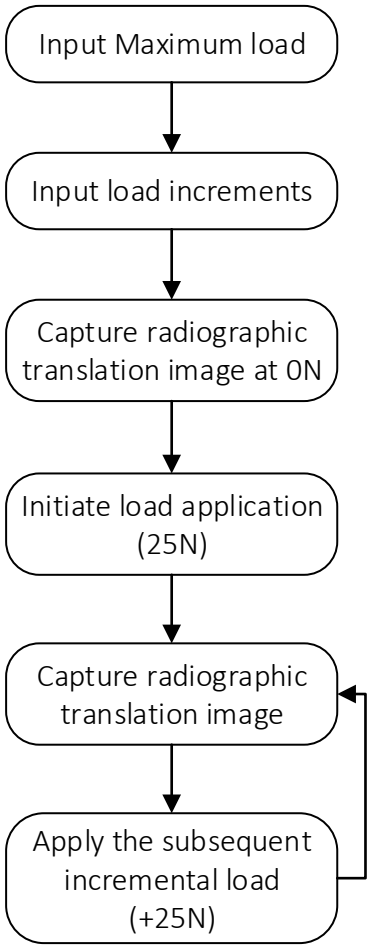

Figure 3.4: Logic diagram for the load application process.

3.7 Feedback Control

The µC is required to regulate the operations of the entire electronics system. Several popular µCs could be utilised for this study, including the Arduino, Raspberry Pi and BeagleBone. The selected µC would require a sufficient number of digital input and output ports, to manage the transfer of data to and from the various components. In addition to supplying power to the components, the µC is required to perform the following functions:

i. Facilitate the operation of a user interface with visual display.
ii. Process the necessary user input variables i.e. maximum load and increments.
iii. Provide control signals for actuator operation.
iv. Interpret the sensor input.
v. Facilitate the communication between the sensors and the actuator to apply the load within a predetermined thresh-hold.

Section II: Mechanical Systems Design

3.8 Load Application System

3.8.1 Introduction and Specifications

The mechanical aspect of the LAS supports and positions the load applicator during testing. The mechanical system for the LAS includes the orientation system needed to apply the required translation load to various aspects of the proximal lower leg. These aspects include the anterior (shin), posterior (calf), medial and lateral surfaces of the proximal lower leg. Design considerations for the mechanical system include a radiolucent structure to avoid interference during radiographic bone translation tracking and the manufacturing method of the various mechanical components.

3.8.2 Design Considerations and Concepts

3.8.2.1 Support Structure

Two design concepts were generated for the support structure of the LAS. These concepts incorporated general and study-specific design considerations as indicated in Table 3.1. Structural integrity, manufacturability and feasibility are general aspects of medical device design considered imperative, particularly with Frugal Biodesign whereby resources and facilities are limited. The weight and radiolucent considerations depend predominantly on the materials selected for manufacturing. Design considerations specific to this study, include the Bilateral Support Structure, AP and ML load application capabilities and the adaptor feature to allow for integration of the LAS with the PSS. The LAS support structure concepts incorporated the material dependant and general considerations, however, prioritised the design considerations specific to this study. Table 3.1 indicates what is considered a design specific consideration, a material specific consideration and a general consideration for the purposes of this study.

Table 3.1: Design considerations for mechanical support structure of the LAS.

Design Considerations	*Type of Consideration*
Bilateral support	Specific[ᵗ]
AP and ML load application ability	Specific[ᵗ]
Adaptor	Specific[ᵗ]
Radiolucency	Material dependent[ᵉ]
Weight	Material dependent[ᵉ]
Manufacturability	General[ᵩ]
Feasibility	General[ᵩ]
Structural integrity	General[ᵩ]

[ᵗ] Specific considerations are design aspects that pertain to this study.
[ᵉ] Material dependent considerations are a feature of the choice of material and its mechanical properties.
[ᵩ] General considerations are incorporated in the design of most, if not all, medical device products.

Concept 1: C-arm Support Structure

The first design concept for the LAS support structure was a C-arm mechanism. This concept was inspired by the operation of the Low Dosage X-ray (LODOX) scanner C-arm. The rotating C-arm allows for AP (90°) as well as lateral (0°) imaging of the subject. A similar design could be exploited to allow for AP and ML load application to the proximal lower leg. The C-arm LAS support structure (attached to the Lower leg support panel (LLSP)) positioned for (A) ML and (B) AP lower leg translation, is illustrated in Figure 3.5.

(A) (B)

Figure 3.5: Concept 1 - (A) The C-arm LAS support structure positioned for ML proximal lower leg translations and (B) the C-arm LAS support structure attached to the lower leg support panel positioned for AP proximal lower leg translation.

The image illustrates the C-arm LAS support structure in the ideation phase of this study. Image (A) shows the C-arm in position for ML proximal lower leg translation and image (B) illustrates the C-arm fitted to the LLSP and in the position for AP proximal lower leg translation. The C-arm structure would be attached to the lateral edge of the LLSP using pins or bolts. The actuator would rotate 90 degrees, within the body of the C-arm, allowing for AP and ML lower leg translation. Either a belt and pulley or a rack and pinion gearing system could rotate the arm within the body of the structure. The actuator would be imbedded in the arm. In addition, the actuator would apply the loads in both extension and contraction according to the required translation direction.

The C-arm support structure would be attached to the lateral edges of the LLSP with pins or bolts. A belt and pulley or rack and pinion mechanism would control the rotation of the arm within the body of the structure. The actuator would be embedded in the arm and rotate therewith. The concept features a complex design structure for the LAS support structure. A radiolucent structure is required for imaging purposes, which implies a construct manufactured from a polymer since some polymers have been found to be radiolucent (Beukes et al. 2017). The significant design challenges faced when developing a C-arm support structure of this nature were determined to be:

1. The actuator would require a stable and mechanically sound structure to support the application of a 250N load as well as the weight of the (potentially large) actuator.

2. Simplicity is a favourable design consideration, to achieve and ensure a minimum overall cost. The design of a C-arm support structure poses the potential for a complex design, eventually resulting in increased material and manufacturing costs.

Concept 2: Unilateral Support Structure

The unilateral load application support structure is a modification of a Bilateral Support Structure concept initially considered (described in Appendix A). This structure was developed to explore the advantages of unilateral laxity measurements. Resorting to a unilateral structure would result in a more lightweight and portable structure due to less material and components used. Furthermore, structural integrity would be more achievable with a more compact design, as compared to a Bilateral Support Structure. The unilateral support structure concept attached to the Laxmeter's lower leg support panel is illustrated in Figure 3.6.

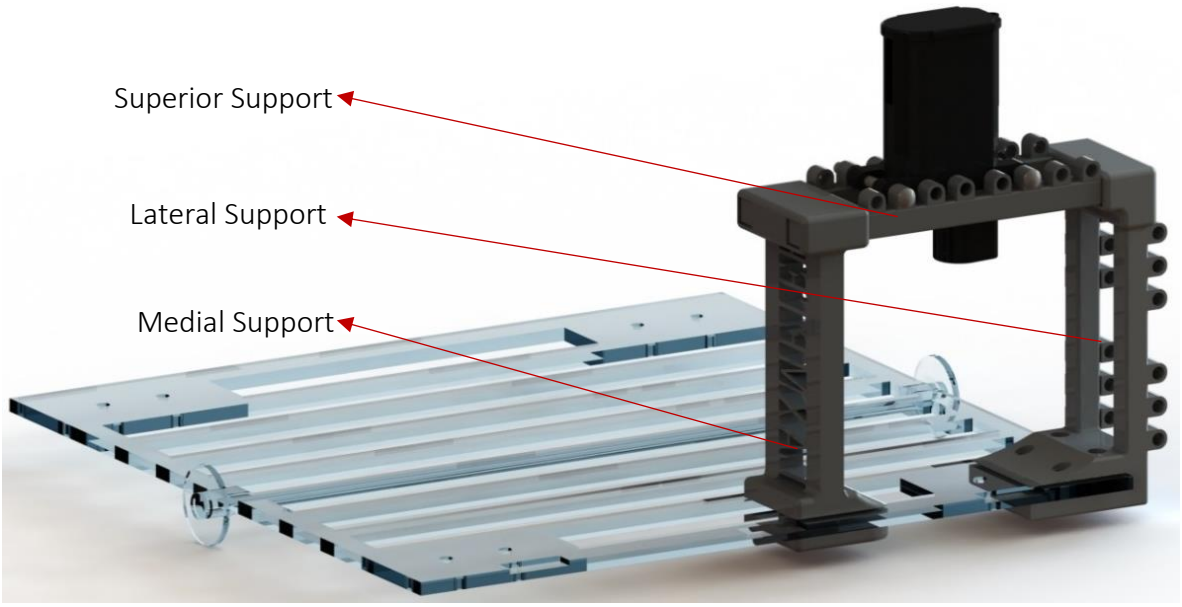

Figure 3.6: Unilateral LAS support structure (including the load applicator) attached to the Laxmeter's LLSP.

The image illustrates the unilateral LAS support structure in the ideation phase. The structure would span half the width of the Laxmeter and be fitted to the lower leg panel using pins or bolts. The load applicator would be attached to the lateral and superior supports of the unilateral support structure to induce AP and ML proximal lower leg translation. The unilateral support structure concept would be capable of inducing proximal lower leg translation of one limb. The structure would be removed and reassembly on the opposite side of the LLSP to compare both limb laxity results.

This concept investigates the advantages of a simpler and more compact design, in an attempt to ensure feasibility, affordability and structural integrity. The concept consists of three main elements: the lateral, medial and superior supports. This concept considered the way in which the load applicator would attach to the structure and accounted for human variation in femoral length and overall body width. This was achieved by allowing the actuator to translate both vertically and horizontally, along the lateral and superior supports. In addition, the concept considered the assembly of all three supports with a sleeve and cotter type joint mechanism. Finally, the concept would attach to the Laxmeter's LLSP by means of either pins or bolts.

Concept Selection – LAS Support Structure

The two LAS support structure concepts were rated according to the feasibility of the design. The criterion for evaluation was based on the design considerations and weighted according to their significance, subjectively. A necessary screening process was used (as indicated in Table 3.2) whereby, each concept was rated according to how best it met the weighted criterion. This process was used to filter out the most appropriate concept for the Laxmeter LAS support structure. A sample calculation of the total rating is provided below according to Eq. (3.1).

Table 3.2: LAS support structure concept selection.

Selection Criterion (weight)/ Concepts	*Radiolucent (3)*	*Structural integrity (3)*	*Manufacturability (3)*	*Weight (2)*	*Practicality (3)*	*Assembly (2)*	*Total*	*Rank*
1	3	1	1	1	1	1	22	2
2	2	3	3	3	3	3	45	1

Sample calculation: The total score for Concept 1 was calculated as follows:

$$Total = \sum(Criterion\ weight\ \times\ rating) \tag{3.1}$$

$$= (3 \times 3) + (3 \times 1) + (3 \times 1) + (2 \times 1) + (3 \times 1) + (2 \times 1)$$

$$= 22$$

Based on the results as indicated in Table 3.2, Concept 2 was ranked the most feasible design for the development of the LAS support structure. The final design outcome is documented in Section 4.4 The Laxmeter.

3.8.2.2 Load Application Components

The point/ area of contact between the LAS and the participant would need to be monitored to provide a feedback in the form of a load reading. Load sensors would need to be mounted onto the contact points to provide the required applied load reading. Various load sensor technologies exist, and therefore, an appropriate sensor would need to be selected according to feasibility and availability.

A load applying force-sensing pad (FSP) on either side of the proximal lower leg would be an ideal means of applying bidirectional loads, thereby inducing AP and ML translation. The FSPs would need sufficient surface area to allow for the mounting of the load sensors. In addition, the LAPs would need to be a simple design to allow for ease of manufacturing. However, the material for manufacturing would be a crucial design consideration as this would affect the load readings. The material selection process would take into consideration the sensors that would be used to measure the load applied to the proximal lower leg. The way in which the senor measures the load applied would require specific material properties.

3.9 Patient Support Structure

3.9.1 Introduction

The Laxmeter PSS consists of a configuration of panels assembled by hinges, aimed at creating the ideal laxity measurement testing conditions. Figure 3.7 illustrates the patient positioned on the PSS, whereby the lower leg is rested on top of the LLSP. The upper leg and the distal end of the lower leg require securing, thereby eliminating unwanted lower limb displacement and restricting translation to the proximal lower leg. Each panel is designed with specific features to ensure efficient and accurate laxity.

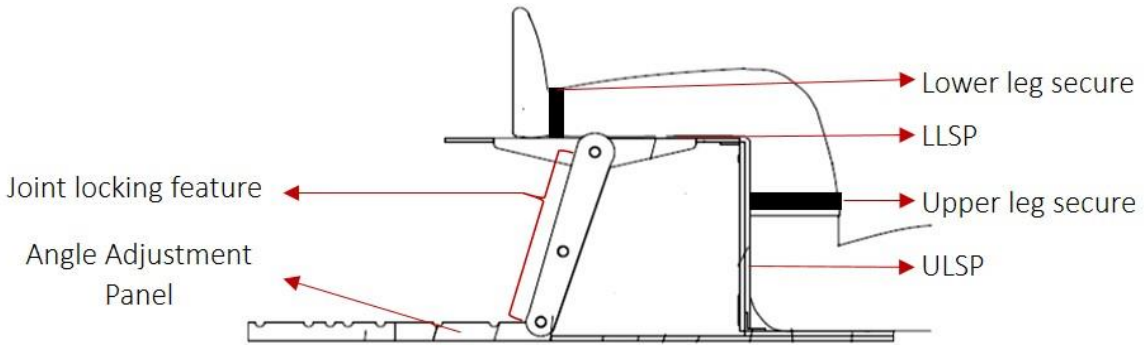

Figure 3.7: Ideal patient position as provided by the Laxmeter PSS for laxity measurement procedures (Image credit: (Sivarasu and Patnaik 2014b)).

3.9.2 Lower Leg Support Panel

The LLSP design requires various modifications (to the original Laxmeter, according to Sivarasu and Patnaik (2014b)) for multi-ligament laxity measurement procedures. The panel is the central point for the Laxmeter's laxity measurement procedures. The design considerations for the LLSP are as follows:

- Sufficient structural integrity to support the lower leg
- Secure the distal lower leg
- Allow for attachment of the LAS
- Track AP and ML proximal lower leg translation
- Allow for radiographic imaging of bone translation (radiolucency)

The LLSP requires sufficient structural integrity to support the lower leg weight of a patient whose size is above average. Anthropometrics will be considered to design an appropriate panel. The panel would require a means of preventing ML translation of the distal lower leg during collateral ligament laxity measurements and preventing anterior translation during ACL laxity measurement tests. The translational load is applied to aspects of the proximal lower leg, and therefore, the LAS would need to be attached to the LLSP. Limited information is available outlining a reliable means of tracking ML bone translation. Therefore, the design of the LLSP would need to incorporate an efficient and accurate bone translation tracking system. Lastly, the LLSP construct should not interfere with the radiographic image produced when capturing the bone translation. Therefore, a radiolucent structure is required, allowing the X-rays to sufficiently penetrate the panel and allow for a high-quality undistorted X-ray image.

3.9.3 Upper Leg Support Panel

The upper leg support panel (ULSP) is adjacent to the LLSP (as indicated in Figure 3.7) and connected by a configuration of hinges. The intersection between the two panels creates the angle of knee flexion required for that specific laxity measurement test (as elaborated in Section 3.9.4 Joint Locking Feature). The ULSP features work in conjunction with those of the LLSP to ensure accurate and reproducible laxity measurement results. The ULSP has the following features:

- Provides upper leg support
- Secures the upper leg
- Provide windows for non-tested limb

Upon placing a patient onto the PSS, the ULSP should remain parallel and in contact with the upper leg (thigh). The panel's primary purpose is to support the upper limb and secure it at angles of knee flexion greater than and equal to 90°. The angle between the ULSP and LLSP provides for the required knee joint flexion angle. The ULSP should incorporate a means of securing the upper leg to prevent femoral translation during the procedure.

Note that the simultaneous elevation of both legs can be found to be awkward and results in women experiencing immense discomfort. This position (as indicated in Figure 3.8) results in potential skin exposure of the thigh region, which is regarded as social taboo amongst more conservative populations (Sivarasu and Patnaik 2014b). As a result, windows or openings should be incorporated into the panel design.

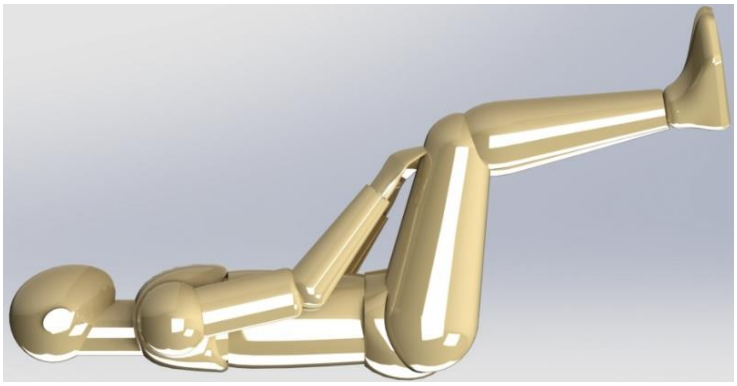

Figure 3.8: Position regarded taboo for conservative women (2014) (Image credit: (GrabCAD 2017)).

Femoral length variation was considered a secondary feature and would be accommodated for, by elevating the subject's pelvis using Plexiglas® sheets of various thicknesses (if short) and the height adjustment feature of the LAS (if long).

3.9.4 Joint Locking Feature

3.9.4.1 Introduction

The joint locking feature is an essential component in the function of the Laxmeter. The feature is a novel innovation in knee joint laxity measurement devices. Existing devices focus on measuring the laxity of the knee joint ligaments at one specific angle. The Laxmeter would allow for the measurement of ACL, PCL, MCL and LCL laxities at multiple, predefined, degrees of flexion. The feature would incorporate the following considerations:

- A selection of knee joint flexion angles
- A stable construct with sufficient integrity
- A simplistic design

Two concepts were considered for the joint locking feature. Both incorporated the above-mentioned considerations, focussing on the number of joint angles and producing a structurally sound device. However, the simplistic design consideration proved to be the deciding factor, due to available time, manufacturing and monetary resources.

3.9.4.2 Design Concepts

Concept I: A Modified Scissor Jack

The Scissor Jack is a traditional mechanism used to raise a range of objects including motor vehicles and large crates. The concept makes use of a four-bar linkage system and a lead screw mechanism to lift the object from the surface of elevation. The use of a lead screw allows for controlled and intricate height adjustment. Figure 3.9 illustrates a Scissor Jack, designed for the Laxmeter's joint locking feature, incorporating a four-bar linkage system and a lead screw mechanism.

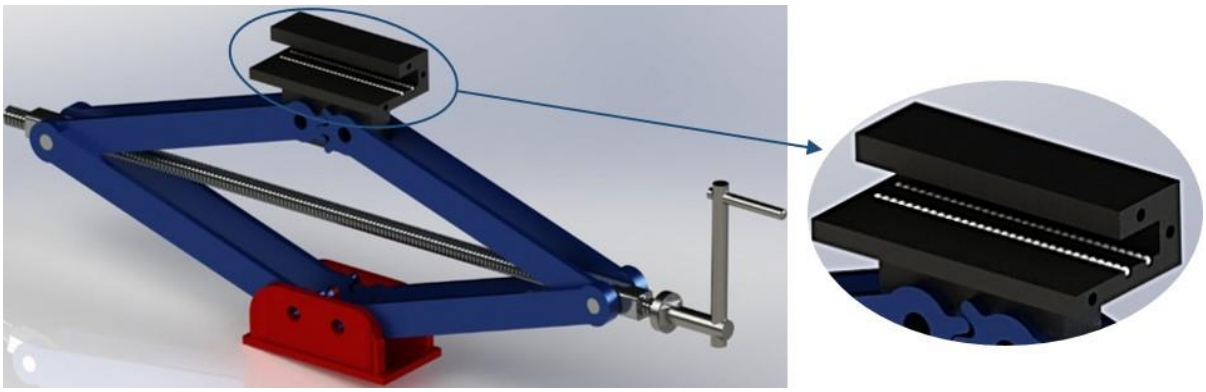

Figure 3.9: Four-bar linkage system Scissor Jack with lead screw height adjustment mechanism designed for the joint locking feature, highlighting the specialised linear ball bearings.

The image shows the joint locking feature Scissor Jack concept, which makes use of a crank to rotate a lead screw connecting the two lateral intersections of the jack. The rotation of the lead screw due to the applied torque results in the inward translation of the two most lateral connections. This inward translation results in the elevation of the LLSP.

This concept would make use of two Scissor Jacks to elevate the LLSP to a specified height and, thereby, adjust the knee joint angle. The use of two Scissor Jacks (located on either side of the PSS) would be required to ensure the sound stability of the PSS. The base plate of the Scissor Jack would be fitted to the Angle Adjustment Panel. As the height of the jack is adjusted, thereby elevating the LLSP, the jack's upper pad will slide along the length of the LLSP, using specialised linear motion ball bearings (as illustrated in Figure 3.9). This will ensure that the LLSP maintains a horizontal configuration, relative to the X-ray bed, at all angles of knee joint flexion. The concept allows for finer increments of knee flexion, allowing the operator a wider range or increased specificity of knee joint angles for laxity measurement testing. The use of such a scissor jack mechanism for LLSP elevation purposes would be an ideal means of achieving the required knee joint flexion angle.

However, including the Scissor Jack concept into the Laxmeter design, from a whole device perspective, would increase complexity and cost. Furthermore, the time for manufacture of two large scale, radiolucent and structurally sound modified jacks would be extensive due to the intricacy of the design.

Concept II: The Parallel Supports

The Parallel Supports concept consists of two arms located on either side of the PSS and is an adaptation of the mechanism described by Sivarasu and Patnaik (2014b). As illustrated in Figure 3.10, the superior end of each arm pivots about the centre of the LLSP's lateral edge and the inferior ends engage in selected notches located on the Angle Adjustment Panel. Each notch corresponds to a specific degree of LLSP elevation and as a result a specific angle of knee joint flexion. To achieve the required angle of knee joint flexion, a locking mechanism will be required to securely maintain the horizontal configuration of the LLSP and the selected knee joint flexion angle. The concept would incorporate all design considerations as indicated in Section 3.9.4.1 Introduction. The concept is simplistic in design, suitably elevates and supports the LLSP and allows for a selection of knee joint flexion angles. The concept embodies all three primary design considerations for the joint locking feature. Secondary considerations include manufacturability of each part and cost effectiveness. Figure 3.10 illustrates the use of a Parallel Supports concept for elevating an LLSP like panel.

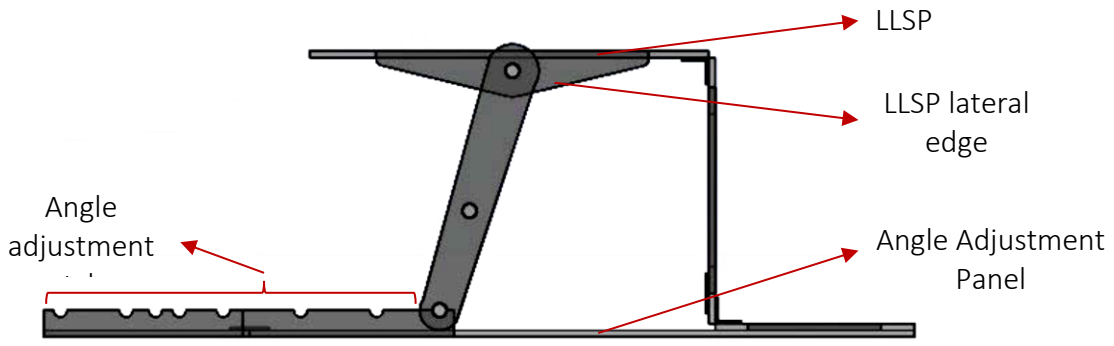

Figure 3.10: Parallel support concept for the joint locking feature (Image credit: (Sivarasu and Patnaik 2014b)).

The image illustrates the joint locking feature Parallel Supports concept currently being implemented by the existing Laxmeter Prototype. The supports are used to adjust the LLSP to ULSP angle, while maintaining a horizontal LLSP configuration, engage with a select angle adjustment notch corresponding to a particular knee joint flexion angle and support the loads experienced by the LLSP.

Concept Selection: Joint Locking Feature

The basis of the joint locking feature concept selection is manufacturing time, complexity and as a result cost effectiveness. The Parallel Supports concept would be easier to manufacture. The Scissor Jack concept would need complex machining whereas the parallel support mechanism could potentially be laser cut in a matter of minutes. Therefore, Concept II: The Parallel Supports would be considered for further development.

3.9.5 Storage Considerations

One of the primary functions of the PSS is to provide the ideal ergonomic patient position for knee joint laxity measurements. This is achieved by placing the patient's lower extremities onto the device and conducting the laxity measurement tests. This implies that, to support the weight of an overweight patient, the structure would need to be large and structurally rigid. In addition, the need for a radiolucent structure implies the need for thicker panels or additional structural supports, which adds to the weight of the device.

The primary consideration regarding storage features, is the device's ability to fold up into a compact configuration of the panels. This feature would contribute to the device's transport and storage capabilities. The panels and hinges would need to be designed and configured to allow for convenient and straightforward storage as well as setup. Current devices are compact and therefore convenient to handle and store away. Therefore, it is essential for the Laxmeter to incorporate storage features to make an effective impact on the market.

Section III: Systems Integration

3.10 Adaptor Design

Integrating the LAS and the PSS is a key feature of the Laxmeter design. The medial, lateral and superior supports of the LAS support structure, and the LLSP, will be designed for integration of the two systems. The adaptor design would require the following considerations to be met:

- Ease of integration
- Maintain a lightweight system

Ease of integration or assembly of the two systems is crucial to allow for the efficient use of time when carry out a laxity measurement testing procedure. An easy assembly process is preferred, allowing the user more time for laxity measurement testing and results processing. An arduous assembly process would result in the user being unwilling to use or even purchase the device. The use of additional components to allow for systems integration would impact the overall weight consideration. Maintaining a lightweight structure is an essential overall design requirement for the Laxmeter. The adapter design allows for the assembly of the entire Laxmeter device, producing a fully functional multi-ligament laxity measurement stress radiography device.

4 Design Outcomes

4.1 Load Application System

4.1.1 Electronics Design

The electronics system design and development is outlined in this section of the study. The electronic system components required for the LAS consist of an actuator, microcontroller, LCD, power supply, interfacing circuitry and a motor driver circuit. The selection and implementation of these components are discussed below as well as the electronic system operations.

4.1.1.1 Actuator Selection

The actuator selected for this study would require the following functional specifications, derived from the overall study objectives:

I. Apply a load of 250 Newtons (N)
II. Apply the load in a linear motion
III. Apply the load in extension and retraction
IV. Apply 25N incremental loads in the range of 0N to 250N, with a ±5N accuracy
V. Compact for storage and LAS integration purposes

The actuator selected was the SKF® CAHB-10, ACME (screw), Electric Linear Actuator (as shown in Figure 4.1). A variety of CAHB-10 direct current (DC) actuators are available with varying stroke lengths (50mm to 300mm), voltage (V) requirements (12 or 24 V) and maximum applied loads (120N to 1000 N).

The CAHB-10 12V, 500N, 100mm stroke actuator was selected for the LAS. This actuator meets the requirements of this study i.e. applying a 250N linear load, in increments of 25N in both extension and retraction. Additionally, a 100mm stroke length was considered a compact option that allows for storability, transportability and ease of integration with the LAS support structure.

Figure 4.1: The SKF CAHB-10, ACME Screw, DC Electric Linear Actuator utilised for application of the incremental loads to the various aspects of the proximal lower leg (image credit: (SKF 2013)).

The image illustrates the SKF CAHB-10 Electric Linear Actuator selected as the linear actuator for the LAS.

The 12V actuator was selected for the LAS as it allows for an increased current range (0.8-3 amperes) when compared to the 24V actuator (0.48-1.8 amperes), as indicated in Figure 4.2. The wider operational current range allows for easier control of the actuator in the relatively small operating range of 0-250N. The 500N actuator was selected to ensure the 250N specification was met while maintaining safe operational conditions.

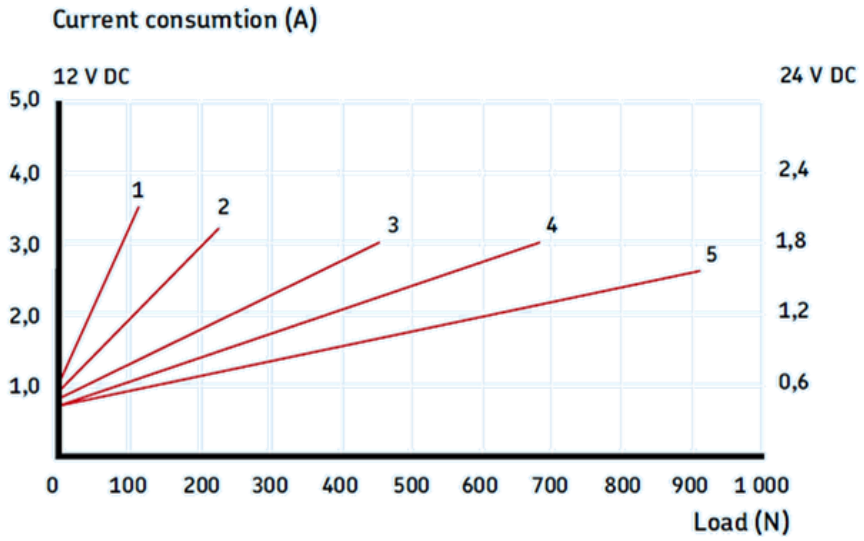

Figure 4.2: The current-load plots for various 12V (left) and 24V (right) SKF CAHB-10, ACME (Screw), DC Electric Linear Actuators.

The image illustrates the graphical curves (1-5) indicating the maximum loads applicable by the several SKF CAHB-10 ACME, DC Electric Linear Actuators available and the amount of operational current required to apply a particular load, distinguishing between the 12V and 24V models. For example, curve 3 (the selected actuator) can apply a maximum load of approximately 450N and operates within a current range of 0.8-3A for the 12V model and 0.48-1.8A for the 24V model.

The CAHB-10 actuator is controlled by regulating the input operational current to achieve a specified load. The 500N actuator (Curve 3 in Figure 4.2) has a current range of approximately 0.8-3 Amperes (A) for the 12V model and 0.5-1.8A for the 24V model. The 12V actuator model allows for a greater operational current range, thereby allowing for better control, particularly considering the need to apply the load in 25N increments for data collection and graphical representation purposes.

In addition, the CAHB-10 linear actuator features a self-locking mechanism which prevents motor failure as a result of applying a specified load for too long a period. This feature is particularly attractive for the application of incremental loads. The actuator applies a set load, locks in position and switches off the motor. This provides the operator with sufficient time to capture and store a radiographic image of the translation result. The self-locking feature eliminates the concern of motor failure due to the time delay. The actuator is designed to be maintenance free, reliable, dust and shock resistant as well as lightweight (RScomponets 2017).

The 100mm stroke length specification was selected considering the 95th percentile male calf diameter in conjunction with the LAS structural design (further elaborated upon in Section 4.1.2.2 Anthropometric Study). The distance from the LLSP and the superior support of the LAS support structure, with the inclusion of a 95th percentile male calf diameter, would accommodate for a 100mm stroke actuator. A 200mm stroke CAHB-10 actuator was considered too large, as the overall retracted length would be 345mm. The retracted length of the 100mm stroke actuator is 243mm.

4.1.1.2 Microcontroller and Display

An Arduino Uno R3 microcontroller (µC) development board (as illustrated in Figure 4.3) was selected to perform the processing functions to operate the LAS. The µC has sufficient processing specifications regarding clock speed, flash memory and RAM (Random Access Memory) for the LAS operation software. Additionally, the µC has sufficient input and output pins for the circuitry including a Pulse Width Modulation output pin to control the actuator. The full specifications of the µC can be found in Appendix B.

Figure 4.3: The Arduino Uno R3 microcontroller development board used to perform the operations of the LAS (image credit: (Arduino 2017)).

The ITead LCD1602 Key Shield 1.0 display (as illustrated in Figure 4.4), developed for the Arduino Uno, was found to be suitable for displaying the load readings produced by the load sensors and allowing the operator control of the actuator and the loads applied. The Shield features a built-in six button interfaces as indicated in Figure 4.4, which allows the operator to:

B1. Initiate the testing sequence and apply the subsequent load
B2. Manual actuator retraction
B3. Zero the posterior-medial force sensor
B4. Zero the anterior-lateral force sensor
B5. Manual actuator extension
B6. Reset the test sequence once completed

Figure 4.4: LCD1602 Key Shield 1.0 display developed by ITEAD STUDIO.

The image illustrates the LCD1602 Key Shield 1.0 display used to display and control the operations of the LAS.

4.1.1.3 Power Supply

A sufficient power supply unit (PSU) was required for the Laxmeter's LAS electronics. The power supply is needed to power the microcontroller, LCD display, motor driver and linear actuator. The maximum voltage, current and power requirement of all primary circuitry components are indicated in Table 4.1.

Table 4.1: Maximum operating voltage, current and power required by the primary circuitry components.

Components	*Maximum voltage (V)*	*Maximum current (A)*	*Maximum power (W)*
µC	20	0.8	2.2
LCD	5.5	0.04	0.22
Driver	46V (operating supply)	4	25
Actuator	12	3.2	N/A

The component requiring the largest operating voltage is the actuator. The linear actuator requires 12V and a maximum of 3A for operation. The µC needs 5V for operation, which is derived from the NCP1117 5V regulator on the Arduino Uno development board. The LAS electronics were supplied with power from a 12V 5A AC-DC PSU adaptor which provided sufficient current for all electronic components. The addition of a 1Ω 5-Watt (W) sensitivity resistor was incorporated into the circuit to measure, display and regulate the current being drawn by the actuator motor. This was a safety provision integrated into the system to prevent damaging the linear actuator, as the 5A current supply exceeded the maximum allowable actuator current.

4.1.1.4 Motor Driver Selection

The motor driver is required to control the extension and retraction of the linear actuator for load application. The selection and implementation of the primary electronic components as well as the electronic system operations are discussed below.

The linear actuator identified and selected in Section 4.1.1.1 Actuator Selection can apply the 250N load bi-directionally. The polarity of the voltage supplied to the actuator would need to be switched to achieve this bidirectional function. An H-bridge motor driver provides this functionality with 5V logic inputs which are well-suited to the Arduino Uno. An L298N Dual H-bridge Motor Control Driver was selected to drive the linear actuator. Note, only one full H-bridge unit is used for the LAS. The pin connection schematic of the L298N Driver is illustrated in Figure 4.5.

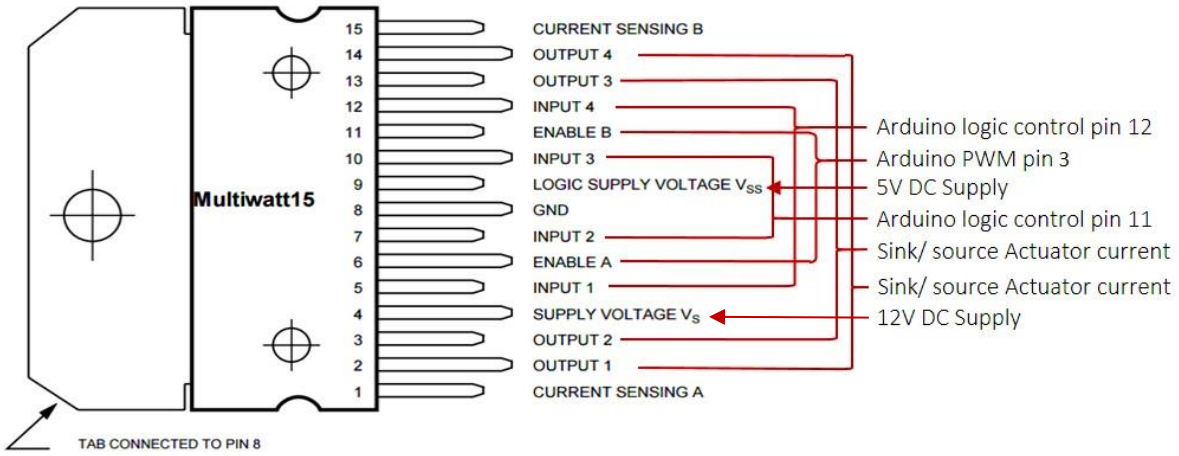

Figure 4.5: L298N Dual H-bridge Motor Control Driver pin connections (Image credit: (STMicroelectronics 2000)).

The illustration indicates the connections of the L298N motor driver to the primary components of the LAS.

The 12V, 5A PSU was connected to the L298N Driver as well as to the µC. The L298N requires a 5V input power supply for the internal logic; thus, an L7805 voltage regulator circuit (shown in Figure 4.6) was connected to the logic supply voltage pin V_{ss} (pin 9) on the L298N Driver. Additional components included four Schottky diodes to regulate the bidirectional translation and light emitting diodes to visually signal the circuit power status (red), actuator extension (green) and actuator retraction (red). Figure 4.6 shows the circuit diagram used to achieve bidirectional translation of the linear actuator.

Figure 4.7 illustrates the physically built circuit to control the bidirectional translation of the actuator. The L298N Dual H-bridge Motor Control Driver, L7805 5V voltage regulator, linear actuator connection and PSU socket are indicated in Figure 4.7. A heat sink was attached to the L298N Driver to absorb and dissipate the excessive heat generated during laxity measurement procedures.

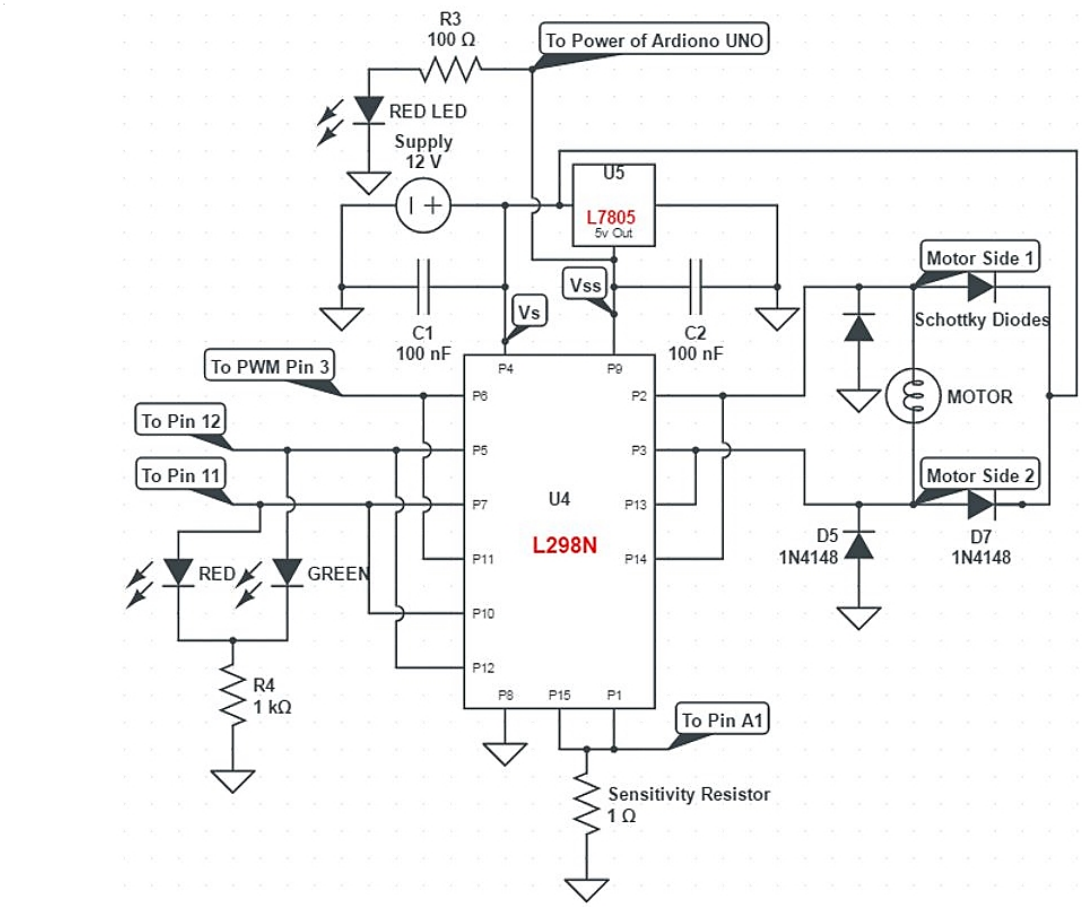

Figure 4.6: Circuit diagram of components used to regulate the bidirectional translation.

The image shows the motor driver circuit diagram, indicating the primary components used for bidirectional translation of the linear actuator. The primary circuitry components include an L298N Dual H-bridge Motor Driver, an L7805 voltage regulator, a linear actuator motor, the Arduino Uno and several additional electronic interfacing components.

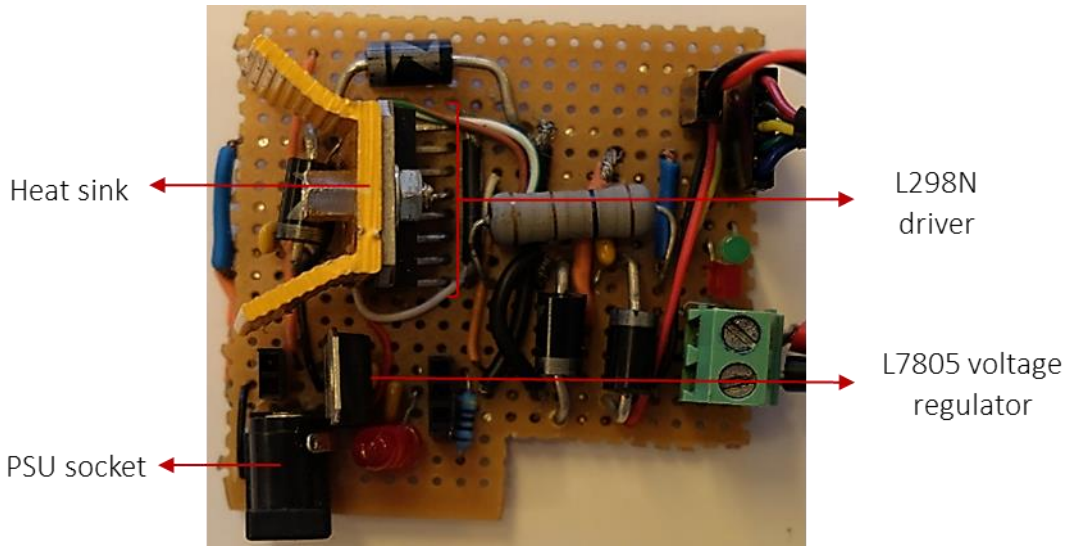

Figure 4.7: The Motor Driver circuitry built to control the bidirectional translation of the linear actuator.

4.1.1.5 Force Feedback

The LAS required a means of accurately measuring the load applied to the proximal lower leg, considering the FSPs detailed in Section 4.1.2.4 Force-Sensing Pads, developed to interface with the patient's lower limb. A strain gauge amplifier circuit was selected as an appropriate means of measuring the applied load. A full Wheatstone bridge strain gauge configuration was used to measure the strain experienced by each FSP during loading, and convert it to an equivalent load (Newtons) reading displayed on the LCD1602 Key Shield display. The full Wheatstone bridge consisted of two primary strain gauges placed on the non-contact surface of each pad and positioned in the centre and parallel to the length of the pad, which measured the strain due to the load applied. The full Wheatstone bridge was completed by two auxiliary "dummy" strain gauges. These auxiliary gauges were positioned perpendicular to the primary gauges and served the function of accounting for heat fluctuations during laxity measurements. Figure 4.8 illustrates the configuration of the strain gauge sensors on (A) the posterior-medial and (B) the anterior-lateral FSPs.

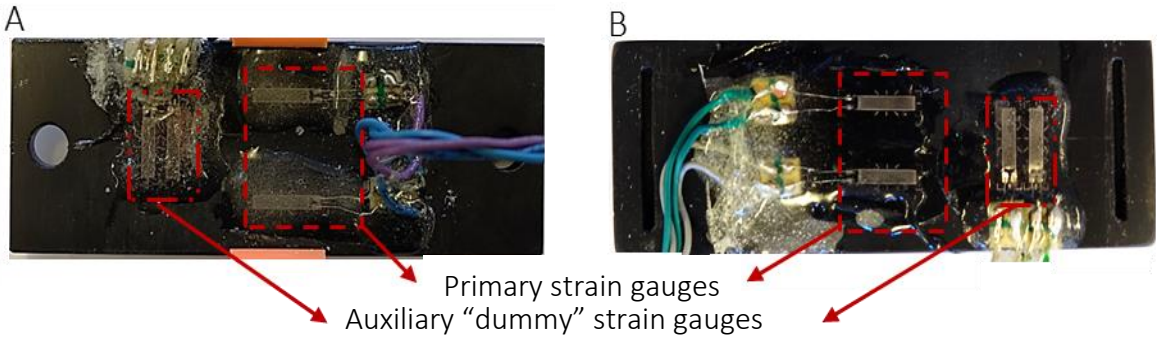

Figure 4.8: Strain gauge configuration on the non-contact surfaces of (A) the posterior-medial and (B) anterior-lateral FSPs.

The image illustrates the strain gauge (force sensor) configuration on the FSPs. The primary strain gauges are placed in the centre of the FSPs, parallel to the length of the pads. The function of the primary gauges is to measure the strain during the laxity measurement procedures. The auxiliary 'dummy' strain gauges compensate for the heat generated during laxity measurement procedures to improve the stability and the accuracy of the force readings.

The Wheatstone bridge was connected to an AD8223 instrumentation amplifier (as illustrated in Figure 4.9) to amplify the changes in resistance measured by the strain gauges. The gain would be set by a variable resistor (POT shown in Figure 4.9) which was calibrated to maximise the measured output range across 0-250N. Since the Arduino operates using a single supply (+5V), the measured signal from the Wheatstone bridge would need to be biased by 2.5V to account for changes in applied force direction. The instrumentation amplifier would be fed a reference bias voltage of 2.5V from a unity gain circuit connected to a voltage divider and supplied with 5V as shown in Figure 4.9. The strain gauge amplifier circuit measurement result output would, thereafter, be fed to the Arduino analogue inputs, which would be converted using an Analogue to Digital Converter (ADC) value- Newton transfer function (detailed in Section 4.1.1.6 Calibration Procedure) before it is relayed to the LCD.

Figure 4.9 illustrates the strain gauge amplification circuit diagram for measuring the load applied to the patient's lower limb. Two strain gauge amplification circuits were built, one for each of the FSPs. Figure 4.10 illustrates the end product of the Laxmeter's strain gauges amplification circuit.

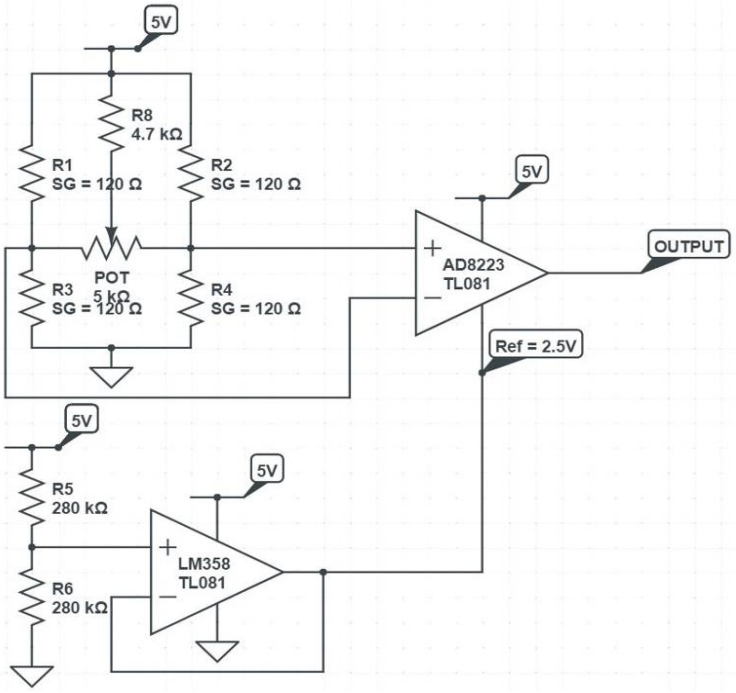

Figure 4.9: Strain gauge amplification circuit for measuring the load applied by the LAS.

The image shows the strain gauge amplification circuit for measuring the load applied by the actuator. The circuit makes use of a full Wheatstone bridge configuration to measure the strain experienced by the FSPs. Two primary strain gauges were configured to measure the strain applied and two auxiliary gauges compensated for the heat fluctuations on the pads, thereby improving the measurement accuracy.

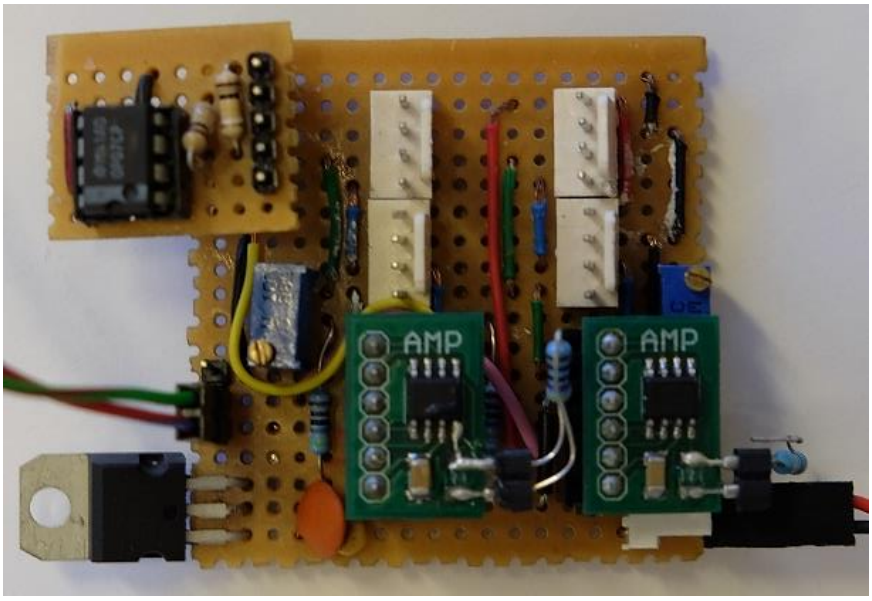

Figure 4.10: The physically built strain gauge amplification circuit to measure the loads applied to the proximal lower leg.

4.1.1.6 Calibration Procedure

The calibration process involved loading the FSPs from 0N to 250N in 25N increments to obtain sufficient data points to produce a Force to ADC value curve, from which the transfer function was derived. The posterior-lateral and anterior-medial FSPs were mounted onto an Instron 3365 Dual Column Universal Testing Machine (as illustrated in Figure 4.11), which applied the 25N incremental loads to the FSPs. At each Instron force reading, the ADC value was read from the LCD and recorded. The Instron force versus ADC value readings were used to plot the near linear graphs shown in Figure 4.12.

Figure 4.11: The anterior-lateral FSP mounted onto the Instron 3365 Dual Column Universal Testing Machine for calibration.

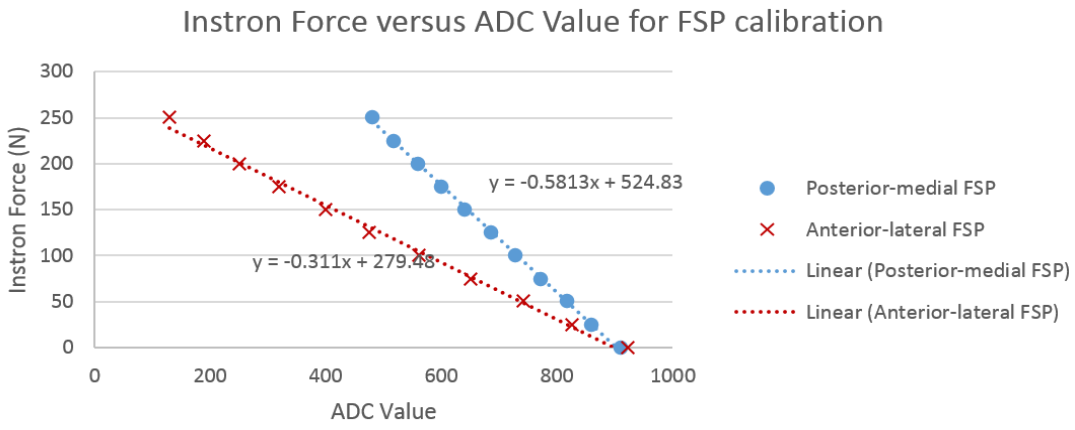

Figure 4.12: Near linear graph for the FSPs, obtained during the calibration procedure.

The image illustrates the near linear graphs obtained by recording the ADC readings produced by the strain gauges at each Instron incremental load applied. The gradients of these curves were used to compute the transfer function needed to convert the strain gauge amplifier voltage readings into Newton readings.

The gradients of the graphs were integrated into the transfer function, which converted the ADC readings to force readings in Newtons. The transfer function equation variables differed for each FSP. The ADC - Force transfer function equations is indicated by Eq. (4.1).

$$Force = (ADC\ value - rest\ reading) \times (graph\ gradient) \times (correction\ factor) \quad (4.1)$$

4.1.2 Mechanical Design

Section 3.8.2.1 Support Structure outlined the process carried out to select the appropriate mechanical structure used to support the actuator and allow for multi-directional load application. The concept selection process filtered out Concept 2: Unilateral support structure as the most feasible concept for the Laxmeter's LAS. The concept was further developed to produce the final iteration, addressing the drawbacks of the initial iteration. The structural features were designed to achieve the following:

1. A symmetrical and aesthetically appealing design
2. Accommodate the size and weight of the linear actuator
3. Adaptor component to attach the linear actuator to the LAS support structure
4. Height and width of the support structure to accommodate human variation in proximal lower leg (calf) diameter
5. Adaptor design for the fitment of the LAS to the Laxmeter PSS

4.1.2.1 Load Application System Concept Development

The final iteration of the LAS support structure embodied aesthetic appeal, structural integrity, affordability, durability, symmetry and simplicity. The design was carried out on SolidWorks (a 3D CAD and computer-aided engineering software) to investigate the functionality of the structure. The structure consists of three supports (superior, medial and lateral) as well as the actuator housing; all manufactured from cast Nylon. Cast Nylon possesses adequate mechanical strength properties, is locally available (in Cape Town, South Africa), machinable and cost effective. The three supports make up the LAS support structure whereas the actuator housing allows for the attachment of the linear actuator to the support structure. Figure 4.13 illustrates the mechanical component assembly of the Laxmeter's LAS, whereby the actuator, contained within the housing, is attached to the lateral support of the support structure. The FSPs (detailed in Section 4.1.2.4 Force-Sensing Pads) are fitted to the end of the linear actuator.

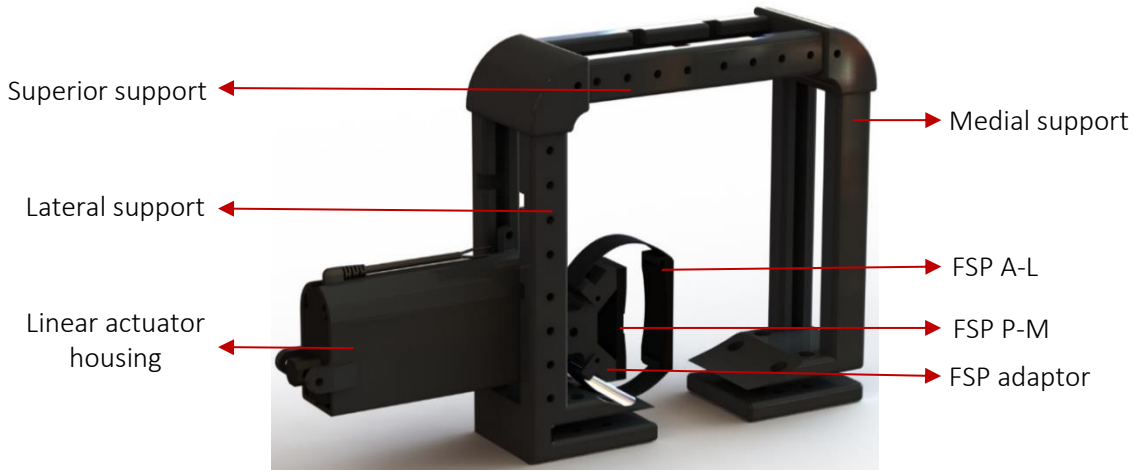

Figure 4.13: The fully assembled LAS including the support structure, the linear actuator contained within the actuator housing and the FSPs (anterior-lateral and posterior-medial).

The image illustrates the LAS assembly used to induce tibial translation by applying a 250N load to the proximal lower leg. The assembly consists of the support structure (medial, lateral and superior), the actuator housing, the FSP (push and pull) as well as the FSP adaptor.

4.1.2.2 Anthropometric Study

To establish the overall dimensions of the LAS support structure, the relevant anthropometric lower limb features of the 95th percentile male were investigated. The bodily feature influential to the design would be the proximal lower leg or calf circumference. The diameter of the proximal lower leg depends largely on the soft tissue structures (muscle and fat) surrounding the bone. However, this portion of the leg would need to be considered as the limb would be placed within the confines of the support structure. The anthropometric data for the typical 95th percentile, 40-year-old American male in the year 2000, according to NASA (2008) is indicated in Table 4.2.

Table 4.2: Anthropometric parameters used for design of LAS support structure (information credit: (NASA 2008)).

Property	*Specification*
Gender	Male
Age	40 years
Percentile	95th
Calf circumference (C)	414mm
Hip Breadth	390mm

Based on the parameters stated in Table 4.2, the diameter of a 40-year-old, 95th percentile male's calf was calculated to be 131.78mm. The linear actuator described in 4.1.1.1 Actuator Selection has a maximum stroke length of 100mm. Therefore, to accommodate for a calf diameter of 131.78mm and a 100mm maximum linear actuator stroke length, the height and width of the LAS support structure were designed to be approximately 231.78mm. The addition of an SF was considered; however, this would result in a rather large structure, which impacts on the overall weight of the device and was therefore not implemented. The final overall dimensions of the LAS structural support are indicated on the design drawings in Appendix C. For comparative purposes, Table 4.3 was considered, which indicates the calf circumference of a typical American male, 20 years and older (between the years 2003 and 2006), according to McDowell et al. (2008).

Table 4.3: The calf circumference values for a typical American male 20 years of age and older, between 2003 and 2006 compared to the findings according to NASA (2008) i.e. 414mm (information credit: (McDowell et al. 2008; NASA 2008)).

Percentile	*Calf circumference (mm)*
50th	375 < 414
75th	409 < 414
95th	471 > 414

According to the findings by McDowell et al. (2008) and the 414mm calf circumference designed for, the LAS support structure accommodates for more than 75 percent of the typical male population in the US. This is valid for the US population between the years 2003 and 2006. The 95th percentile calf circumference, according to McDowell et al. (2008), will need to be considered for future iterations of the LAS support structure.

4.1.2.3 Load Application System Support Structure

The lateral and medial supports are designed to be almost identical, and the superior support resembles the lateral support mid-section. This design creates a more aesthetically appealing construct and accommodates for available manufacturing techniques. The initial Concept 2 design was asymmetrical and would be challenging to manufacture with the resources available in the UCT Faculty of Health Science's (FHS's) mechanical workshop.

The lateral, medial and superior supports were designed to achieve unilateral multi-ligament laxity measurements. The design focused on two crucial design considerations: 1. Support the linear actuator's weight as well as the reaction forces generated due to the load applied and 2. Allow for adjustable positioning of the linear actuator to achieve multi-ligament laxity measurements and account for human variation in proximal lower leg diameter and hip breadth. The supports make use of a sleeve and cotter joint mechanism (as illustrated in Figure 4.14), which allows for effortless assembly of the support structure and a secured joint.

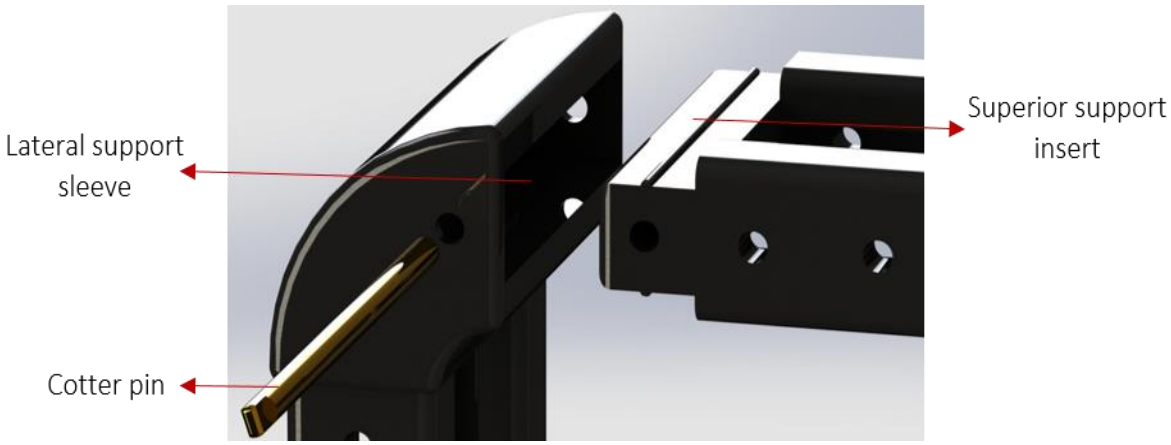

Figure 4.14: Sleeve and cotter type joint allowing for LAS support structure ease of assembly and disassembly.

The image illustrates the exploded view assembly of the LAS support structure's lateral and superior supports. The superior support is fitted to the lateral support sleeve and fixed in position by a cotter pin.

The primary function of the LAS support structure is to support the linear actuator when applying the required load to the proximal tibia. All three supports consist of two parallel members, which accommodate the breadth of the actuator and the actuator housing. Each member compromises of an inward facing, C-shaped cross section (as illustrated in Figure 4.15), which would allow for mounting the linear actuator to the structure. This C-shaped cross-sectional profile was designed to accommodate two bearings situated on either side of the actuator housing, allowing the housing to travel along the length of the supports. This allows for the actuator to be appropriately positioned as required and fixated with pins. In addition, the C-shaped cross section mimics a C-beam, thereby improving the structural integrity of the construct. Position fixation apertures (as indicated in Figure 4.15), which allow for appropriate positioning of the linear actuator on the structure, are located on the superior and lateral supports. The apertures allow the actuator to account for human variation in proximal lower leg (calf) diameter, overall hip breadth and femoral length.

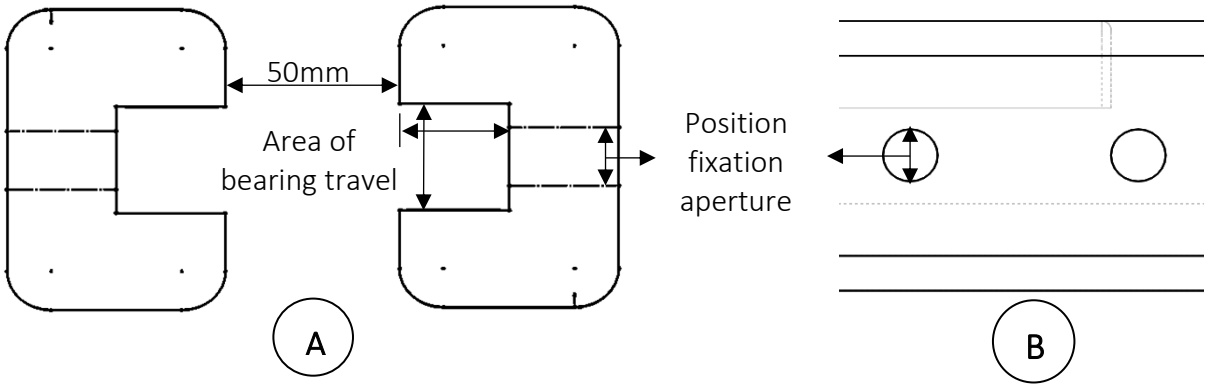

Figure 4.15: (A) C-shaped cross-sectional profile of the Parallel Supports and (B) side view of the force application system's support structure beams.

The image illustrates (A) the C-shaped cross section of the lateral and superior supports (sectioning through the parallel members) as well as (B) a side view of the parallel members. The Parallel Supports are spaced 50mm apart to accommodate for the actuator housing. The C-shaped cross section supports bearings located on the actuator housing to travel along the length of the lateral and superior supports. The actuator housing is then fixed into the required position by inserting pins through the position fixation apertures.

The linear actuator applied the necessary load in both retraction and extension. The support structure accommodated the linear actuator housing between the parallel members of the lateral and superior supports only. The parallel members on the superior and lateral supports were designed to be multi-functional. The medial support's parallel members were designed to support the loads (the weight of the actuator when fitted to the superior support and all reaction forces) and achieve symmetry for aesthetic appeal.

4.1.2.4 Force-Sensing Pads

Two FSPs were designed as part of the LAS (illustrated in Figure 4.16), to measure the load applied to the proximal lower leg. The posterior-medial pad would apply a load during extension of the linear actuator. This action would translate the tibia either posteriorly or medially, according to the position of the actuator on the LAS support structure. The anterior-lateral pad would apply a load to the proximal lower leg during retraction of the linear actuator. This action would result in an anterior or lateral translation of the tibia according to the position of the linear actuator on the LAS support structure. A posterior-medial FSP adaptor (indicated in Figure 4.16) attached the posterior-medial pad to the linear actuator head. The adaptor features strap connections i.e. anterior-lateral adaptors, which allows for the attachment of the anterior-lateral pad with Velcro® straps to the linear actuator. Two primary and two auxiliary strain gauges were fitted to each pad to measure the applied load. The strain gauges would use the deflection of the pads to measure the load applied.

The FSPs were manufactured out of Ertalyte as opposed to cast Nylon. Although Ertalyte (a radiolucent polymer) has a higher yield strength and elastic modulus compared to cast Nylon, the material is substantially more expensive. This conservative approach to design was taken due to the need for minimal deflection and sufficient strength. The deflection calculations for both Ertalyte and cast Nylon FSP were carried out using MD Solids. The sample calculation for the anterior-lateral Ertalyte pad is provided below.

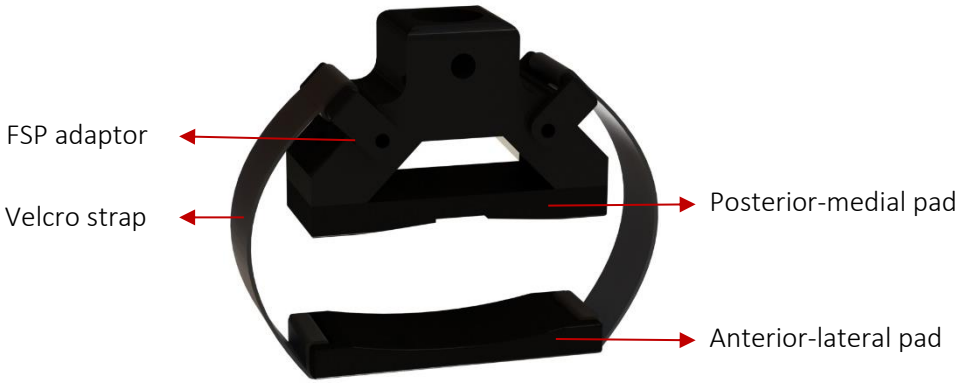

Figure 4.16: The FSPs designed to apply the incremental loads to various aspect of the proximal lower leg.

The image illustrates the assembly of various components designed to induce proximal lower leg translation. These components include the posterior-medial pad, anterior-lateral pad, FSP adaptor and the Velcro straps.

The first step was to identify the load distribution (free body diagram) across the length (l) of the pads. To calculate for the worst-case scenario, a point load (P) of 250N was modelled as opposed to a distributed load (as indicated in Figure 4.17). The Modulus of Elasticity (E) for Ertalyte® was found to be 3500MPa. The moment of inertia (I) and thereafter the deflection of the pad was calculated using MD Solids (a mechanics of materials engineering student's assistive software) and verified by means of hand calculations (applying Eq. (4.2)) according to Budynas et al. (2011). The width (b) and height (h) of the cross section of the plate are 32mm and 6mm respectively. Figure 4.17 illustrates both the free body diagram and the deflection curve of the anterior-lateral FSP.

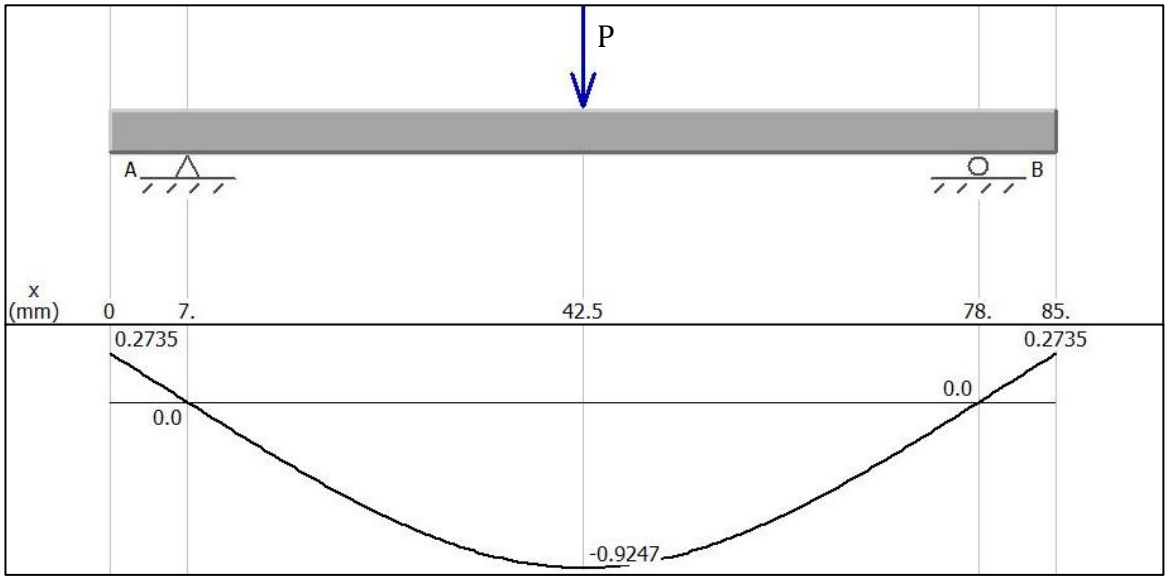

Figure 4.17: Free body diagram simulating the worst-case loading experienced by the anterior-lateral pad.

The image illustrates the simulation (free body diagram and deflection curve) of the worst-case loading scenario of the anterior-lateral FSP. The loading scenario was used to measure the deflection of the Ertalyte® FSPs (0.9247mm) and thereby determine the feasibility of using the material as opposed to Nylon.

Therefore, the deflection may be calculated as follows:

$$\delta = \frac{-Pl^3}{48(EI)} \tag{4.2}$$

$$\therefore \delta = \frac{-Pl^3}{48\left(E\left[\frac{bh^3}{12}\right]\right)}$$

$$= \frac{-(250)(71 \times 10^{-3})^3}{48\left((3500 \times 10^6)\left[\frac{(32 \times 10^{-3})(6 \times 10^{-3})^3}{12}\right]\right)}$$

$$= -0.925mm\ (3.s.f.)$$

The -0.925mm deflection (less than 1% of the actuator's stroke length) is favourable for this study and the manufacturing of the FSPs. The posterior-medial Ertalyte® pad produced a deflection of -0.693mm due to the distance between supports (64.5mm) being less than that of the anterior-lateral pad (71mm). The results for the cast Nylon pads (elastic modulus of 2.76GPa) were -1.173mm for the anterior-lateral pad and -0.879mm for the posterior-medial pad (GPlastics 2012). As a result, the Ertalyte® pads were selected for the FSPs due to the minimal deflection and superior strength of the pads.

4.2 Patient Support Structure

This section of the study outlines and describes the various components that make up the Laxmeter's PSS. The structure provides for the ideal patient position during laxity measurement procedures. In addition, the structure would potentially improve laxity measurement reproducibility by fixating the knee joint flexion angle. The various structures designed to make this possible, are detailed in this section.

4.2.1 Material Selection

Various materials were considered for manufacturing the PSS. The primary materials considered were Plexiglas®, polycarbonate, carbon fibre reinforced plastics (CFRPs) and pure carbon fibre panels. The primary material characteristic considerations were radiolucency, rigidity, weight and structural integrity; however, cost was a large decision determining factor. Although carbon fibre and CFRP would be ideal due to their strength, light weight and radiolucent characteristics, the cost of carbon materials are incomparable to that of Plexiglas® and polycarbonate, as indicated in Table 4.4.

Table 4.4: Cost comparison of a 1 X 1 X 0.008 m sheet of the materials considered for the Laxmeter PSS (as quoted by Maizeys Plastics and Advanced-fibreform).

Material	*Cost (ZAR)*	*Elastic Modulus (MPa)*
Plexiglas ®	1350.69	3000
Polycarbonate	1470.87	2600
Carbon fibre	20,270.00	228 000

The material selected for manufacturing all panels was Plexiglas®. The material was chosen due to its rigidity, low-cost, local availability and radiolucency. The cost difference between Plexiglas® and polycarbonate is minimal; however, Plexiglas® is the more rigid of the two with an elastic modulus of 3300MPa while that of polycarbonate which is 2600MPa (Evonik 2017; ToolBox 2017).

4.2.2 Lower Leg Support Panel

4.2.2.1 Dimensions

The LLSP is the most multifaceted Laxmeter panel, due to the operation of the device. This panel consists of various features, which allow for all objectives achievable by the Laxmeter. The LLSP encompasses the following features:

- Support a portion of the patient's lower leg weight.
- Support knee joint flexion angle locking.
- Contribute in accurate bone translation tracking.
- Fixate the distal portion of the lower leg.
- Allow for the attachment of the LAS (support structure).

The LLSP would need to support the weight of the 95th percentile adult male's lower leg. This affects both the dimensions of the panel and the material selected for manufacture (Plexiglas® as detailed in Section 4.2.1 Material Selection). The panel was designed to fit onto an average X-ray bed. A typical average width of an X-ray table pad is approximately 600mm (Medical 2015; Medline 2016; CCushions 2017). The lower leg length of the 95th percentile male is estimated to be 599mm (Island 2017). Therefore, the panel was designed to accommodate for the lower leg length of the 95th percentile male and the width of an X-ray bed (as indicated in Figure 4.18).

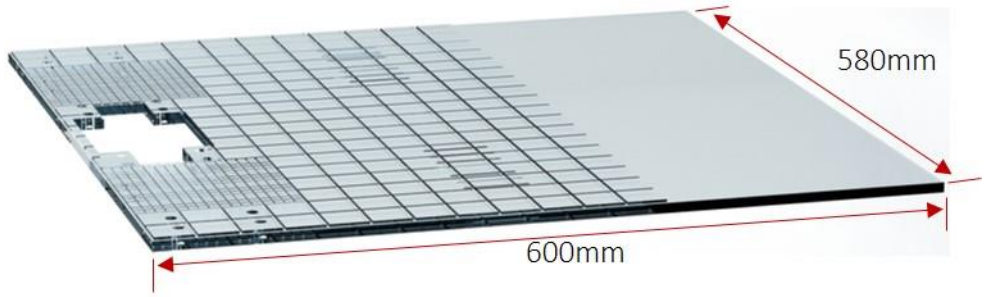

Figure 4.18: Orthographic view of the LLSP CAD model.

The image illustrates the 8mm thick LLSP (580mm wide and 600mm long), which was designed to fit on top of a 600mm wide X-ray bed and accommodate for the 95th percentile male's lower leg length of 599mm.

The 8mm thick panel was verified with Ansys® Finite Element Modelling (FEM) student edition software. This version of the software is limited in functionality, however, it was considered sufficient when modelling components, individually. An 8mm thick panel was selected to reduce the overall weight of the device, as this was a key design consideration for this study (portability and storage). A 10mm and 12mm thick panel were considered, however, the finite element models revealed that the 8mm panel would sufficiently support the loads applied to the LLSP.

4.2.2.2 Structural Analysis

ACL and PCL Laxity Measurement Procedure

The FEM simulation considered the two reaction forces experienced by the LLSP as a result of the 250N load applied by the lateral and medial LAS supports as well as the reaction forces due to the ankle fixation. To determine the reaction forces due to ankle fixation, the loads acting on the lower leg needed to be considered. The ankle fixation loads were calculated by considering the free body diagram of the lower leg during the 250N loading (illustrated in Figure 4.19) and determining the reaction force between the heel and the LLSP.

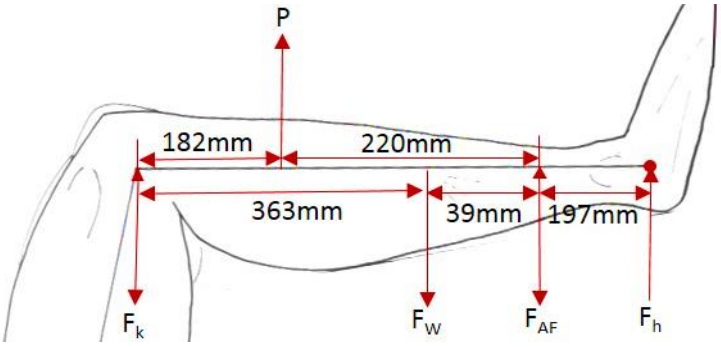

Figure 4.19: The free body diagram of a 95th percentile male's lower leg when subjected to the 250N load during ACL laxity measurement procedures (data credit: (NASA 2008; Island 2017)).

The image illustrates the free body diagram of a 95th percentile male's lower leg during the ACL laxity measurement procedure. The loads which act on the lower leg are: the reaction forces experienced by the knee joint (F_k) as well as the heel on the LLSP (F_h), the reaction force experienced by distal lower leg due to the Velcro® strapping (F_{AF}), the lower leg weight (F_W) and the 250N load (P) applied to induce tibial translation.

The reaction forces experienced by the LLSP due to ankle fixation and heel contact were calculated. The reaction forces were obtained by solving the summation of forces acting on a body (Eq. (4.3)) and the summation of moments about the knee (Eq. (4.4)) simultaneously.

$$P = 250N, \qquad F_W = 64N, \qquad \text{(Detailed below)}$$

$$\sum F = 0, \sum M_k = 0, \sum M_h = 0,$$

$$\sum F = 0 : -F_k + P - F_W - F_{AF} + F_h = 0 \qquad (4.3)$$

$$\therefore F_k + F_{AF} = 186 \qquad \text{Assume } F_h = 0N \text{ (Detailed below)}$$

$$\sum M_k = 0: (P \times 182) - (F_W \times 363) - (F_{AF} \times 402) + (F_h \times 599) = 0 \qquad (4.4)$$

$$\therefore -402F_{AF} + 599F_h = -22268 \qquad \text{Assume } F_h = 0N$$

$$\therefore F_{AF} = 55.39N \ (2.d.p.)$$

Therefore, solving Eq. (4.3) and Eq. (4.4) simultaneously results in the following:

$$\therefore F_{AF} = 55.39N \, , F_h = 0N \, , F_k = 130.61N \ (2.d.p.)$$

The weight of a 95th percentile male's lower leg (F_W) was calculated according to the density and length parameters provided by University of Rhode Island, (2017). The density and length of the lower leg segment were found to be 1.09kg/unit length and 0.599m. Therefore, the mass of the lower leg could be calculated as follows: 1.09 x 0.599 = 0.65kg (2.d.p.). However, this value was assumed incorrect. Therefore, it was assumed that the unit length for the density was decimeters, resulting in a lower leg mass of 6.5kg. This was considered a more realistic value. The weight of the lower leg was therefore calculated as follows: 6.5 x gravitational acceleration (g) = 6.5 x 9.81 = 64N. Since F_k, as well as F_{AF}, are located at fixed supports, and no external forces are being applied between F_{AF} and F_h, it can be assumed that F_h = 0N. The force due to the fixation of the ankle using the Velcro® strap (F_{AF}) was applied to the LLSP to more accurately simulate the ACL laxity measurement procedures. All forces applied to the LLSP FEM simulation are indicated in Figure 4.20.

Figure 4.20 illustrates the Total Deformation of the LLSP, simulating the right knee joint ACL laxity measurement conditions, indicating a maximum deformation of 0.964mm (3.s.f). This result, which will be mirrored about the centre line for the left knee, indicates that the 8mm Plexiglas® panel has a negligible deflection during ACL laxity measurement procedures. The peak deflection, located at the lateral LAS support structure, is due to the attachment of the support to the edge of the LLSP. The edge acts similar to a cantilever beam (due to the support being located between the two 125N loads) with a load applied to the end, resulting in a larger deflection.

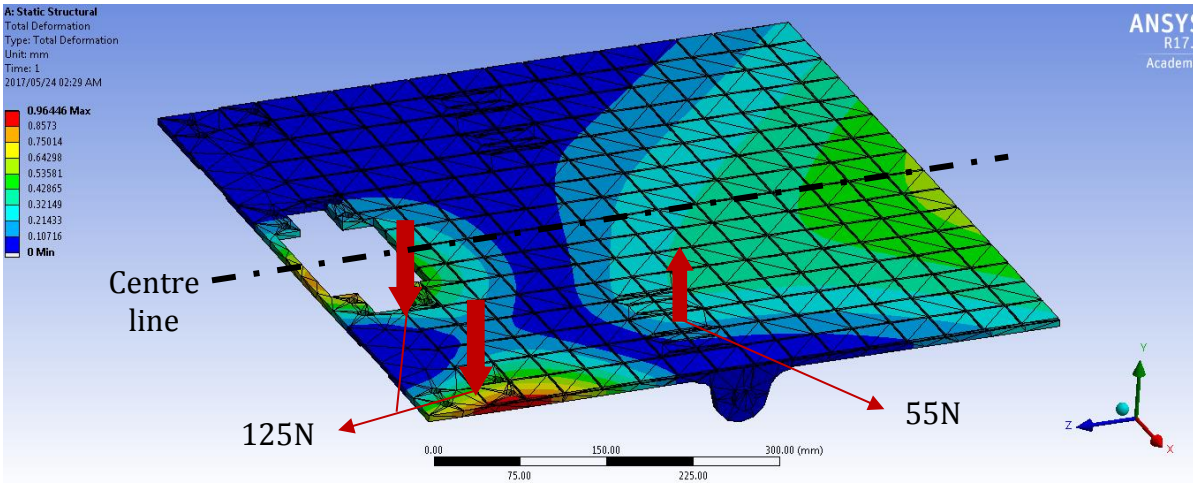

Figure 4.20: Finite Element Model for Total Deformation, simulating the right knee joint ACL ligament laxity measurement procedure using Ansys® FEM student edition software.

The image illustrates the Static Structural FEM simulation for the right knee ACL laxity measurement procedure. The maximum deflection of the LLSP as a result of the various loads was found to be 0.964mm (3.s.f.). This result considered the reaction forces experienced by the LLSP due to the LAS lateral and medial supports (125N each) as well as the reaction force due to ankle fixation (55N). The weight of the 95th percentile male's lower leg was considered in calculating the reaction forces on the LLSP and the 250N load applied to the limb.

Figure 4.21 illustrates the Equivalent (von-Mises) stress FEM of the LLSP, indicating a maximum stress of 4.28Mpa (2.d.p.) when loaded according to the ACL laxity measurement procedures. The maximum Equivalent stress experienced by the LLSP does not exceed the yield strength of the material (80MPa) and therefore, the panel proves sufficient for use during ACL laxity measurement procedures (Plexiglass(R) 2013).

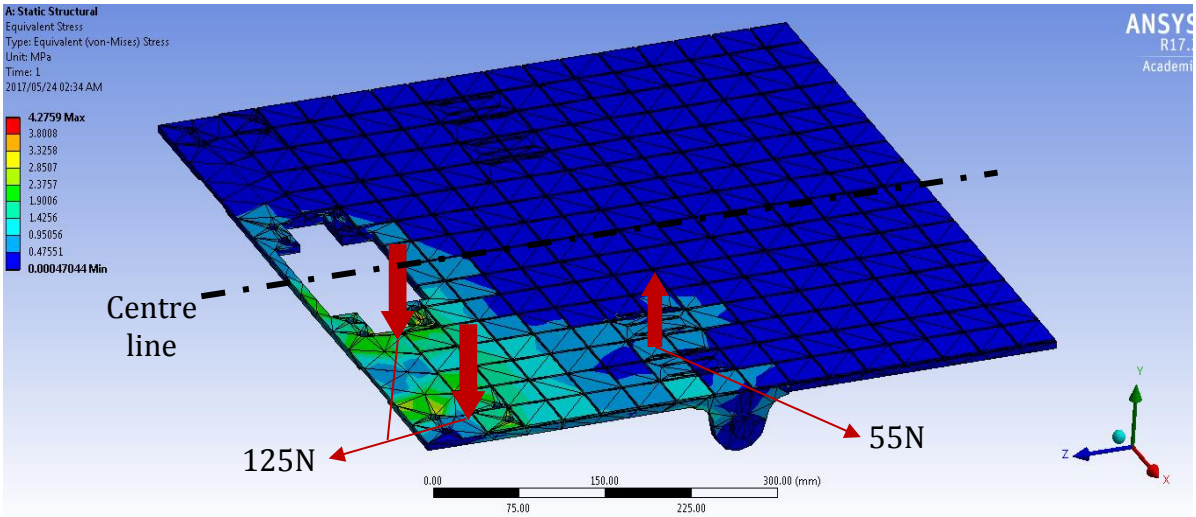

Figure 4.21: Finite Element model for Equivalent Stress, simulating the ACL ligament laxity measurement procedure using Ansys® FEM student edition software.

The image illustrates the Static Structural FEM simulation for the ACL laxity measurement procedures. The maximum Equivalent (von-Mises) Stress experienced by the LLSP as a result of the loads was found to be 4.28MPa (2.d.p.). This result considered the reaction forces experienced by the LLSP due to the LAS lateral and medial supports (125N each) as well as the reaction force due to ankle fixation (55N). Since the Equivalent (von-Mises) Stress was less than the yield strength of Plexiglas® (80MPa), it can be concluded that the LLSP would not fail during ACL laxity measurement loading.

The LLSP FEM analyses of the PCL laxity measurement procedure produced a Total Deformation value of 0.998mm (3.s.f.) and an Equivalent (von-Mises) Stress of 4.49MPa (2.d.p.) respectively. This Total Deformation result was negligible as the deflection would not affect the laxity measurement results. The Equivalent (von-Mises) Stress did not exceed the yield strength of Plexiglas® (80MPa), indicating a sound structure during PCL laxity measurement procedures.

MCL and LCL Laxity Measurement Procedure

Simulating MCL and LCL laxity measurement procedures using FEM, required additional components attached to the LLSP (the lateral and medial supports bolted onto the LLSP). Ansys® could not be used for the structural failure analysis. Therefore, LLSP structural integrity during MCL and LCL laxity measurements was verified by means of manually calculating the bearing and tension experienced by the LLSP. The lateral and medial supports of the LAS support structure were fixed to the LLSP with four M10 bolts (8 in total), which will be further discussed in Section 4.3 Integration Adaptor System. The LLSP structural design needed to account for failure due to bearing and tension on the panel as a result of the bolted connection. This involved calculating the SFs for the various modes of failure i.e. bearing and tension on members according to Budynas and Nisbett (2011). The SF calculations considered the yield strength (S_Y) of the Plexiglas® LLSP as well as the load applied to the proximal lower leg (P) and were carried out as follows (Plexiglass(R) 2013):

Bearing on the LLSP:

The safety factor (SF_{bm}) concerning the bearing on the LLSP, calculated according to Eq. (4.7) was calculated by determining the bearing Area (A_b) according to Eq. (4.5), the bearing stress (σ_b) according to Eq. (4.6) and the tensile yield strength ($S_{y\text{-}Plexiglas®}$) of Plexiglas®. Additional considerations for calculating SF_{bm} were the thickness of the LLSP (t) and the diameter of the bolts (D). A 2x2 M10 bolt configuration was used for the fixation mechanism.

$$A_b = 4(t \times D) \tag{4.5}$$

$$t = 8mm, D = 10mm$$

$$\therefore A_b = 4(0.008 \times 0.01) \; = \; 3.2 \times 10^{-4}\, mm^2$$

$$\therefore \sigma_b = \frac{P}{A_b} = \frac{250}{3.2 \times 10^{-4}} = 781.250\, KPa \tag{4.6}$$

$$P = 250N$$

$$\therefore SF_{bm} = \frac{S_{y-Plexiglas^{(R)}}}{\sigma_b} \; = \; \frac{80 \times 10^6}{781.250 \times 10^3} \; = 102.4 \tag{4.7}$$

$$S_{y-Plexiglas^{(R)}} = 80MPa$$

An SF of 102.4 indicates a severely overdesigned fastening mechanism. The use of a single M4 Nylon bolt results in an SF value of 10.24, which remains an overdesign. An acceptable SF concerning the bearing on the LLSP due to the fastening mechanism would be between 2 and 3. However, the SF indicates that the member will not fail due to bearing stress on the LLSP.

Tension on the LLSP:

The safety factor concerning the tension on the LLSP (SF_{tm}) as calculated according to Eq.(4.10), was determined by considering the tensile area (A_t) according to Eq. (4.8), the tensile stress (σ_t) according to Eq. (4.9) and the tensile yield strength ($S_{y\text{-}Plexiglas®}$) of Plexiglas®. In addition, the calculation considered the width of the lateral support at the point of contact with the LLSP (t_s), the bolt diameter (D), the number of M10 bolts in a row (N) and the thickness of the LLSP panel (t). A 2x2 M10 bolt configuration was used to ensure stability and structural integrity.

$$A_t = \big(t_s - (N \times D)\big)(t) \tag{4.8}$$

$$t_s = 90mm, N = 2$$

$$\therefore A_t = \big(0.09 - (2 \times 0.01)\big)(0.008) \; = \; 5.6 \times 10^{-4}\, mm^2$$

$$\therefore \sigma_t = \frac{P}{A_t} = \frac{250}{5.6 \times 10^{-4}} = 444.429\, KPa \tag{4.9}$$

$$\therefore SF_{tm} = \frac{S_{y-Plexiglas^{(R)}}}{\sigma_t} \; = \; \frac{80 \times 10^6}{444.429 \times 10^3} \; = 179.2 \tag{4.10}$$

As seen from the previous SF calculation concerning the bearing on the LLSP, the safety factor result of 179.2 indicates an overdesigned fastening mechanism. The SF_{tm} (tension on the LLSP) safety factor result, using a single M4 Nylon bolt, would result in a safety factor of 220.16, indicating severe overdesign. However, the safety factor result (SF_{tm} = 179.2) indicates that the LLSP will not fail due to tensional stress on the members.

The 600 x 580 x 8mm Plexiglas® LLSP was designed to be structurally sound, to sufficiently support all loads subjected to the panel as a result of knee joint ligament laxity measurements. The structure would need to withstand the loads generated during all four major ligament laxity measurement procedures at multiple fixed degrees of flexion. All structural analyses were conducted on a horizontal LLSP. This was due to the LLSP maintaining a horizontal configuration throughout all laxity measurement procedures.

4.2.2.3 LLSP Hinge Arch

The Laxmeter concept selected to lock the knee joint flexion angle in place was a pin and slot mechanism. This mechanism was adopted from the previous device, seeing as the eliminated concepts were found to be infeasible. The LLSP features two hinge arches (as illustrated in Figure 4.22) bolted to the centre of the lateral edges of the panel. These hinge arches extend the LLSP downward and consist of a cross-sectional profile as illustrated in Figure 4.22. This profile is concentric with that of the locking mechanism, which will be further detailed in Section 4.2.4 Joint Locking Mechanism.

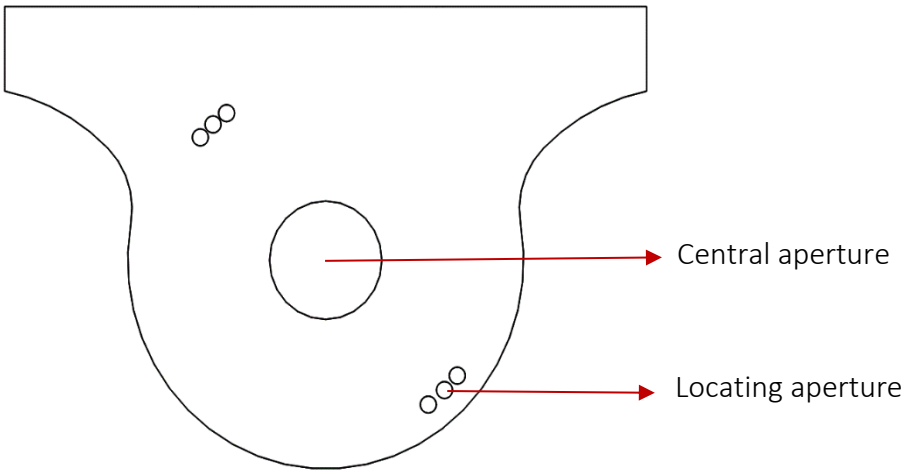

Figure 4.22: Cross section profile of the knee joint locking add-on Sections for the LLSP.

The image illustrates the side view of the LLSP hinge arch, which is bolted to the centre of the lateral edges of the panel. The arches allow for the attachment of the Joint Locking Mechanism to the LLSP. The proximal section of the parallel support arms was designed to be concentric with the central aperture of the arch. The locating apertures allow the operator to select a particular knee joint flexion angle.

4.2.3 Upper Leg Support Panel

The ULSP was designed with two key feature considerations: 1) Windows to limit posterior region exposure and 2) fixation points for securing the upper leg during laxity measurement procedures. Women are reported to experiencing discomfort when lying in the required position for Laxmeter laxity measurement procedures (Sivarasu and Patnaik 2014b). The patient position during laxity measurement procedures is indicated in Figure 4.23.

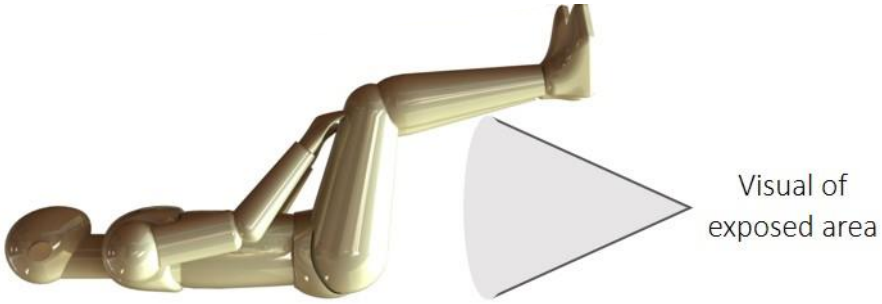

Figure 4.23: Patient position during Laxmeter, knee joint, laxity measurement procedures.

The image illustrates the patient position when placed on the PSS. The position requires the patient to elevate their lower limb, thereby exposing the posterior region. This is considered taboo amongst women from more conservative backgrounds.

As illustrated in Figure 4.23, the lower limb is elevated thereby exposing the patient's posterior region. This exposure can be reduced by integrating windows into the ULSP, which allows the patient to rest their non-tested limb on the X-ray bed. In addition, during ACL and PCL laxity measurement procedures, a lateral radiographic image is captured to measure the laxity of the ligament. With both limbs on the LLSP, it is challenging to identify the right limb from the left, from the 2-dimensional (2D) X-ray image. Therefore, by placing the non-tested limb through the window, the translation image obstruction is eliminated. Slots were cut into the three columns of the panel (as illustrated in Figure 4.24) to accommodate for the Velcro® straps, used for upper leg fixation due to the radiolucent properties of the Velcro® material.

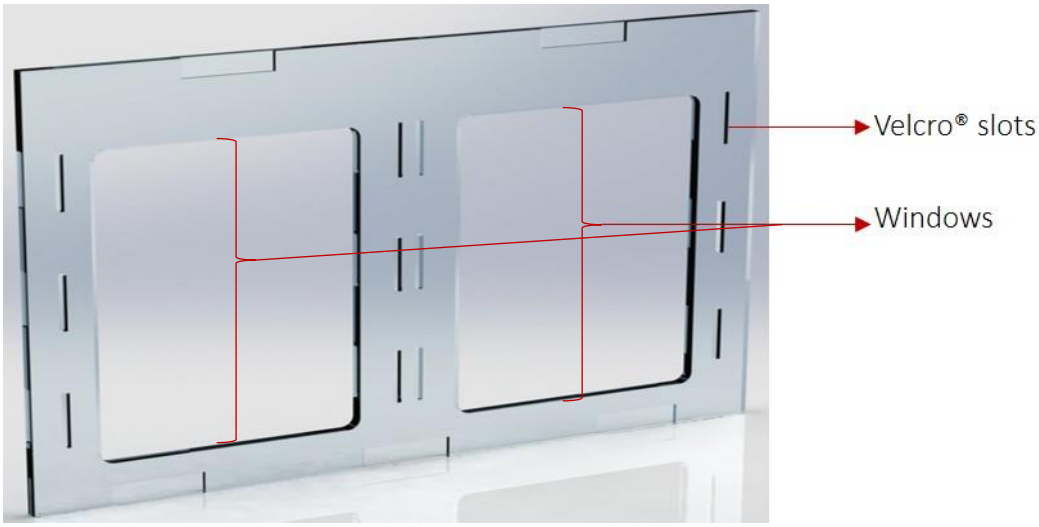

Figure 4.24: The ULSP designed to accommodate for posterior region exposure and lateral image limb differentiation discrepancies as well as upper leg fixation.

The image illustrates the ULSP design to support the LLSP during laxity measurement test procedures. Furthermore, special design considerations include windows for the non-tested limb to limit posterior region exposure as well as eliminate the need to differentiate the right limb from the left during ACL and PCL laxity measurement procedures. In addition, the panel features Velcro® slots to allow for upper leg fixation.

The PCL laxity measurement procedure FEM structural analysis was considered the worst-case load scenario. Therefore, the ULSP was analysed in a 90° position, considering a 130.61N (2.d.p.) load being applied in the negative y-direction. The analysis revealed a negligible Total Deformation of 0.308mm (3.s.f.).

4.2.4 Joint Locking Mechanism

The PSS replicated a four-bar linkage system (illustrated in Figure 4.25). However, to maintain a fixed configuration (since all linkage junctures are hinge joints), one juncture would need to be locked in position. In addition, the length of one or more linkages would need to be adjustable to maintain a rhomboidal configuration as per the required knee joint flexion angle (Θ). This particular panel configuration simulates the LLSP in a permanent horizontal position, parallel to the X-ray bed. These feature requirements were integrated into the joint locking mechanism (JLM) design.

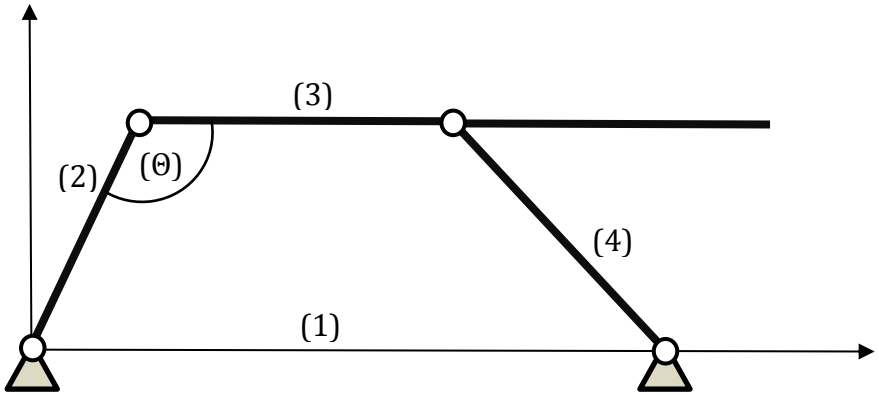

Figure 4.25: Four-bar linkage system used as the basis of the Laxmeter's PSS design.

The image illustrates the PSS four-bar linkage configuration of panels. The image labels the Angle Adjustment Panel + Fold Assist Panel (1), the ULSP (2), the LLSP (3), the parallel support arms (4) and the angle of knee joint flexion (Θ).

The JLM allows the Laxmeter to carry out all four laxity measurement techniques at various fixed degrees of knee joint flexion. Three primary components make up the JLM. These include:

- The parallel support arms
- The LLSP hinge arches
- The Angle Fixation Slots

The parallel support arms form the fourth linkage in the PSS 4-bar linkage configuration (as indicated in Figure 4.25). The LLSP hinge arches are attached to the centre of the LLSP's lateral edges. The Angle Fixation Slots are attached to the edges of the Angle Adjustment Panel. The superior ends of the support arms pivot about the LLSP hinge arches. The inferior ends of the support arms pivot about the Angle Fixation Slots. As the superior end of the parallel support arms rotate about the hinge arches, the arms are fixed into position to obtain the required knee joint flexion angle by inserting two pins (one on either side of the Laxmeter) that fit into specific apertures. The apertures in the support arms are concentric with the apertures in the hinge arches to lock the JLM and fixate the required knee joint flexion angle. Figure 4.26 illustrates the JLM, emphasising the knee joint flexion angle fixation mechanism by inserting a pin into the required aperture, to maintain a horizontal LLSP and fixate the knee joint flexion angle.

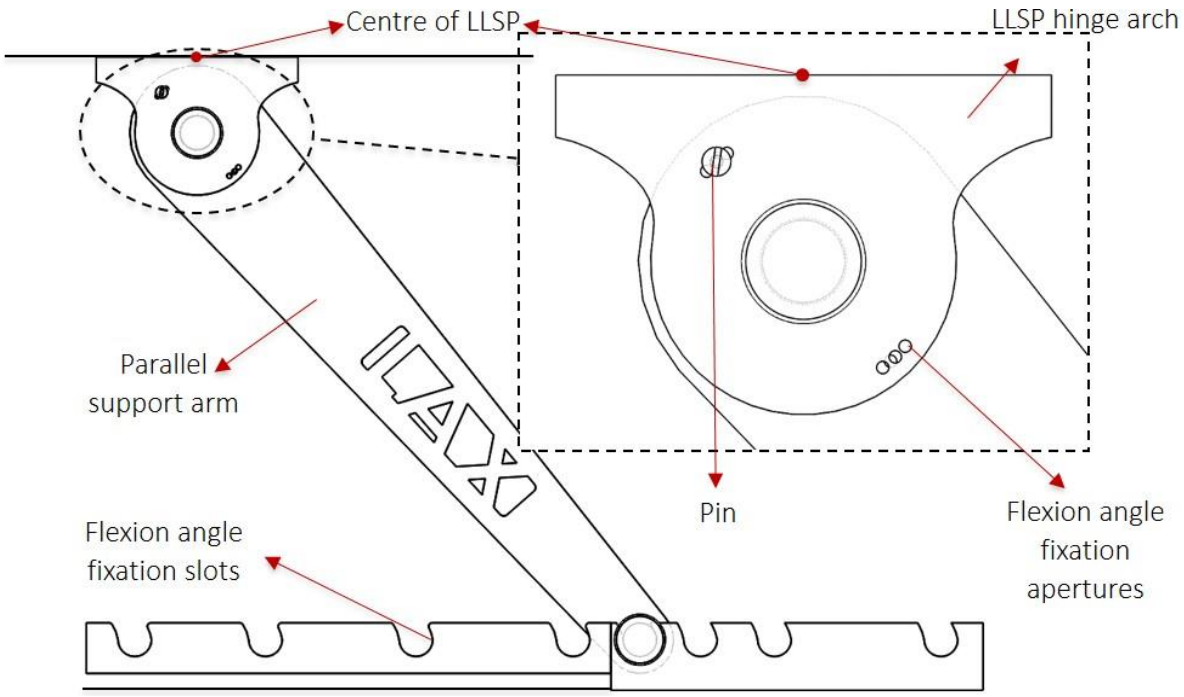

Figure 4.26: The JLM designed to fixate the knee joint flexion angle by inserting a pin.

The image illustrates the JLM used to select the required knee joint flexion angle and maintain a rhomboidal panel configuration. The flexion angle fixation apertures in the hinge arches become concentric with the apertures in the parallel support arm to select the required angle. The pin is inserted to fix the juncture in place to maintain the linkage configuration.

The joint fixation slots allow for the length adjustment of Angle Adjustment Panel, thereby allowing for the selection of the required knee joint flexion angle, while maintaining the rhomboidal panel configuration. Figure 4.27 illustrates examples of the four-bar linkage rhomboidal PSS panel configuration knee joint flexion angle adjustment. The length of the Angle Adjustment Panel + Fold Assist Panel linkage is adjusted to obtain the required knee joint flexion angle and maintain a rhomboidal panel configuration.

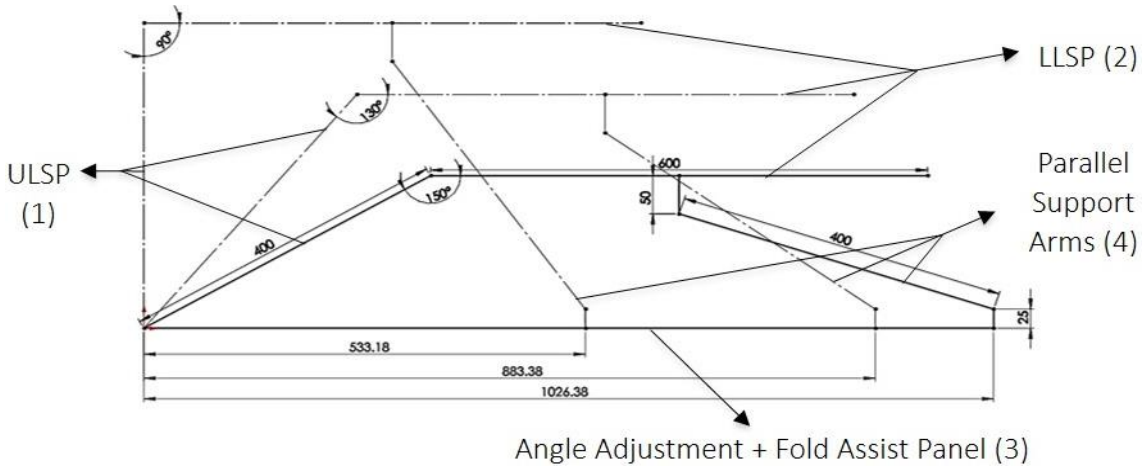

Figure 4.27: Length adjustment of the Angle Adjustment + Fold Assist Panel allowing for knee joint flexion angle adjustment.

The image illustrates the mechanism of adjusting the length of the Angle Adjustment Panel + Fold Assist Panel to achieve a specific knee joint flexion angle. Examples provided are for 90°, 130° and 150° flexion angles.

4.2.5 Storage Features

The storage features of the Laxmeter provided for portability and ease of storage. This consideration encompasses a lightweight device, ease of assembly and disassembly as well as manageable overall dimensions for carrying, moving or transportation (particularly concerning the PSS). The details of these features are detailed below.

4.2.5.1 Weight

The PSS was designed using 8mm thick Plexiglas® sheets, excluding the support arms and the LLSP hinge arches, which were manufactured from 12mm thick sheets. All FEM analyses and calculations related to the panels were based on the 8mm thick panels. This was to ensure that the overall weight of the PSS was kept to a minimum. In addition, large windows were sectioned into the Angle Adjustment Panel, ULSP and the Fold Assist Panel. The PSS had a total weight of 64N, as compared to Laxmeter Prototype One, which weighed 240N.

4.2.5.2 Ease of Assembly and Disassembly

Load Application System

The two subsystems of the Laxmeter (LAS and PSS) were considered separately when designing the storage capabilities. The LAS support structure assembled by utilising the sleeve and cotter joint type mechanism. This allowed for timely assembly and disassembly as well as ease of storage. The entire LAS can be disassembled and packaged within a 310x220x145mm container. Assembled in the ACL and PCL laxity measurement configuration (as illustrated in Figure 4.28), the dimensions of the LAS are 455x296x98mm.

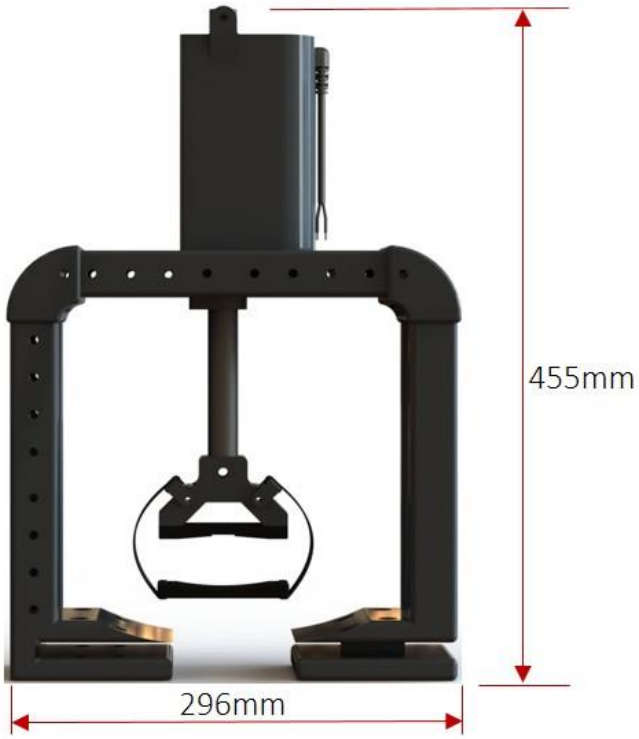

Figure 4.28: The LAS assembly in the ACL and PCL laxity measurement configuration.

The image illustrates the LAS in the ACL and PCL laxity measurement configuration, whereby the actuator is placed on the superior support of the LAS support structure. The components allowed for timely assembly and disassembly, improving the storage capabilities of the Laxmeter.

Patient Support Structure

The storage capability of the PSS was a key design outcome of this study. The sheer size of the structure, meant that the need for foldability was essential. The dimensions of the LLSP and ULSP were designed considering various anthropometric parameters. The Fold Assist Panel and the Angle Adjustment Panel, however, were specifically designed to collapse the PSS to allow for storage. The folded PSS (as illustrated in Figure 4.29) was designed to be 600x600x40mm.

The various panels would make up three layers when folded. The dimensions of the LLSP and ULSP were fixed at 600x580x8mm and 380x580x8mm; indicating that the LLSP would make up the first layer (1) and the ULSP a portion of the second layer. The Fold Assist Panel was, therefore, designed to be 220x600x8mm, completing the 600mm length of the second layer (2). Finally, the Angle Adjustment Panel was designed to be 600x600x8mm, thereby making up the final layer (3) of the assembly. All layers are indicated in Figure 4.29. The Angle Adjustment Panel, however, included the Angle Fixation Slots (8mm thick) that needed to be accounted for during folding. This is the reasoning behind the 580mm width of the LLSP and the ULSP. The Angle Fixation Slots would thus be the lateral borders of the PSS when folded. In addition, the Angle Fixation Slots required a base length of 1040mm to achieve the 0˚- 90˚ (from full extension) angles of knee joint flexion. This length exceeded the length of the Angle Adjustment Panel + Fold Assist Panel (820mm). Therefore, the Angle Fixation Slots were sectioned at the end of the Angle Adjustment Panel and reconnected with a hinge. The hinge allowed the free Angle Fixation Slot cut off sections to fold outward and be positioned adjacent to the PSS. Finally, the orientation of each hinge, connecting the panels and additional Sections, was crucial to allow for the folding configuration of the panels.

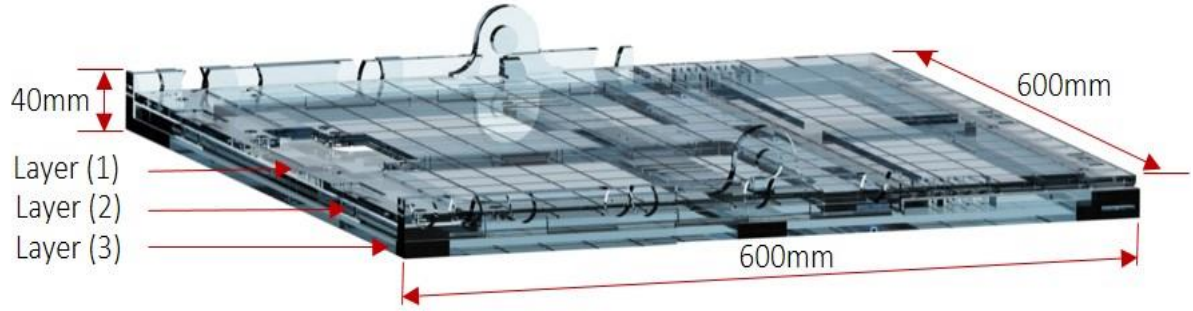

Figure 4.29: The PSS in the folded configuration, for storage and portability.

The image illustrates the folded configuration of the PSS, indicating the 600x600x40mm overall dimensions of the subsystem. The various layers of the PSS are shown whereby: Layer (1) is the LLSP, Layer (2) is the ULSP, as well as the Fold Assist Panel and Layer (3), is the Angle Adjustment Panel.

4.3 Integration Adaptor System

Integrating the LAS and the PSS would allow for the Laxmeter to carry out the necessary laxity measurement procedures. It facilitates ease of assembly and disassembly. The LAS and PSS integration modifications were as follows:

- PSS
    - Central Locking Mechanism Slot with bolt apertures
- LAS
    - Sleeve and cotter joint mechanism
    - Inferior sleeve for lateral support fixation
    - Inferior sleeve for medial support fixation

The Central Locking Mechanism Slot was designed for an effortless and time-efficient means of fixing the LAS support structure's medial support to the LLSP. The profile of the slot is illustrated in Figure 4.30. The large area allows for the insertion of the medial support's inferior sleeve. The support is then shifted laterally, thereby fixing it in place. The bolt apertures allow for the insertion of four M10 Nylon bolts to secure the component in the required position.

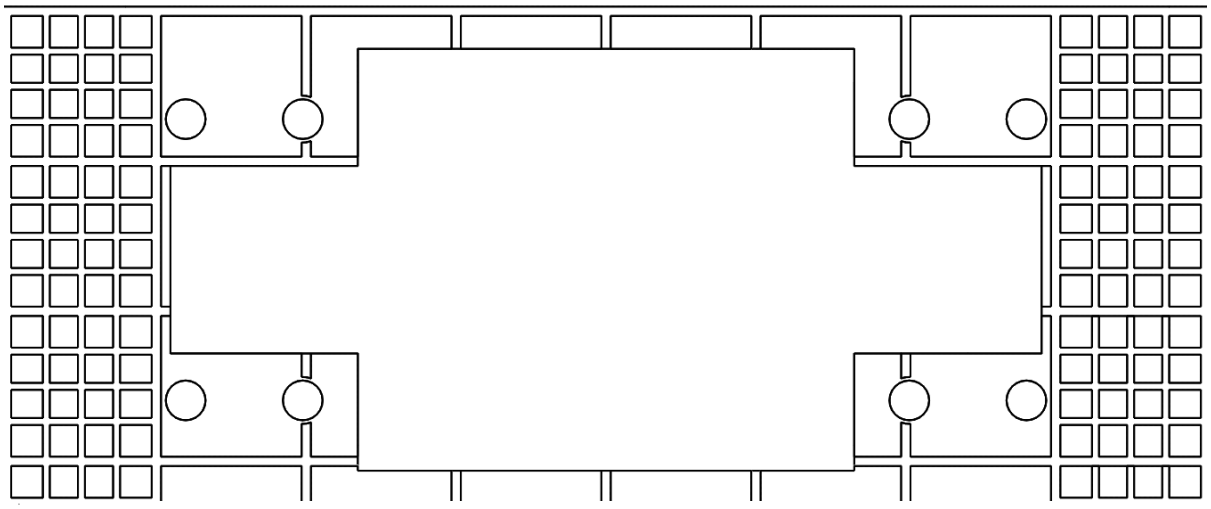

Figure 4.30: Central Locking Mechanism Slot profile.

The image illustrates the profile of the Central Locking Mechanism Slot located on the LLSP. The slot facilitates the attachment of the medial LAS support to the LLSP. This profile considers both the right and left limb laxity measurement procedures.

The use of a sleeve and cotter joint system facilitates the integration of the two systems. Upon securing the medial LAS support, the superior support would be attached. Thereafter, the lateral support would be attached to the superior support and simultaneously slide onto the edge of the LLSP. The inferior section of the lateral LAS support had a sliding fit onto the edge of the LLSP. For both the right and left sides of the panel, the LLSP features a total of sixteen apertures, eight on each side. Considering one side, in particular, four apertures allow for the fixation of the medial support and the remaining four allow for the fixation of the lateral support. Once the assembled LAS support structure has been attached to the LLSP, the device is ready for laxity measurement stress radiography procedures.

The inferior sleeves of the medial and lateral LAS supports were modified to accommodate for integrating the two subsystems, illustrated in Figure 4.31. The medial support's inferior sleeve could be considered a three-layer section. The top and bottom layers are 105.5 x 90mm, which would be accommodated for by the central area of the Central Locking Mechanism Slot, which is 121 x 94mm. The lateral notch areas (42 x 42mm) of the Central Locking Mechanism Slot were sized to accommodate the middle layer of the medial LAS support's inferior sleeve (40 x 40mm). The medial support would be placed through the central area of the Central Locking Mechanism Slot, to where the middle layer is in plane with the LLSP. The medial support would be shifted laterally, to fit the middle layer into the notch of the Central Locking Mechanism Slot. Figure 4.31 illustrates the assembly of the medial LAS support and the LLSP. Once in position, four M10 Nylon bolts were used to fasten the supports to the LLSP.

The lateral support makes use of a layer system, similar to that of the medial support. However, the middle lateral was designed as a lateral connection stretching along the width of the lateral aspect of the support. This created a C-shaped sleeve (as illustrated in Figure 4.31), which accommodated for the LLSP fitting between the top and bottom layers. Four M10 Nylon bolts were used to fix the lateral support to the LLSP.

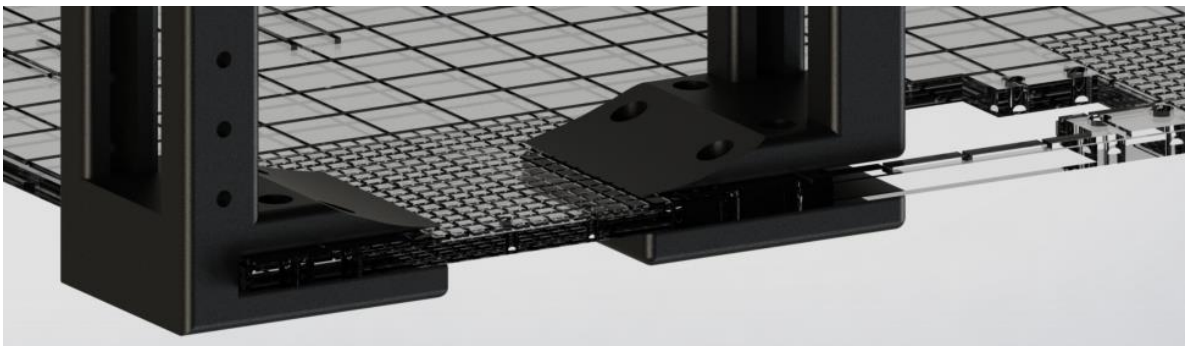

Figure 4.31: Integration Adaptor Design for attaching the LAS to the LLSP.

The image illustrates how the Integration Adaptor design functioned to attach the LAS support structure to the PSS's LLSP.

4.4 The Laxmeter

Integrating the two subsystems (the LAS and PSS) resulted in a functional Laxmeter Prototype equipped for experimental laxity measurement procedures. Figure 4.32 illustrates the fully assembled Laxmeter Prototype and a patient placed, in the appropriate position, on top of the device. Figure 4.33 illustrates the PSS and LAS in the folded and dissembled configurations for transport and storage.

An additional feature integrated post-manufacturing was a radiopaque scale feature, to allow for real-time bone translation tracking. The scale was achieved by means of embedding a radiopaque substance (Barium powder) within the rectangular grooves located on the surface of the LLSP. The area in the knee joint imaging region was more densely populated with smaller square grooves. This LLSP radiopaque scale would assist with MCL and LCL bone tracking, however, an add-on scale was developed that would stand upright to track ACL and PCL bone translations.

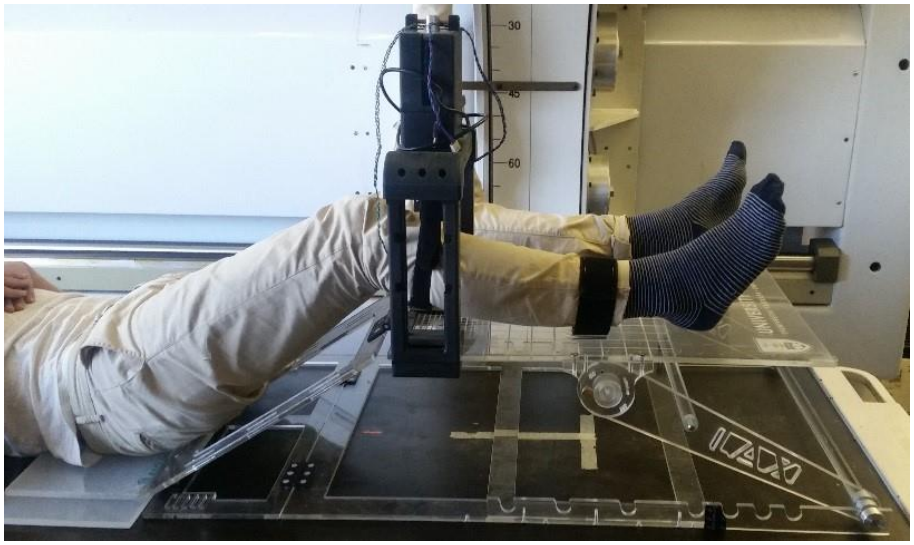

Figure 4.32: The fully assembled Laxmeter Prototype, placed on the LODOX scanner examination table (model credit: Ameen Bardien).

The image illustrates the fully assembled Laxmeter Prototype placed on the LODOX scanner examination table. The participant placed on the devices indicates the patient position during and ACL or PCL laxity measurement procedure, at 150° knee joint flexion angle.

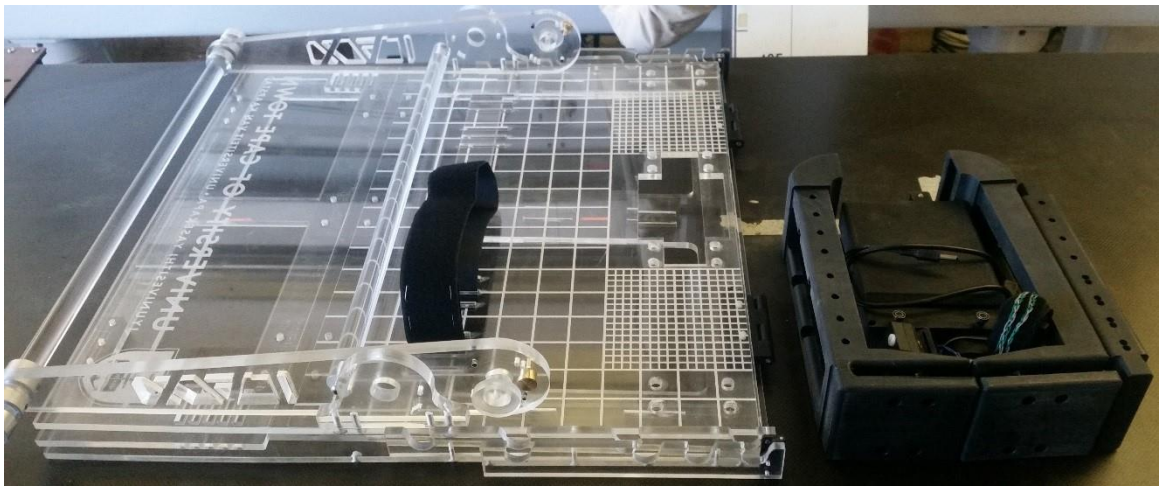

Figure 4.33: Storage configuration of the Laxmeter's PSS and LAS.

4.5 Failure Modes and Effects Analysis

4.5.1 Overview

Failure Modes and Effects Analysis (FMEA) is a subjective systematic approach to identify and quantify all potential ways in which a design can fail. The analysis model allows for the prioritisation of risks to identify critical design flaws that would need to be addressed in future iterations. The risks are prioritised according to the potential severity impact (S), probability of occurrence (O) and detectability (D) of the failure modes. This section describes the FMEA of the Laxmeter on a subsystem basis to improve the design recommendations for future iterations of the device.

4.5.2 Severity, Occurrence and Severity Scales

The systematic approach of analysing the potential failure modes and effects is based on a step by step process which involves:

1. Identifying the potential modes of failure
2. Identifying the effects/ consequences for each mode
3. Rating the severity each effect
4. Identifying the root causes for each failure mode
5. Rating the probability of occurrence of each root cause
6. Identifying controls and indicators of failure
7. Rating detectability of each mode or root cause
8. Calculating the risk priority number (RPN) of each root cause
9. Provide recommendations for future iterations based on prioritised risks

The RPN quantifies the risks associated with the modes of failure for the device. The RPN is calculated by multiplying the appropriate S, O and D ratings assigned to each effect. A 0-10 rating scale is used to effectively allocate appropriate S, O and D values. Table 4.5, Table 4.6 and Table 4.7 indicate the scales used to rate the S, O and D values as well as calculate the appropriate RPNs are indicated in Table 4.8.

Table 4.5: Severity Impact Rating scale

Score	*Severity Impact*
1	None - Unnoticed
2	
3	
4	
5	
6	
7	
8	
9	
10	Injury/ Render unusable

Table 4.6: Probability of Occurrence Rating Scale

Score	*Occurrence Probability*
1	Failure is unlikely
2	
3	
4	
5	
6	
7	
8	
9	
10	Failure is highly likely

Table 4.7: Detection Probability Rating scale

Score	*Detection Probability*
1	Controls certain to detect
2	
3	
4	
5	
6	
7	
8	
9	
10	Absolutely not detectable

4.5.3 FMEA model

Subsystems	*Potential Modes of Failure*	*Potential Effects of Failure*	*S*	*Potential Cause(s) of Failure*	*O*	*Current Controls*	*D*	*RPN*
LAS	Support structure buckling	Unable to apply load	10	Design flaw	3	X-ray image inspection	2	60
			10	Lack of material strength	3	X-ray image inspection	2	60
	Inability to accommodate calf diameters	Unable to perform procedure	10	Design flaw	4	Patient would not fit	1	40
	Inability to apply specified load	Additional interpolation	3	Programming / Control error	4	Visual inspection on LCD	1	12
	Inability to retract or extend actuator post procedure	Injury to the patient	10	Programming / Control error	7	Visual inspection on LCD/ X-ray	1	70
	In accurate application of load	Inaccurate results	7	Programming / Control error	7	Incomparable results to existing studies	5	245
	Sliding of anterior-lateral FSP on joint contours	Inaccurate laxity measurement results	7	Cloth-like behaviour of Velcro®	8	X-ray image inspection	2	112
	Anterior-lateral FSP slippage	Inability to apply the 250N load	6	Velcro® strap release	8	X-ray image inspection	5	240
PSS	Inability to support subject weight	Unable to perform procedure	10	Hinges contorting	6	Visual inspection/ panel failure	2	120
			10	LLSP failure (bending)	6	Visual inspection/ panel failure	4	240
			10	ULSP failure (buckling)	7	Visual inspection/ panel failure	3	210
			10	JLM pin failure (shear)	2	LLSP would fall	1	20
	Inability to withstand all loads associated with laxity measurement procedures	Unable to perform procedure	10	Hinges contorting	9	Visual inspection	4	360
			10	LLSP failure (bending)	6	Visual inspection/ panel failure	5	300
			10	ULSP failure (buckling)	10	Visual inspection/ panel failure	4	400
			10	JLM pin failure (shear)	3	LLSP would fall	1	30
	Patient limbs shift during loading procedures	Inability to apply the 250N maximum required load	8	Velcro® strap release	7	Inability to apply 250N load / visual inspection	1	56
			8	Insufficient securing of patient	7	Inability to apply 250N load / visual inspection	1	56

Table 4.8: FMEA model for Laxmeter, using a subsystem approach.

Table 4.8 indicates that the most probable modes of failure (with the highest RPNs) would be the PSS' s inability to withstand all loads associated with the laxity measurement procedures (including the 250N load, the weight of the subject's lower leg and the reaction forces generated) due to the ULSP buckling and the hinges contorting. Additional modes of failure that present a high RPN include: the inability of the LLSP to support the weight of the test subject as well as all loads associated with the laxity measurement procedures. Notable failure methods for the LAS would include the inaccurate application of the required loads as a result of programming errors as well as anterior-lateral FSP slippage due to Velcro® strap release when measuring ACL and LCL laxities.

These modes of failure would need to be prioritised for future iterations of the Laxmeter stress radiography device. Thereafter, and FMEA would need to be carried to ensure that the RPN values of the prioritised methods of failure indicated in Table 4.8 are significantly reduced to ensure a fully functional Laxmeter prototype with minimal risk of failure.

5 Experimental Methodology

5.1 Overview

This chapter details the experimental procedures for *in vitro* functional verification of the Laxmeter as a multi-ligament laxity measurement stress radiography device. Detailed information about the research hypothesis, the study population, the experimental setup and procedure, the data retrieval and analysis process, usability of the device, safety features and ethical considerations are provided in this chapter.

The experimental portion of this study consisted of three phases:

Phase 1: The *in vitro* functional verification experimental trial.

Phase 2: A comparative study of existing laxity measurement study results to the Laxmeter's performance.

Phase 3: Provide design and procedural recommendations for further iterations and experimental studies.

The study utilises standard laxity measurement procedures to determine the efficacy of the device (Bickley and Prabhu 2003; Lubowitz et al. 2008). The laxity measurement procedures would be attempted for ACL, PCL, MCL and LCL at predefined knee joint flexion angles. These angles were defined according to standard laxity measurement procedures, to allow for Phase 2 of the experimental portion of this study (Lubowitz et al. 2008). The experimental methodology flow chart is illustrated in Figure 5.1.

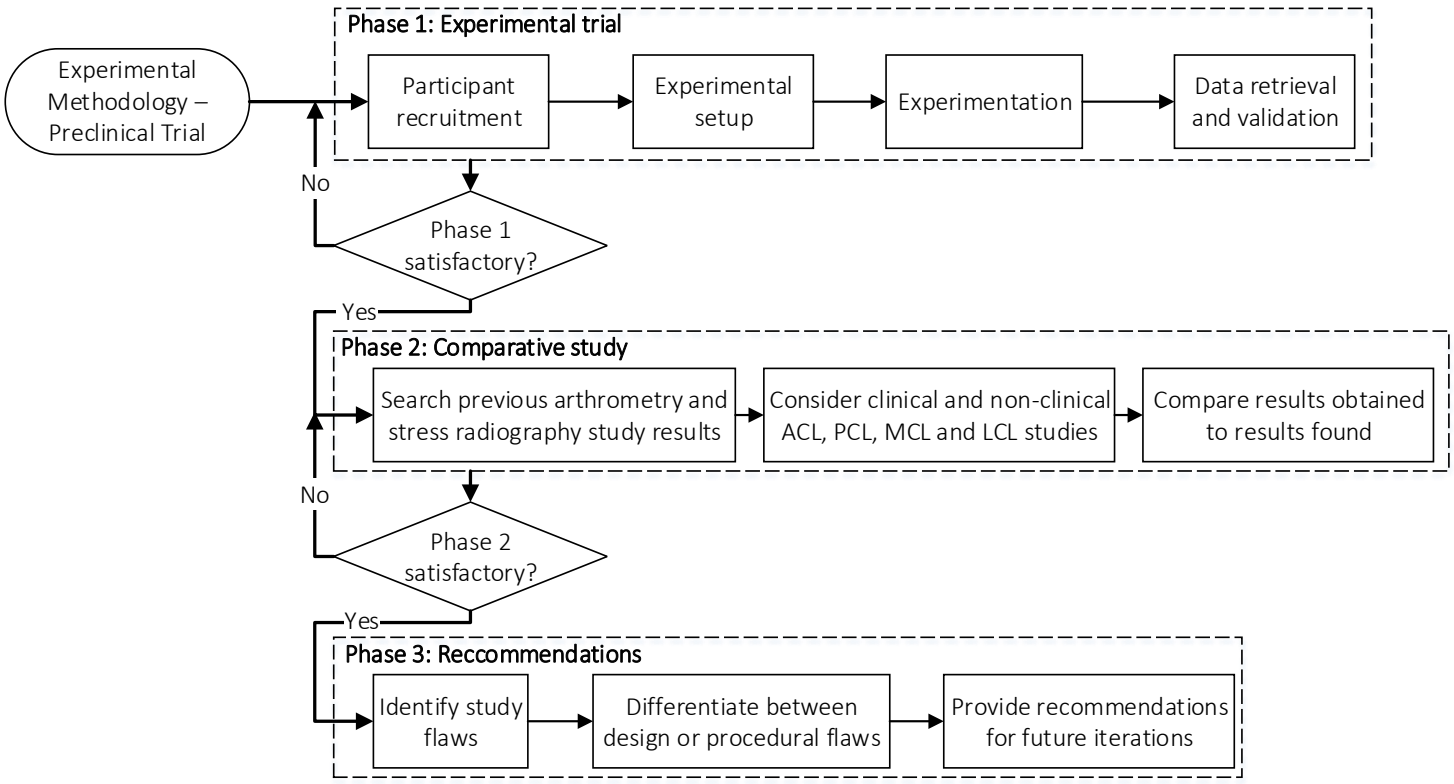

Figure 5.1: Experimental Methodology Flowchart.

5.2 Research Hypothesis

The causal research hypothesis (H_C) of this study is divided into two statements:

1. A laxity measurement stress radiography device that allows for and induces anteroposterior (AP) and mediolateral (ML) lower leg translation for measuring the laxity of the ACL, PCL, MCL and LCL at various flexion-extension angles will improve the physician's overall assessment of the knee injury.
2. Providing anatomical support and creating the ideal patient position during laxity measurement tests as well as fixating the patient's pelvis will improve the reproducibility and accuracy of the laxity measurement test results.

The alternative hypothesis (H_A) for this study is stated as follows:

A. A laxity measurement stress radiography device that allows for and induces AP and ML lower leg translation for measuring the laxity of the ACL, PCL, MCL and LCL at various flexion-extension angles will not improve the physician's overall assessment of the knee injury.
B. Providing anatomical support and creating the ideal patient position during laxity measurement tests as well as fixating the patient's pelvis will not improve the reproducibility and accuracy of the laxity measurement test results.

Phase 1

5.3 Experimental Procedure

5.3.1 Participant Recruitment

The *in vitro* verification of the study was conducted on a single fresh frozen cadaver. The test subject was subject to the availability of fresh cadavers provided by the FHS Anatomy Department, at UCT. The only exclusion criterion required intact knee joint ligaments, verified by cause of death report and visual inspection. Fresh cadavers are the preserved bodily remains (by process of freezing) of deceased people yet to undergo the embalming process. The bodily structures (muscles, ligaments and bones) of fresh cadavers are more likely to retain their natural mechanical properties as compared to embalmed cadavers. It was assumed that the cadaver had healthy knee joints and intact ligaments. Table 5.1 shows the general patient details of the cadaver provided for the experimental procedure.

Table 5.1: Test subject details.

Parameters	*Patient Details*
Age (Years)	74
Weight (kg)	73
Height (m)	1.74

5.3.2 Experimental Setup

The experimental procedure for stress radiography requires the use of an X-ray modality. The LODOX scanner was included as part of the experimental equipment setup for this study. The LODOX control program (STATSCAN) was specifically set to scan the knee joint (at 90kV and 200mA) and positioned according to the ligament under examination. The specific positions of the LODOX C-arm are indicated in Table 5.2 and shown in Figure 5.2.

Table 5.2: Experimental setup details for the different laxity measurement procedures.

Ligaments	*Patient Position*	*Angle of Flexion*	*Translation Direction*	*C-arm Position*	*Actuator position*
ACL	Supine	30° & 90°	Anteriorly	AP (90°)	Superior
PCL	Supine	30° & 90°	Posteriorly	AP (90°)	Superior
MCL	Supine	0° & 30°	Medially	Lateral (0°)	Lateral
LCL	Supine	0° & 30°	Laterally	Lateral (0°)	Lateral

The Laxmeter PSS was assembled and positioned against the inferior edge of the X-ray table surface. The knee joint flexion angle was set according to the specified ligament laxity measurement procedure (as indicated in Table 5.2). The LAS support structure was attached to the PSS (LLSP) and secured using Nylon bolts. The cadaver was placed on to the PSS, in the required position (as illustrated in Figure 5.2). In the case of ACL and PCL laxity procedures, the non-tested limb was put through the ULSP window, as illustrated in Figure 5.2(A). This was done to eliminate the interference of the non-tested limb during stress radiographic image capturing. In the case of MCL and LCL laxity measurement procedures, the position of the non-tested limb would not affect the stress radiography image, as a result, both limbs were placed on the LLSP, as illustrated in Figure 5.2(B).

The LODOX C-arm was appropriately positioned over the knee joint. The radiographic image encompassed the proximal half of the lower leg and the distal half of the upper leg. The X-ray source, situated on the C-arm of the scanner, was be positioned at 760mm from the scanning bed for lateral imaging purposes. In the case of AP imaging, the scanner was placed in the standard configuration with a fixed horizontal position from the scanning bed. However, the bed was lowered, creating a 240mm vertical distance between the radiation source and the table surface. This was done to prevent the C-arm from colliding with the actuator during scanning.

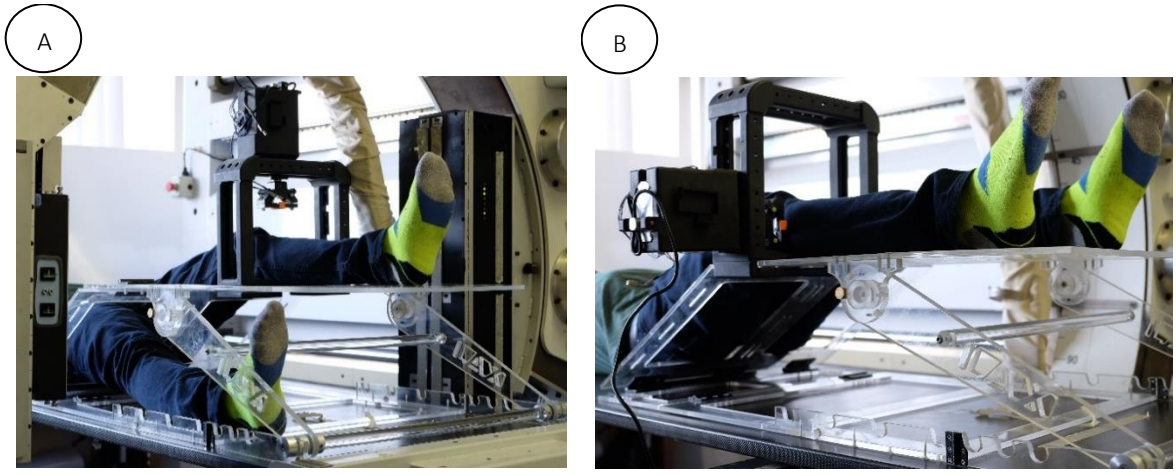

Figure 5.2: Test subject position when placed on the Laxmeter for (A) ACL and PCL as well as (B) MCL and LCL ligament laxity measurements.

The image illustrates (A) the patient placing their leg through the ULSP window during ACL & PCL laxity measurement procedures and (B) the patient placing both legs on the LLSP during MCL & LCL laxity measurement procedures. The patient positions are in consideration of the LODOX C-arm position and the non-tested limb interference during stress radiography image capturing. For (A) ACL and PCL procedures, the scanner is in the AP position whereas, for (B) MCL and LCL procedures the scanner is in the lateral position.

Once the subject was appropriately positioned on the PSS for the specified test, various body structures required securing, to inhibit unwanted movement, prior to commencing the procedure. The Velcro® straps were used to secure the subject's upper leg and the distal portion of the lower leg to the PSS. In addition, the subject's pelvis was securely fastened to the X-ray table using Velcro® strapping. This served a dual purpose: 1) inhibit pelvic movement and 2) neutralise the pelvic position to improve procedural reproducibility. The purpose of securing the subject to the PSS and the X-ray table was to ensure that translation was limited to the proximal lower leg during laxity measurement procedures.

Thereafter, the linear actuator and FSPs were attached to the LAS support structure and the subject's proximal lower leg. The electronics were connected, thereby completing the setup for the measurement procedures. The linear actuator, and the LODOX C-arm, were positioned accordingly (as indicated in Table 5.2).

5.3.3 Experimentation

The *in vitro* functional verification process through preclinical cadaver based laxity measurement trials was conducted as per the recommended standard techniques outline by Lubowitz et al. (2008). The techniques described by Lubowitz et al. (2008) correspond to the techniques described in Bates' guide to physical examination and history taking (Bickley and Prabhu 2003). Figure 5.3 summarise the entire experimental procedure.

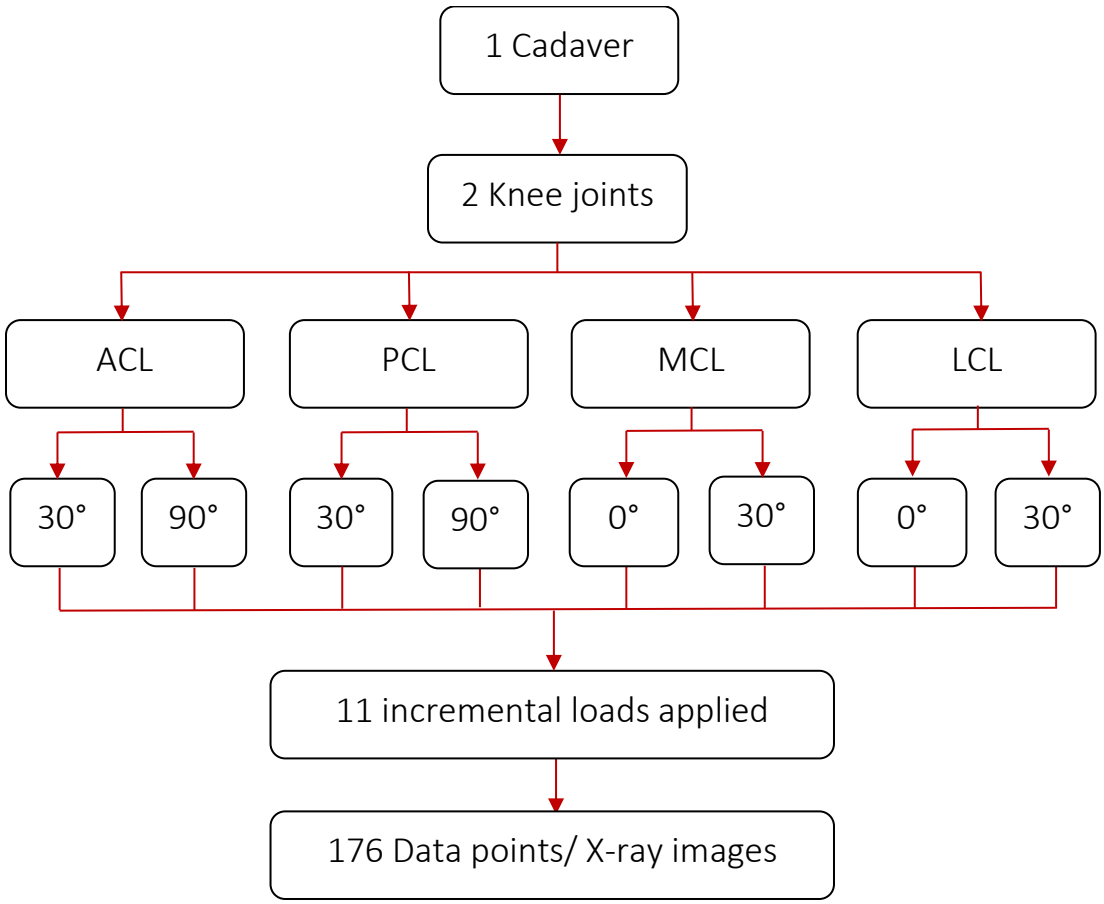

Figure 5.3: Experimentation procedural overview.

Once the test subject was appropriately positioned and secured to the Laxmeter setup, the testing procedure commenced. Table 5.3 indicates the standard measurement techniques utilised for this study.

Table 5.3: The laxity measurement techniques utilised by the Laxmeter to evaluate the Laxity of particular ligaments in the knee joint.

Ligaments	*Technique*
ACL	Anterior Drawer Test
PCL	Posterior Drawer Test
MCL	Valgus Stress Test
LCL	Varus Stress Test

5.3.3.1 ACL – Anterior Drawer Test

The Anterior Drawer Test required the subject to be in the supine position with the knee joint flexed to either 30° (from full extension) or 90°. The position of the hip joint depended on the degree of knee joint flexion. The linear actuator was placed on the superior LAS support (as illustrated in Figure 5.4(A)) and positioned above the tibial tuberosity of the lower leg. The proximal portion of the lower leg was strapped to the linear actuator with an FSP on both the anterior and posterior surfaces of the lower leg. The load was then applied to the posterior aspect of the lower leg, specifically on the medial and lateral intersections of the hamstrings by retracting the extended linear actuator. This was done until the anterior-lateral FSP read 250N. The proximal lower leg slid forward, allowing for the laxity measurement of the ACL.

5.3.3.2 PCL – Posterior Drawer Test

The Posterior Drawer Test required the subject to be in the supine position with the knee joint angles flexed to 30° (from full extension) or 90°. The distal portion of the subject's lower leg was constrained. The linear actuator was positioned as described for the Anterior Drawer Test and the lower leg was strapped to the linear actuator with an FSP on both the anterior and posterior surfaces of the proximal lower leg. The load was then applied to the anterior face of the lower leg by extending the fully retracted linear actuator. This was done until the posterior-medial FSP read 250N. The posterior translation of the tibia allowed for the laxity measurement of the PCL, however, isolated PCL tears are rare (Bickley and Prabhu 2003).

5.3.3.3 MCL – Abduction Stress Test

The Abduction (Valgus) Stress Test required the subject to be in a supine position and the knee joint flexed to 0° (full extension) and 30° (from full extension). Additionally, the subject's leg was abducted approximately 30° from the sagittal plane. The distal portion of the lower leg was constrained, particularly on the medial aspect. The linear actuator was placed on the lateral LAS support (as illustrated in Figure 5.4(B)) and positioned adjacent to the fibula. The subject's proximal lower leg was strapped to the linear actuator with FSPs on both the medial and lateral aspect of the lower leg. The load was applied to the lateral aspect of the knee by means of a pushing force as a result of extending a retracted linear actuator. This was done until then posterior-medial FSP read 250N. This arrangement opened up the knee joint on the medial side to measure the laxity of the MCL.

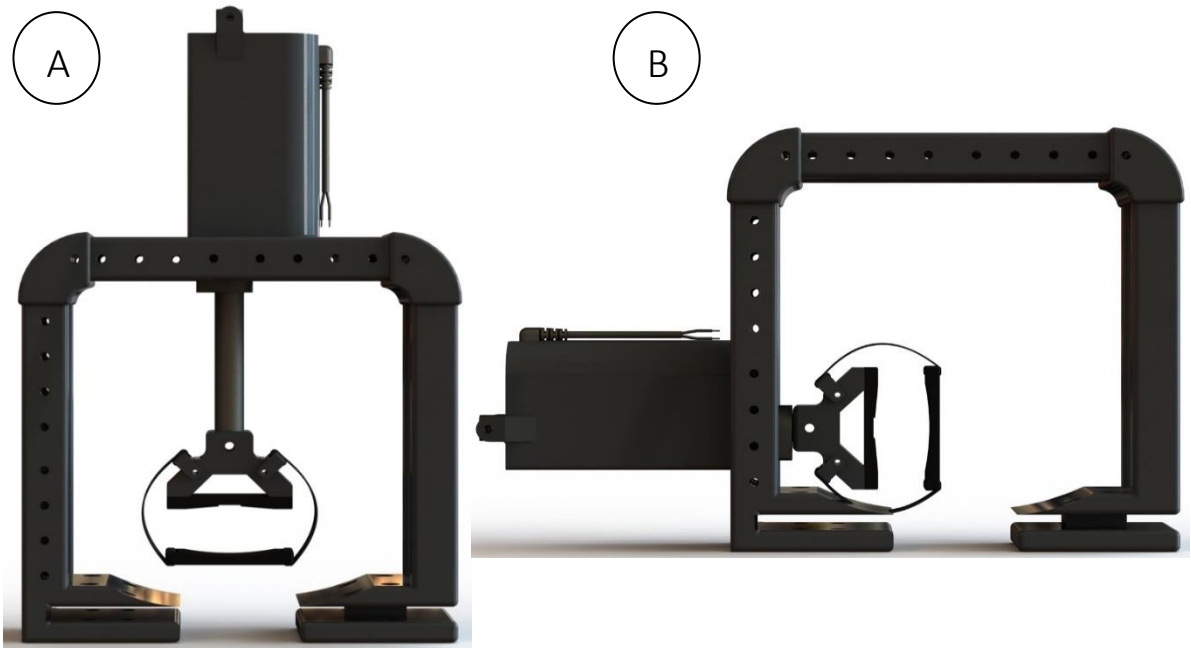

Figure 5.4: The linear actuator in position for (A) ACL and PCL as well as (B) MCL and LCL laxity measurements.

The image illustrates the linear actuator attached to: (A) the superior support of the LAS support structure during ACL and PCL laxity measurement procedures as well as (B) the lateral support of the LAS support structure during MCL and LCL laxity measurement procedures.

5.3.3.4 LCL – Adduction Stress Test

The Adduction (Varus) Stress Test required the subject to be in the supine position with the knee joint flexed to 0° (full extension) and 30° (from full extension). The subject's leg was abducted approximately 30° from the sagittal plane of the body. The distal portion of the lower leg was constrained, particularly on the lateral aspect of the leg. The linear actuator was placed on the lateral support as illustrated in Figure 5.4(B). The proximal portion of the lower leg was strapped to the linear actuator with the FSPs on both the medial and the lateral aspect of leg. The load was applied to the medial aspect of the knee joint by means of retracting an extended linear actuator. This was done until the anterior-lateral FSP read 250N. This particular arrangement opened up the knee joint on the lateral side, which made it possible to measure the laxity of the LCL.

5.4 Radiographic Data Retrieval

The loads applied to the proximal lower leg were done so in 25N increments. At each increment, a radiographic (X-ray) image of the bone translation was captured and recorded as a data point. A total of eleven data points were recorded for each laxity measurement procedure. A laxity measurement procedure was defined according to a specified limb (right or left) and a particular ligament at a predefined angle of joint flexion. Table 5.4 indicates the incremental loads applied to the proximal lower leg for each laxity measurement procedure. The initial data point (0N) was the origin/ resting position prior to load application. Both the right and left knee joints were tested for comparative purposes, to identify any discrepancies between limb translations, due to unforeseen ligament damage or irregularities.

Table 5.4: Incremental loads applied to the proximal lower leg for each laxity measurement technique.

Load (N)	*Data Point*
0	1
25	2
50	3
75	4
100	5
125	6
150	7
175	8
200	9
225	10
250	11

Each stress radiographic image or data point (as illustrated in Figure 5.5) was captured and stored on the LODOX scanner operating computer and an external memory drive. The radiographic images were stored as DICOM files to allow for contrast manipulations during data analysis. An organised method of storing the images was carried according to the following example:

Subject number – Right or left knee – Ligament – Degree of flexion – incremental load.DCM

Example: Subject 1 – Right knee – ACL – 30 deg – 25N.DCM

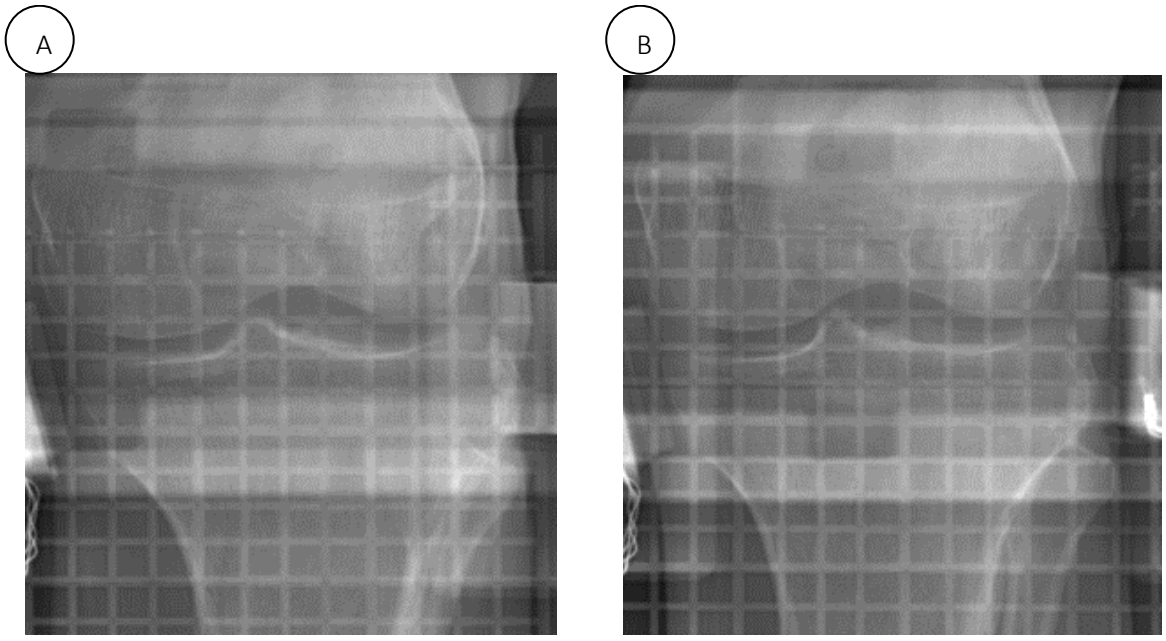

Figure 5.5: Stress radiography images obtained during 0° (full extension) left knee joint flexion, MCL laxity measurement procedures, at: (A) 0N and (B) 250N.

The image illustrates the laxity measurement stress radiographs captured by the LODOX scanner for the following procedure: Subject 1 - Left knee – MCL – 0 deg. – (A) 0N and (B) 250N.

5.5 Data Analysis

The translation of the lower leg relative to the femur was measured, verified and validated. The offset of the tibia was measured in comparison to the position prior to load application (0N). RadiAnt DICOM (DCM) Viewer software was used to analyse the stress radiography images. The program is open source and has a built-in measuring tool, which was used to measure the bone translation and as a result, the knee joint ligament laxities. The measurement technique described by Staubli and Jakob (1991)was adopted to measure the laxity of the ACL and PCL. However, the technique described by Jacobsen (1976) was used to determine the laxity of the MCL and LCL.

The MCL and LCL laxity measurement technique described by Jacobsen (1976)and Liu et al. (2013), as shown in Figure 5.6, was considered an appropriate and reproducible means of measuring the knee joint bone distraction. The technique describes a configuration of four lines. The first line was drawn tangential to the tibial condylar plateaus. The second line was drawn tangential to the femoral condyles. The third line was drawn perpendicular to the first line and adjacent to the tibial condyle on the aspect of the bone to be measured. The laxity measurement result was the distance between lines one and two, along line three.

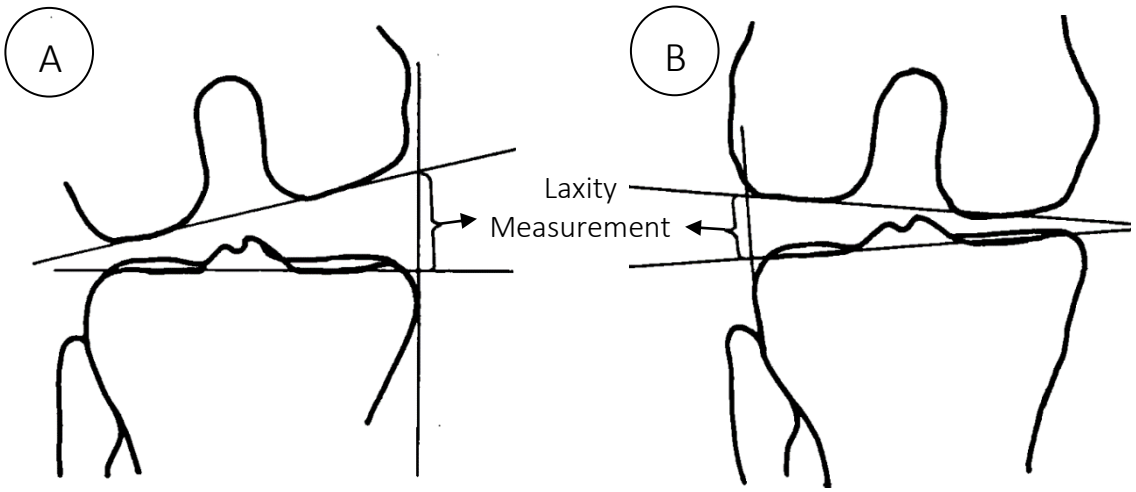

Figure 5.6: Laxity measurements, by means of bone distraction, for the (A) MCL and (B) LCL (image credit: (Jacobsen 1976)).

The image illustrates the laxity measurement technique according to Jacobsen (1976) and Liu, et al. (2013). This laxity measurement methodology was adopted for this study as it was considered the most reproducible means of measuring bone distraction and laxity.

The ACL and PCL laxity measurement technique (shown in Figure 5.7) described by Staubli and Jakob (1991) was considered the most appropriate and reproducible means of measuring the bone distraction. A configuration of lines was used to measure the tibial translation. The first line was drawn along the projected posterior tibial cortex (PTC). A second and third line was drawn tangential to the most posterior aspect of the medial and lateral tibial plateaus, parallel to the PTC. A fourth and fifth line was drawn tangential to the most posterior aspect of the medial and lateral femoral condyles, parallel to the PTC. The average distance between the second and fourth lines as well as the third and fifth lines defined the laxity of the ACL and PCL.

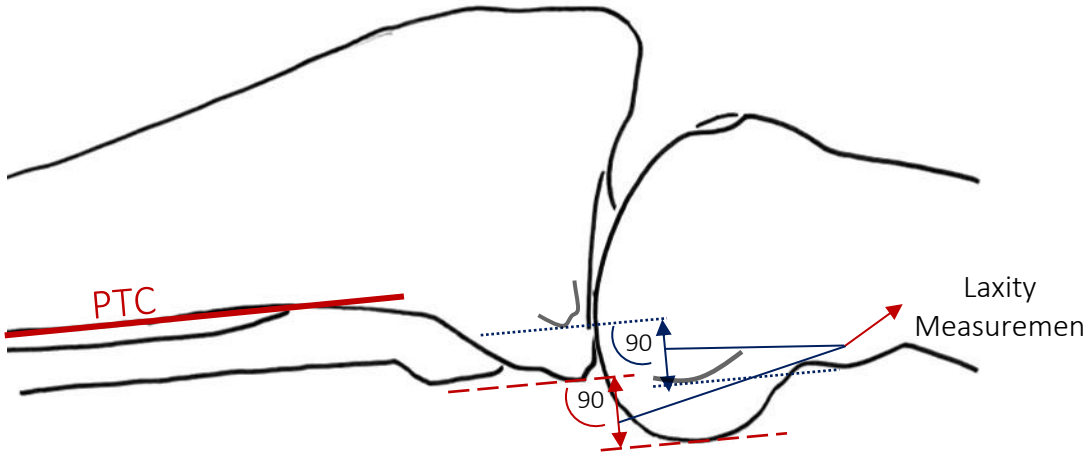

Figure 5.7: Laxity measurement, by means of bone distraction, for the ACL and PCL (image credit: (Staubli and Jakob 1991)).

The image illustrates the laxity measurement technique described according to Staubli & Jakob (1991). This technique was assumed to be the most appropriate and reproducible means for measuring ACL and PCL laxity at various degrees of knee joint flexion.

Phase 2

5.6 Outcome Measures

5.6.1 Research Study

The results obtained for the laxity measurement data analysis were processed and compiled. A graphical representation was produced allowing for the comparison of the left and right knee joint laxity measurement results. In addition, the distraction and translation results were further represented in a manner which allowed for the comparison of laxity measurements from previous studies using similar measurement and analysis techniques. The selection criterion for previous studies used for comparative purposes included:

- Arthrometer and stress radiography results.
- Clinical and cadaver trials.
- A range of loads, between 0N and 250N, applied to the knee joint.
- Consider laxity measurement results indicating range and standard deviations.
- Only healthy knee joints.
- ACL, PCL, MCL and LCL laxity measurements.

To prove the functional efficacy of the Laxmeter as a multi-ligament laxity measurement device, the study results were compared to that of existing research. A positive indication of the Laxmeter's potential functional efficacy was a similar/ comparable laxity measurement result. A similar or comparable laxity measurement result was determined when the Laxmeter's measurement result fell within the range or standard deviation according to existing studies.

5.6.2 System Usability

The Laxmeter was designed, taking into account the assembly and disassembly process of the device. The assembly process was designed to be timely and efficient. The entire setup process of the device involved placing the device on the table, unfolding the PSS and adjusting the knee joint angle. The subject was put on the structure and firmly secured in position, and the LAS fitted to the PSS. Finally, the FSPs were zeroed, and the testing sequence could commence.

The ISO (International Organisation for Standardisation) 9241-210: 2010 provides the minimum requirements for human-centred design principles and activities for the given life-cycle of computer-based interactive systems. The standard provides recommendations for, and assists with, the management of the design processes and the importance of how human-system interaction can be enhanced by hardware and software components of interactive systems. The standard provides assistance and recommendations to improve the usability of the system/ device. The standard considers effectiveness, efficiency and satisfaction as an evaluation criterion. Effectiveness describes how well the system meets the design requirements; efficiency describes the resources expended to achieve effectiveness and satisfaction describes the human factor acceptance as well as willingness to use the system.

The Laxmeter, however, was operated by an internal party during the cadaver trial. Therefore, evaluating system usability would be biased and subjective. As a result, the system usability was evaluated by considering whether the device was able to carry out the necessary laxity measurement procedures (effectiveness), the resources required to achieve effectives and the ease at which this was accomplished. This was an important consideration since the device was designed to accommodate for ease of use.

Phase 3

5.7 Provide Future Recommendations

The nature of this study yields scope for improvement outlined by recommendations to improve future iterations of the Laxmeter and prove the efficacy of the device. Recommendations were provided as a result of the experimental study. The laxity measurement methodology is of equal importance to the design methodology. Both the procedure and the device design was considered and the appropriate recommendations would be made. The nature of a device design study is that the theoretical and the physical aspects of design, inevitably do not always coincide. This is the basis of why a functional experimental (preclinical) trial or study is essential, leading to a full scale clinical trial, for a device in the field of biomedical engineering.

5.8 Ethical Considerations

5.8.1 Informed Consent and Approval

The study was conducted on a full bodied, fresh frozen cadaver. An ethics application was filed to the Human Research Ethics Committee (HREC) of the UCT. Ethical approval was mandatory prior to commencing the laxity measurement procedures. The UCT FHS Anatomy Department had to be informed that no incision would be made on the cadaver during the experimental study. The protocol for this experimental study was reviewed by two senior academic staff members, prior to filing for the HREC approval, to ensure ethical conduct was implemented during the study. The cadaver was treated with the utmost respect as the operator was fully aware of the ethical procedures and requirements. The approval was granted and the award letter from the HREC has been attached in Appendix D.

5.8.2 Privacy

The cadaver's identity was concealed, including any personal information. All data retrieved during the study was labelled as Subject 1, to ensure that the identity of the deceased remained confidential. The study considered all personal participant-related information confidential for its entire duration.

6 Experimental Outcomes

6.1 Introduction

This section details the quantitative outcome of the Laxmeter's efficacy as a multi-ligament laxity measurement stress radiography device. The validation of functionality, usability and integrity was achieved using a single cadaver trial (illustrated in Figure 6.1). The various laxity measurement procedures were carried out, the radiographs were processed and the measured Translation (laxity) vs Load Applied values were plotted. A statistical analysis of the results was not possible due to the inadequate sample size. A comparison would be drawn between the ligament laxities measured from the right and left knee joints to assess reproducibility and verify the assumed intact state of the subject's ligaments. The efficacy of the device was demonstrated by comparing the results obtained from this study (interpolated average laxity of the left and right knee joints) to previous knee joint ligament laxity measurement studies. The limitations of the Laxmeter will be detailed in this chapter, to provide informed recommendations (design and procedural based) for future iterations and validation procedures.

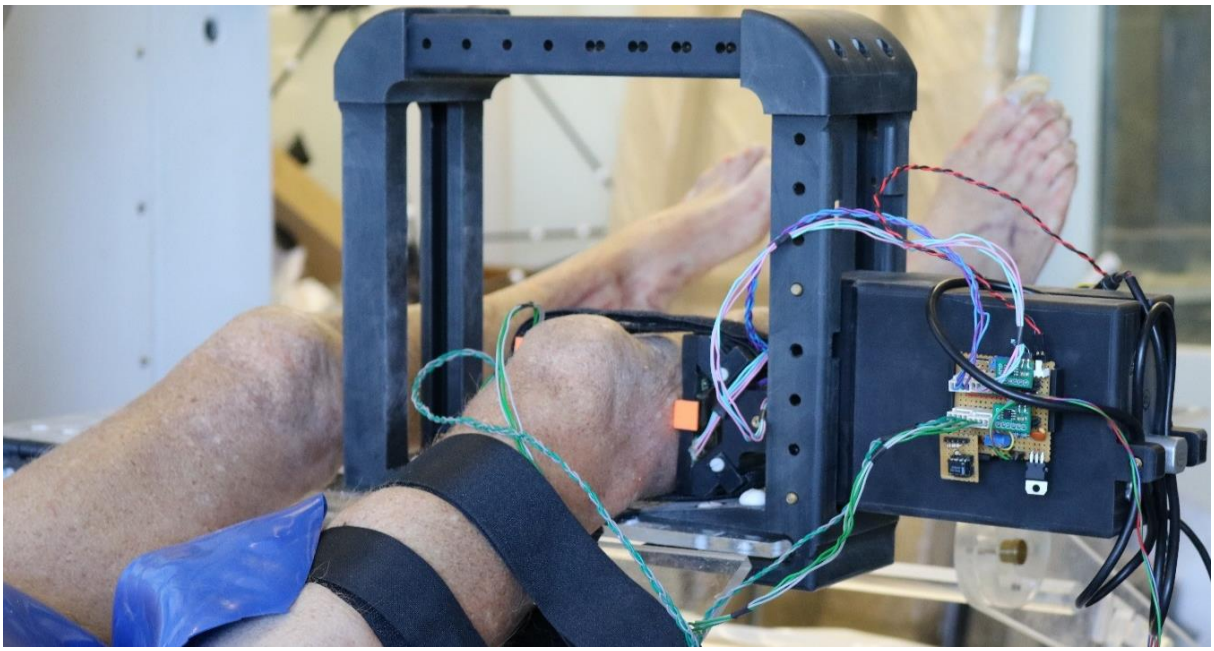

Figure 6.1: MCL laxity measurement procedure (at 30° flexion) before initiating the Laxmeter cadaver trial.

The image illustrates the test subject (cadaver- Subject 1) placed on the Laxmeter and safely secured, before initiating the MCL laxity measurement procedure for the right knee joint.

Table 6.1 compares the Laxmeter's interpolated average ACL, MCL and LCL laxity measurement results, at 30˚ knee joint flexion, to those obtained from previous laxity measurement studies. The ACL results fell within the range of most previous ACL laxity measurement studies, suggesting the Laxmeter's potential to measure ACL laxity accurately. The MCL and LCL results were inconclusive given the limited existing studies, however, in comparison to the more recent research, the Laxmeter performed on par with existing devices.

Table 6.1: The Laxmeter's linear average (right and left knee joint) laxity measurement translation results, in millimetres (mm), at 30° knee joint flexion as a result of various applied loads compared to results obtained from previous studies.

	Load Applied (N)						Sample size
	89[¶]	100	134[¶]	150	200	250	
Anterior Cruciate Ligament (ACL)							
[*‡¶]The Laxmeter	1.6[¶]	1.82	2.48[¶]	2.80	3.78	4.76[¶]	1 cadaver
[*§¶](Markolf et al. 1976)		4.44 ± 2.2[¶‡‡]					35 cadaver knees
[*§](Robinson et al. 2006)				3.5 - 4[‡‡]			18 cadaver knees
[*§¶](Sbihi et al. 2004)				3.28 ± 1.2[¶††]			16 cadaver knees
[*§](Daniel et al. 1985)	2.8-11						33 cadavers
[†‡](Jacobsen 1976)					0 - 7[††]		50 participants
[†§](Boyer et al. 2004)	4.2 ± 2.4[††]						147 participants
[†‡](Boyer et al. 2004)						3.0 ± 3.6[††]	147 participants
[†§¶](Collette et al. 2012)			2.3 ± 0.85[¶††]				15 participants
[†§¶](Collette et al. 2012)			3.15 ± 0.9[¶††]				15 participants
[†§](Leferve et al. 2014)						5 +[‡‡]	139 participants
Medial Collateral Ligament (MCL)							
[*‡]The Laxmeter	0.62[¶]	0.71	0.99[¶]	1.11	1.52	1.92	1 cadaver
[†‡](Jacobsen 1976)	5.5 - 11						50 participants
[†‡**](Liu et al. 2013)				1.1 ± 0.9[**††]			19 participants
Lateral Collateral Ligament (LCL)							
[*‡]The Laxmeter	1.13[¶]	1.29	1.79[¶]	2.02	2.76	3.49	1 cadaver
[†‡](Jacobsen 1976)	9.2 - 16.9						50 participants
[†‡](Jacobsen 1977)	0.1 - 1.8[††]						151 participants

The previous laxity measurement studies considered, were categorised according to the test subject as well as the laxity measurement device used. A study can be categorised as a cadaver study (*) or a clinical study (†). In addition, the two laxity measurement device classifications were considered namely: a stress radiography device (‡) and an arthrometer (§). In some cases, the laxity measurement results at 30° knee joint flexion and a particular load were interpolated (¶) to achieve a more comprehensive comparison with the Laxmeter's results. In addition, due to limited availability of MCL laxity measurement studies, a post ligament reconstruction surgical study (**) was considered. If the Laxmeter's results fell within the standard deviation (±) or range (-) as found by existing studies, the positive result is indicated with the symbol (††). A small variance in the results comparison is shown by the symbol (‡‡), and a negative result is indicated by omitting a symbol.

6.2 MCL Procedural Results

The results from the MCL laxity measurement procedures are detailed in this section. The stress radiographs for the MCL laxity measurements were processed, and the data plotted accordingly. The standardised laxity measurement procedures required measurements to be carried out at both 0° (full extension) and 30° (from full extension) knee joint flexion. Both the right and left knee joint MCL laxity measurement results are shown for comparative purposes.

6.2.1 0˚ Knee Flexion

Figure 6.2 illustrates the results obtained for the MCL laxity measurement procedures at 0° knee joint flexion (full extension). The figure shows the bone distraction at a specific load compared to the initial position i.e. the initial distance between the tibia and femur, at 0N, which was subtracted from all proceeding measurements to determine the laxity of the ligament.

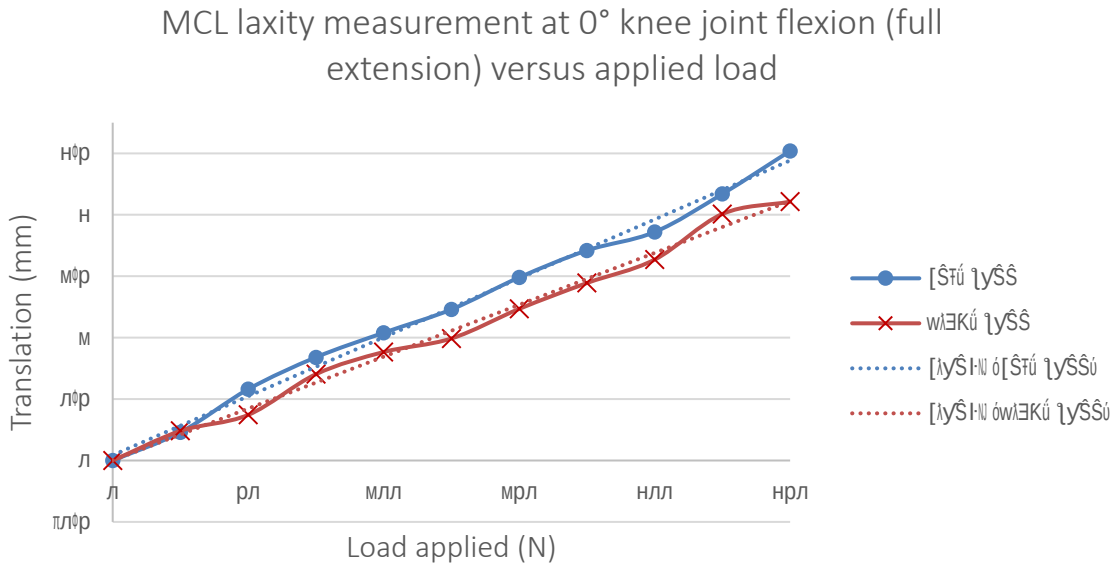

Figure 6.2: MCL laxity measurement results for 0° knee joint flexion (full extension) procedure.

The image illustrates the MCL laxity measurement results at 0° knee joint flexion, for both knee joints. The results indicate a maximum laxity measurement of 2.52mm (left knee), potentially indicating that the ligaments are still intact and healthy.

The MCLs were successfully loaded to 250N and the radiographs captured as well as recorded for each incremental load. The initial position for the right and left knee joints were measured to be 4.72mm and 4.38mm respectively. The bone distraction for the right and left knee joints, as a result of the 250N applied load, was measured to be 6.82 and 6.9 respectively. This resulted in an MCL laxity measurement of 2.11mm for the right knee joint and 2.52mm for the left knee joint. The comparative laxity measurement results between the right and left knee joints were found to varying by 16%, considering the 250N load applied. The laxity measurement procedures yielded satisfying results, on the basis of the maximum bone distraction being 2.52mm. According to the Hughston's grading system, the results indicate that the subject's MCLs are indeed healthy and intact as was assumed prior to undergoing the experimental validation procedure (Phisitkul et al. 2006).

6.2.2 30˚ Knee Flexion

Figure 6.3 illustrates the MCL laxity measurement results, at 30° flexion (from full extension), for the both the right and left knee joints. The figure illustrates the incremental bone distraction from initial position (0N) to final position as a result of the 250N load applied.

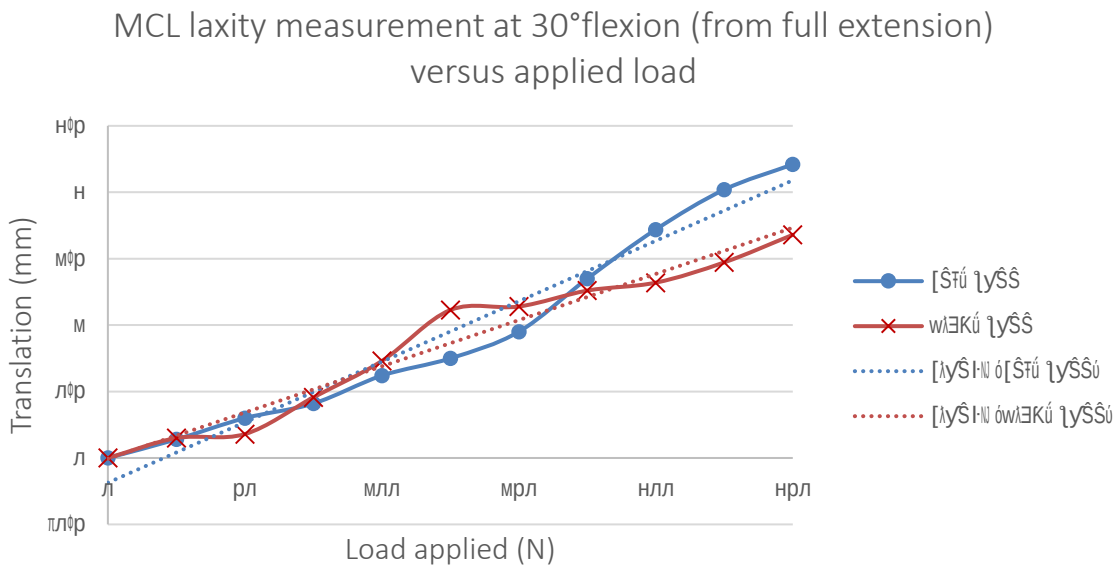

Figure 6.3: MCL laxity measurement results for 30° knee joint flexion (from full extension) procedure.

The image illustrates the MCL laxity measurement results at 30° knee joint flexion, for both knee joints. The results indicate a maximum laxity measurement of 2.21mm (left knee), thereby potentially indicating that the ligaments are still intact and healthy.

The ligaments were successfully loaded from 0-250N, in 25N increments, and the translation radiographs were captured for each incremental load. The initial position bone distraction values for the right and left knees were measured to be 6.72mm and 5.46mm. The final bone distraction measurements for the right and left knees were 8.4mm and 7.67mm. Thereby resulting in a laxity measurement of 1.68mm and 2.21mm, at a load of 250N respectively. The laxity measurement values differed by 23.98%. However, the yielded laxity results indicated that the subject's MCLs were healthy and intact, according to the Hughston's grading system, which supports the assumption made prior to initiating the experimental validation procedure (Phisitkul et al. 2006).

Although previously existing MCL laxity measurement studies that make use of a similar analysis technique as described by Jacobsen (1976) are limited, the Laxmeter's linear average measurements were found to yield inconclusive results in comparison (as indicated in Table 6.1). When compared to a laxity measurement of 5.5-11mm at an 89N applied load, as obtained by Jacobsen (1976), the Laxmeter yielded an linear average laxity of 0.62mm at a 89N load, which is not within the range. However, when compared to a laxity measurement of 1.1mm (with a standard deviation of 0.9mm) at 150 N obtained by Liu et al. (2013), the Laxmeter performed satisfactorily yielding a linear average laxity of 1.11mm at 150N. This is within the standard deviation and therefore produces an acceptable result, suggesting that the Laxmeter could potential perform on par with the techniques described by Liu et al. (2013).

6.2.3 Discussion

The Laxmeter performed satisfactorily considering that the device successfully applied a 250N load to the lateral aspect of the proximal lower legs of the test subject. In addition, the laxity measurement results suggest that the ligaments are healthy as the laxity was measured to be less than the Grade 1+ laxity class (3-5mm), which indicates ligament tenderness but no instability according to Hughston's grading scale (Phisitkul et al. 2006). This result supports the assumption that the ligaments within the subject's knee joints are intact and healthy. The comparative study (indicated in Table 6.1), suggests that the Laxmeter performed satisfactorily (with an linear average laxity of 1.11mm) when compared to a more recent study of a similar nature, which produced a laxity measurement of 1.1 ± 0.9mm (standard deviation) at 150N (Liu et al. 2013). However, considering the results according to Jacobsen (1976), the validity of the Laxmeter as a potential MCL laxity measurement stress radiography devices is inconclusive.

The MCL laxity measurement results, comparing the right and left knee joints differed by 16% for 0° flexion (full extension) and 23.98% for 30° flexion (from full extension). Although the results produced are satisfactory and potentially support the initial assumption made, the difference in the laxity measurement results for the right and left knee joints, however common in previous studies, could be explained by the following (Robert et al. 2009; Collette et al. 2012):

- Human error
- Right lower leg injury
- Procedural limitations

The radiographs were analysed by visually inspecting the images and manually measuring the bone distraction. The technique described by Jacobsen (1976) and Liu et al. (2013) makes use of a configuration of lines to measure the laxity of the ligament. As a result, inaccuracies may occur when determining the specific landmarks, on the radiographs, where the lines need to be drawn.

Before carrying out the laxity measurement procedures, the knee joint was inspected to determine the health of the joint by identifying scars around the joint area. Although the knee joints were found to be healthy and the ligaments intact, the radiographs revealed a severe right leg tibial fracture. Although this injury does not directly affect the knee joint, it could potentially have led to antalgic gait, resulting in overly strained ligaments.

The LAS operated within a load applied accuracy range of ±5N. After applying each incremental load, the actuator locked in position and stalled, thus allowing time for the radiographic image to be taken. During this period, the Velcro® straps released their hold on the limbs while the LODOX scanner was capturing the image. The time taken to capture a radiographic image, along the given scanning area (from the moment the scanner lever was pulled to the time of release) was approximately 20s. As a result, a timelier or less timely stalling period would yield varied laxity measurement results.

6.3 LCL Results

The LCL laxity measurement results are detailed in this section. The stress radiographs were captured and analysed and the results plotted accordingly. The standard laxity measurement procedures for LCL laxity required measurements at a knee joint flexion angle of 0° (full extension) and 30° (from full extension). The results of both the right and left knee joint laxity measurements were plotted and are depicted below.

6.3.1 0˚ Knee Flexion

Figure 6.4 illustrates the laxity measurement results for the LCL at 0˚ knee joint flexion (full extension). The figure illustrates the bone distraction, on the lateral aspect of the knee joint, due to the load applied by the Laxmeter's LAS. The differences between the right and left knee joint laxity measurements are clear and allow for the comparative analysis of the laxity measurements to evaluate the capabilities and reproducibility of the Laxmeter.

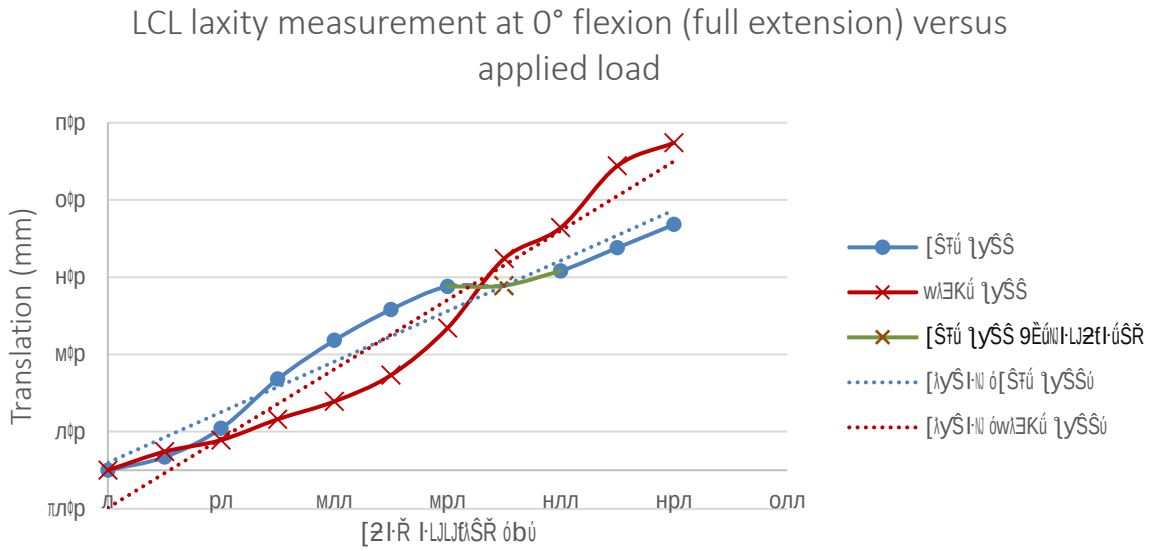

Figure 6.4: LCL laxity measurement results for 0° knee joint flexion (full extension) procedure.

The image illustrates the LCL laxity measurement results at 0° knee joint flexion (full extension), for both knee joints. The results indicate a maximum laxity measurement of 4.24mm (right knee), potentially indicating that the ligaments are potentially lightly sprained in both knees.

The ligaments were successfully loaded to 250N and all but one radiographic image was captured and recorded for each incremental load. The radiographic image captured at the 175N increment, for the left knee, was corrupt and discarded. The initial (0N) bone distraction measurements for the right and left knee joints, were measured to be 8.66mm and 9.32mm respectively. The distraction for the right and left knee joints, as a result of the 250N load, was measured at 12.9mm and 12.5mm. The laxity of the right and left LCLs at 0˚ knee joint flexion (full extension) were 4.24mm and 3.18mm respectively. The final laxity measurement results (at 250N) varied by 25%. The laxity measurement results were satisfactory, indicating a mild sprain of the ligament, considering a maximum bone distraction of 4.24mm according to the Hughston's grading system (Phisitkul et al. 2006). This result supports the assumption that the cadaver has intact LCLs, noting the potential right knee joint LCL sprain.

6.3.2 30˚ Knee Flexion

Figure 6.5 illustrates the results obtained during the LCL laxity measurement procedures, conducted at a knee joint flexion angle of 30° from full extension. Both the right and left knee joint laxity measurements are plotted, to allow for comparison of the results. The depiction of the bone distraction as a result of applying the 0-250N incremental load to the lateral aspect of the knee joint, is illustrated in Figure 6.5.

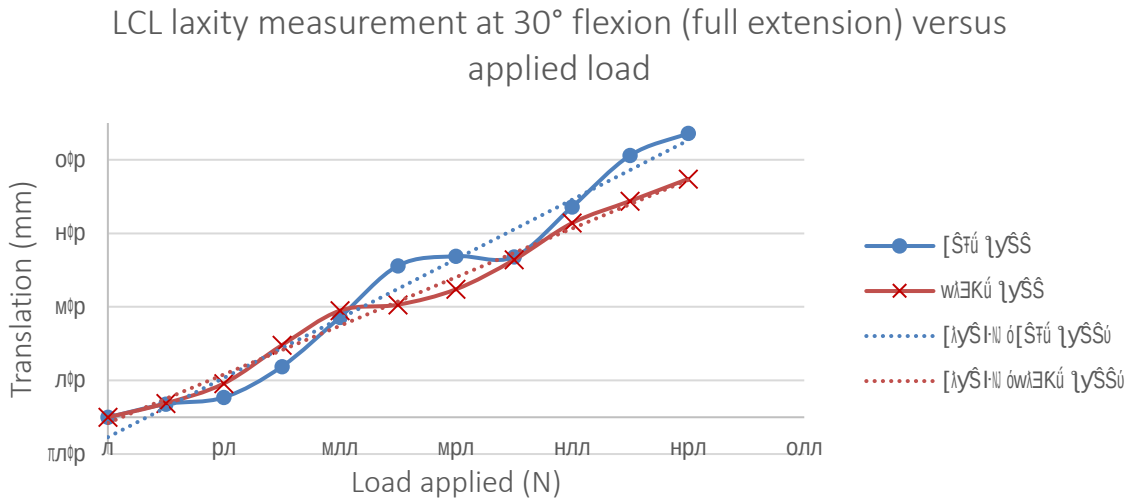

Figure 6.5: LCL laxity measurement results for 30° knee joint flexion (full extension) procedure.

The image illustrates the LCL laxity measurement results at 30° knee joint flexion (from full extension), for both knee joints. The results indicate a maximum laxity measurement of 3.86mm (right knee), potentially indicating that the ligaments are potentially lightly sprained in both knees.

The LCLs were both loaded to a maximum of 250N in increments of 25N. The translation radiographs were successfully captured for each incremental load and analysed using the technique described by Jacobsen (1976) and Liu et al. (2013). The initial rest position (0N) results for the right and left knee joints were measured at 8.36mm and 8.94mm. The bone distraction due to the 250N load was 11.6mm and 12.8mm. As a result, the laxity of the LCLs due to the 250N loads was 3.24mm and 3.86mm. The laxity results differed by 16.06%, however, according to the Hughston's grading scale, both ligaments would be diagnosed as intact but lightly sprained (Phisitkul et al. 2006). This once again supports the assumption that the LCLs within the knee joint are intact, noting the light sprains.

Previous studies concerning LCL laxity measurements, making use of a similar technique as described by Jacobsen (1976), involving arthrometers and stress radiography devices were limited. However, of the studies found, the Laxmeter's measurements yielded an inconclusive comparative result. Compared to a laxity measurement of 9.2-16.9mm at an applied load of 89N, as found by Jacobsen (1977), the Laxmeter yielded a negative result with a linear average laxity of 1.13mm at 89N, which does not fall within the 9.2-16.9mm range. However, when compared to an LCL laxity of 0.1-1.8mm at 89N load, as found by Jacobsen (1977), the Laxmeter performed satisfactorily yielding a linear average laxity of 1.13mm, which is within the desired range. This suggests that the Laxmeter could potentially perform on par with the techniques described by Jacobsen (1977) and effectively perform LCL laxity measurement procedures.

6.3.3 Discussion

The Laxmeter performed satisfactorily in three main areas of the experimental study. First, the Laxmeter was able to successfully apply a 250N load to the medial aspect of the knee joint and induce bone distraction, resulting in a laxity measurement. Second, the laxity measurement results indicated a light sprain of both LCLs, according to Hugston's grading scale. This supports the prior notion that the cadaver possesses healthy knee joints, comprised of intact ligaments. Finally, the comparative study (as indicated in Table 6.1) revealed that the Laxmeter can produce LCL laxity measurement results similar to that of more recent studies i.e. The Laxmeter's linear average laxity of 1.13mm compared to 0.1-1.8mm at 89N (Jacobsen 1977). This suggests that the Laxmeter could potentially perform LCL laxity measurement procedures accurately and reproducibly to compete with existing devices.

Although the LCL laxity measurement results were satisfactory and showed potential, a key point to note was the difference between the right and left knee joint laxity measurement results. The LCL laxity measurement results comparing both limbs indicated a 25% difference at 0° (full extension) and 16.06% difference at 30° (from full extension). These differences in laxity measurement values, and the right knee joint LCL sprain (as 0°knee flexion/ full extension), could be explained by various factors, including those detailed in Section 6.2.3 Discussion. An additional factor, however, was the FSP shifting.

During the LCL laxity measurement procedures, the anterior-lateral FSP shifted slightly (as shown in Figure 6.6). This was due to the non-rigid Velcro® attachment of the FSP to the linear actuator. The use of Velcro® strapping meant that the FSP was not restricted to the operating plane of the actuator. The FSP shifted along the medial aspect of the joint, due to the sloping anatomical structures. The change of position due to the FSP shifting, resulted in a decreased load applied in the actuators operating plane, potentially affecting the accuracy of the laxity measurement results.

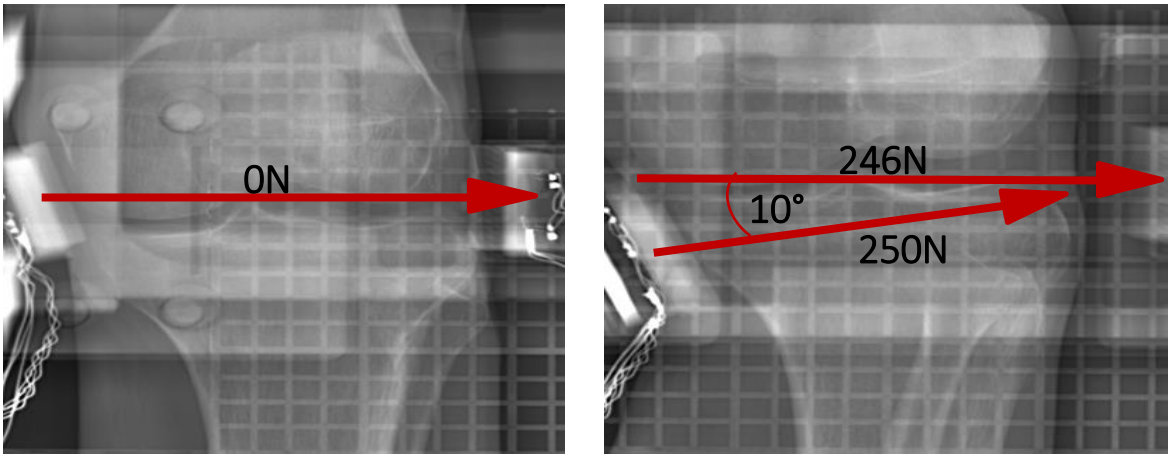

Figure 6.6: Shift of anterior-lateral FSP during left leg LCL laxity measurement procedures at 30° knee joint flexion.

The image illustrates the anterior-lateral FSP shifting as a result of the applied load. The force in the actuator's plane of operation is reduced from 250N to 246N, due to the FSP shift along the medial aspect of the joint.

6.4 ACL Results

The ACL laxity measurement results are detailed in this section. The standard ACL laxity measurements are required at a knee joint flexion angle of 30° and 90°. However, when configuring the Laxmeter for ACL laxity measurements at a 90° knee joint flexion angle, the Laxmeter would not fit beneath the C-arm of the LODOX scanner. The distance between the LODOX scanner table (on its lowest setting) and the C-arm was measured to be 760mm. The height of the Laxmeter in the 90˚ ACL laxity configuration is 865mm, proving that the 90° ACL laxity measurement procedure was found to not be possible with the available equipment. As a result, the ACL laxity measurement procedures were limited to only 30° (from full extension) knee joint flexion angles. Both knee joints underwent the laxity measurement procedure and the results thereof are illustrated in Figure 6.7.

6.4.1 30˚ Knee Flexion

Figure 6.7 illustrates the laxity measurement results for the ACL at 0˚ knee joint flexion (full extension). The figure illustrates the degree of tibial translation due to the load applied by the Laxmeter's LAS. The differences between the right and left knee joint laxity measurements are depicted in the figure and allow for the comparative analysis to evaluate the laxity measurement capabilities and reproducibility of the Laxmeter.

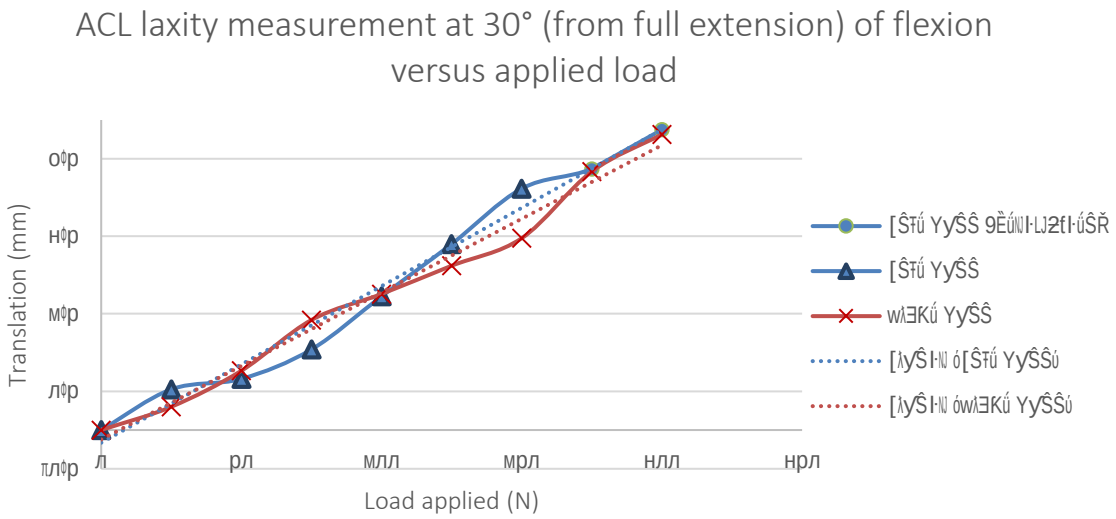

Figure 6.7: ACL laxity measurement results for 30° knee joint flexion (full extension) procedure.

The image illustrates the ACL laxity measurement result for both knee joints at a 30° flexion angle, from full extension. The laxity measurement results indicate a maximum laxity measurement of 3.82mm, which according to the International Knee Documentation Committee (IKDC) criteria, is a nearly normal knee (Kocher et al. 2004). The laxity measurements for the left knee were carried out up to a load of 150N. The laxity measurements results at 175N and 200N for the left knee joint were interpolated by using the linear trend line equation: Translation = 0.0202(Load applied) – 0.1637. The interpolated results for the left leg ACL laxity measurements are indicated clearly.

The ACLs for the right and left knee joints were loaded to 200N and 150N respectively. The radiographs were captured successfully for each incremental load during the process. The tibial translation distances prior to applying the translation load (0N) were measured to be 8.04mm for the right knee and 5.805mm for the left knee. The tibia translation distances post load application were measured at 11.86mm for the right knee joint (at 200N) and 8.92mm for the left knee joint (at 150N). This resulted in an ACL laxity measurement of 3.82mm for the right knee joint and 3.12mm for the left knee joint at a 30° (from full extension) flexion angle. The laxity measurement results at a load of 150N, differed by 20.55%. The laxity measurement results were satisfactory, indicating that the ligaments were nearly normal, according to the IKDC criteria outline according to Kocher et al. (2004). This result supports the assumption that the ACLs within the subject's knee joints were intact and healthy.

6.4.2 Discussion

The Laxmeter performed satisfactorily with regards to the ACL laxity measurement procedures. The laxity measurement results obtained, indicated that the subject would be diagnosed with a nearly normal knee. This possible diagnosis supports the assumption that the ACLs were intact within both knee joints. In addition, the Laxmeter's ACL laxity measurement results were comparable to those obtained by previous studies (as indicated in Table 6.1). The linear average laxity measurement results yielded during the Laxmeter's ACL laxity measurement procedures were within the range and standard deviations of majority of the collected studies. In summation, the Laxmeter performed satisfactorily in nine out of the ten studies (six being positive and three varying slightly), which suggests that the Laxmeter could potentially measure ACL laxity at 30° flexion.

Although the laxity measurement results were found to be satisfactory, several critical notes would need to be established and understood. The reason for solely considering the ACL laxity measurement procedure at 30° knee joint flexion is indicated in Section 6.4 ACL Results. An additional keynote was the difference between the right and left knee joint laxity measurements, which is commonly found as stated in Section 6.2.3 Discussion. The initial and resultant bone distraction values differed and the laxity measurement results varied by 20.55%. The reasons for this variance are similarly outlined in Section 6.2.3 Discussion, which is once again applicable to this particular case. In addition, the anterior-lateral FSP shift, as described in Section 6.3.3 Discussion, applies to the ACL laxity measurement procedure as well.

A notable result was the inability of the system to apply a 250N load to the posterior proximal lower leg. The system was limited to applying a 150N load for the left knee and 200N load for the right knee. The reason for this limitation was the inadequate patient securing system as a result of Velcro® strapping slippage. The distal lower leg LLSP strapping proved to be unable to restrain the lower limb movement during the laxity measurement procedure. The subject's limb slid underneath the strapping as the load was being applied. The right limb was more securely fastened to the Laxmeter PSS during the laxity measurement procedure compared to the left. In addition, the strapping during the right knee joint ACL laxity measurement procedure withheld the load for a longer period. The Laxmeter was fully capable of applying the load; however, slippage was significant enough to cause the actuator to complete a full stroke (extension or retraction) before reaching 250N.

6.5 PCL Results

6.5.1 Discussion

The Laxmeter was designed to measure the laxity of all four major ligaments of the knee joint at multiple fixed degrees of flexion. The standard laxity measurement procedure for the PCL would be the Posterior Drawer Test at 90° and 30° (from full extension) knee joint flexion. Since the Laxmeter configuration i.e. position of the linear actuator is identical to that of the ACL laxity measurement procedure, the Laxmeter would not fit beneath the C-arm of the LODOX scanner at a knee joint flexion angle of 90° (as detailed in Section 6.4 ACL Results). As a result, the 90° knee joint flexion angle PCL laxity measurement procedures were omitted from this study.

The study proceeded to perform the PCL laxity measurement procedures at a knee joint flexion angle of 30° and a maximum applied load of 250N. During the right knee joint procedure, the ULSP, and the hinges attaching the ULSP to the LLSP, began to deform (buckle) as the load was applied to the leg. This meant that the structural integrity of the Laxmeter was insufficient and therefore, incapable of performing the PCL laxity measurement procedures. The ULSP and hinge deformation resulted from attempting to reduce the weight of the structure and increase cost effectiveness, thereby compromising on structural integrity. The ULSP was considered during the design process as a potential failure point, however, the FEM analysis of the ULSP did not examine the moment experienced by the panel as well as the 30° angle. This design limitation could potentially have been identified by modelling and analysing the entire Laxmeter assembly during a PCL laxity measurement procedure. As a result, PCL laxity measurement procedures were omitted from the study due to the potential failure of the PSS.

7 Discussion

7.1 Overall Design

The requirements identified for the Laxmeter were implemented on a subsystem basis i.e. the LAS and the PSS. This allowed for more intricate design management, to better ensure that all design requirements were met. The design outcomes of the Laxmeter can be evaluated on both a subsystem and an assembly basis.

The PSS was designed to support the weight of a 95th percentile male, facilitate the required knee joint laxity measurement procedures and allow for the selection of specific knee joint flexion angles. Additional key design requirements for this study included storage and portability features as well as integration design components. The PSS was manufactured from 8mm Plexiglas® sheets to ensure radiolucency for stress radiography laxity measurement procedures. The structural integrity of LLSP and ULSP PSS panels was verified using Ansys® FEM student edition software. This was done considering the weight of a 95th percentile male and the 250N load applied to the proximal lower leg. The PSS was successfully able to configure to nine fixed knee joint flexion angles, including the standard 0°(full extension), 30° (from full extension) and 90° angles required for the ACL, PCL, MCL and LCL laxity measurement procedures (Lubowitz et al. 2008). In addition, the PSS achieved portability and storability by developing a lightweight and compact system. The 8mm thick Plexiglas® allowed for cost effectiveness and reduced the PSS's weight to 64N (6.5kg). Finally, the PSS was successfully able to integrate with the LAS thus forming the Laxmeter.

The LAS was subdivided into the electronics system and the patient support structure. The electronics system controlled the extension and retraction of the linear actuator (SKF® CAHB-10, ACME Screw, DC Electric, 500N, 100mm stroke length) and measured the force applied to the proximal lower leg. These two functions were integrated, allowing the electronics system to manipulate the actuator to apply a 25N incremental load from 0-250N. The system successfully achieved this feature to within an accuracy of ±5N. The system was entirely controlled by push buttons located on an ITEAD STUDIO LCD1602 Key Shield 1.0 display. The support structure supported the linear actuator during laxity measurement procedures. In addition, the support structure allowed for integrating the PSS as well as the LAS and made AP as well as ML load application possible. The support structure was design to accommodate the linear actuator in various positions providing for AP and ML tibial translation. Also, the structure provided for human variation in proximal lower leg diameter, pelvic width and femoral length. The linear actuator successfully applied the 250N load in all laxity measurement procedural actuator positions.

However, during a certain laxity measurement experimental validation procedure, the PSS deformed approaching failure with increasing load. The ULSP, as well as the Nylon hinges connecting the LLSP to the ULSP, deformed (buckled) during a PCL laxity measurement procedure at 30° (from full extension) knee joint flexion. The ULSP began to buckle under the load, and the Nylon hinges began to contort. This resulted in the Laxmeter's inability to measure PCL laxity at 30° knee joint flexion. This result correlates with the outcome of the FMEA model described in Section 4.5.3 FMEA model. The model predicted the potential failure of the ULSP and the contortion of the hinges, indicating the need for design modifications.

Due to the nature of the study; availability of resources (funding as well as the timeline) and manufacturing time, rapid prototyping and sufficient Prototype testing was not possible. This is a key part of the device design and the developmental process. Future work would need to undergo this process to eliminate structural failures occurring, such as the buckling experienced by the ULSP.

7.2 Validation Experimentation

The experimental laxity measurement procedures were carried out on a single cadaver, assumed to have healthy knee joints and intact ligaments. The FHS Anatomy department at UCT provided the cadaver on condition that no incisions would be made on the body. To induce ruptures in the knee joint would have required the purchasing of a cadaver which was not possible due to the cost capacity of the project. However, future cadaver trials would be effectively validated by the results of a ligament laxity measurement procedure post ligament intervention. The standard laxity measurement procedural protocols, according to Lubowitz et al. (2008), indicate that MCL, as well as LCL procedures, were to be carried out at 0° (full extension) and 30° (from full extension) knee joint flexion and ACL and PCL procedures at 30° and 90° knee joint flexion. This was the procedural protocol followed by the Laxmeter.

The Laxmeter successfully applied the 25N incremental load (from 0-250N) to determine the MCL and the LCL laxity at 0°(full extension) and 30° knee joint flexion. The stress radiographs were captured and the laxity of the ligaments were measured. The laxity measurement results suggested that the test subject had intact MCLs and LCLs, according to Hughston's grading system (Phisitkul et al. 2006). This potentially supports the assumption that the subject's MCLs and LCLs were all intact and healthy. Furthermore, the global laxity measurement comparison study suggests inconclusive results, however, when specifically compared to more recent studies, which utilise a similar technique, the Laxmeter is potentially capable of reliably and accurately measuring MCL and LCL laxity.

The Laxmeter was successfully able to apply 150N and 200N to the posterior aspect of the proximal left and right lower legs for the ACL laxity measurement procedures. The Laxmeter's inability to surpass 150N (for the left knee) and 200N (for the right knee) was due to Velcro® strap slipping during loading. The right limb was more securely fastened than the left, allowing for an increased applied load. However, a comparison between the Laxmeter's laxity measurement results and existing studies of a similar nature revealed that the Laxmeter can potentially accurately measure the laxity of the ACL at 30° knee joint flexion.

8 Conclusion and Recommendations

The presented study set out with the aim to design and experimentally validate a novel multi-ligament laxity measurement stress radiography device (the Laxmeter second iteration/ Prototype) that reliably and accurately measures the laxity of the ACL, PCL, MCL and LCL at multiple fixed degrees of flexion.

For this aim to be met, the primary objectives would need to be achieved. These objects were stipulated as follows:

i. Incorporate structural design changes on the Laxmeter Prototype One, to accommodate multi-ligament laxity measurements at multiple fixed degrees of flexion.
ii. Design and develop an electromechanical linear load applicator with range 0-250N.
iii. Modify the existing Laxmeter to accommodate for convenient storage, portability and straightforward setup.
iv. Perform experimental testing and *in vitro* cadaver functional validation for the suitability of the modified device for multi-ligament laxity measurements.

The objectives were met, in part, through the design process and the experimental functional validation procedure of this study. This section provides the conclusion for the objectives and details recommendations for future expansion and continuation of the research presented.

8.1 Conclusion

8.1.1 Structural Design

The Laxmeter, developed as part of this study, was designed and developed to accommodate multi-ligament laxity measurements at multiple fixed degrees of flexion. This feat was successfully achieved, in part. The Laxmeter was designed as two subsystems, namely 1) the PSS and 2) the LAS. The PSS was designed as a configuration of Nylon hinge coupled panels (LLSP, ULSP, Fold Assist Panel and Angle Adjustment Panel) and two Parallel Supports. The structure was manufactured from 8mm thick Plexiglas® sheets (for its affordability and radiolucent properties) to support the weight of a 95^{th} percentile male. The 8mm thick Plexiglas® panels were sufficiently capable of supporting the relevant loads experienced during knee joint laxity measurement procedures (as verified using FEM analysis). In addition, the PSS accommodated laxity measurement procedures a 0° (full extension), 30°, 40°, 45°, 50°, 60°, 70°, 80° and 90° degrees of flexion. The PSS was designed for and successfully achieved LAS integration to allow for knee joint laxity measurement procedures. However, PCL laxity measurements were not possible due to buckling of the ULSP, and the Nylon hinges contorting. As a result, the Laxmeter was limited to measuring the laxity of the ACL, MCL and LCL at standardised ligament laxity measurement procedural angles.

8.1.2 Electromechanical Linear Load Applicator

The electromechanical linear load applicator or LAS according to the study, was successfully designed to apply a 25N incremental load from 0-250N on the proximal lower leg. The LAS was successfully capable of extending or retracting the SKF CAHB-10 linear actuator to apply the incremental loads. Strain gauge FSPs were used to measure the applied load at the point of contact. In addition, the LAS was successfully able to integrate with the PSS allowing for multi-ligament laxity measurement procedures.

8.1.3 Storage, Portability and Setup

The PSS and the LAS allowed for storability, portability and straightforward setup. The 8mm Plexiglas® panels (including windows sectioned in the panels) allowed for a lightweight and portable system. In addition, the hinge configuration of the panels allowed the PSS to fold up and occupy a space of 600x600x40mm. This allowed for the Laxmeter to be stored up against a wall or in a cupboard. The LAS support structure assembled using sleeve and cotter joints. The disassembled components successfully fit within a space of 310x220x145mm as compared to an assembled configuration which occupies a space of 455x296x98mm. The sleeve and cotter joint mechanism allowed for a timely and straightforward assembly (setup) and disassembly. Integrating the PSS and LAS functioned in accordance with the sleeve and cotter joint mechanism.

8.1.4 Experimental Testing and In Vitro Cadaver Validation

The experimental laxity measurement cadaver validation procedure was carried out successfully, in part. The 25N incremental load (0-250N) was successfully applied to the MCL and LCL. The laxity measurement results suggest that the Laxmeter is capable or accurately and reliably measuring the laxity of the MCL and LCL at 0° (full extension) and 30° (from full extension) knee joint flexion. The results suggested that the test subject's MCLs and LCLs were intact, which supports the assumption (made before initiating the experimental procedure) that the cadaver had healthy knee joints with intact ligaments. The global laxity measurement comparative study results suggested inconclusive results. However, the Laxmeter was found to potentially perform satisfactorily, when comparing the MCL and LCL laxity measurement results to more recent research.

The ACLs were successfully loaded to 200N (right knee joint) and 150N (left knee) respectively at 30˚ knee joint flexion. The 90˚ knee joint flexion laxity measurement procedure was omitted due to the Laxmeter being too large for the LODOX scanner setup. The Laxmeter was unable to apply an increased load to the ACLs due to the Velcro® straps releasing their hold under load. However, the omitted laxity measurements were obtained with interpolation, according to a trend line. The ACL performance suggests that the Laxmeter can potentially accurately and reliably measure the laxity of the ACL at 30° knee joint flexion. The laxity measurement results suggest that the ACLs are both normal intact ligaments. This supports the assumption, made prior to initiating the experimental procedure, that the test subject's knee joints are healthy with intact ligaments. In addition, the global laxity measurement comparison suggests that the Laxmeter can potentially accurately and reliably measure the laxity of ACLs.

Table 8.1 compares the Laxmeter developed in this study (Laxmeter 2.0) to the KT-1000™, the GNRB®, the Telos™ Stress Device and the previously existing Laxmeter (Laxmeter Prototype One). The table shows the significant improvement and potential impact that the Laxmeter has.

Table 8.1: Laxity measurement technique capabilities and limitations of existing laxity measurement devices and techniques. X represents inability to carry out the test, '✓' represents ability to perform the test with reduced reliability, '✓*' represents ability to conduct the test with ergonomically awkward positions, '✓†' represents allowance for test but inability to functionally perform the test and '✓✓' represents full ability to carry out the test.

Existing Devices	*Lachman Test (ACL)*	*Anterior Drawer Test (ACL)*	*Posterior Drawer Test (PCL)*	*Adduction Stress Test (LCL)*	*Abduction Stress Test (MCL)*	*Various degrees of flexion*	*Stress Radiography (radiation)*
KT-1000™	✓	✓✓	✓✓	X	X	X	X
GNRB®	✓✓	✓✓	X	X	X	X	X
Telos™ Stress Device	X	✓	✓	✓✓	✓✓	✓*	✓✓
Laxmeter One	X	X	X	✓†	✓†	✓✓	✓✓
Laxmeter Two	X	✓✓	X	✓✓	✓✓	✓✓	✓✓

Figure 8.1 provides an illustration of the Laxmeter assembly developed and functionally validated during this study. The figure provides both a rendered (A) as well as a physical (B) depiction of the device prior to and post manufacturing.

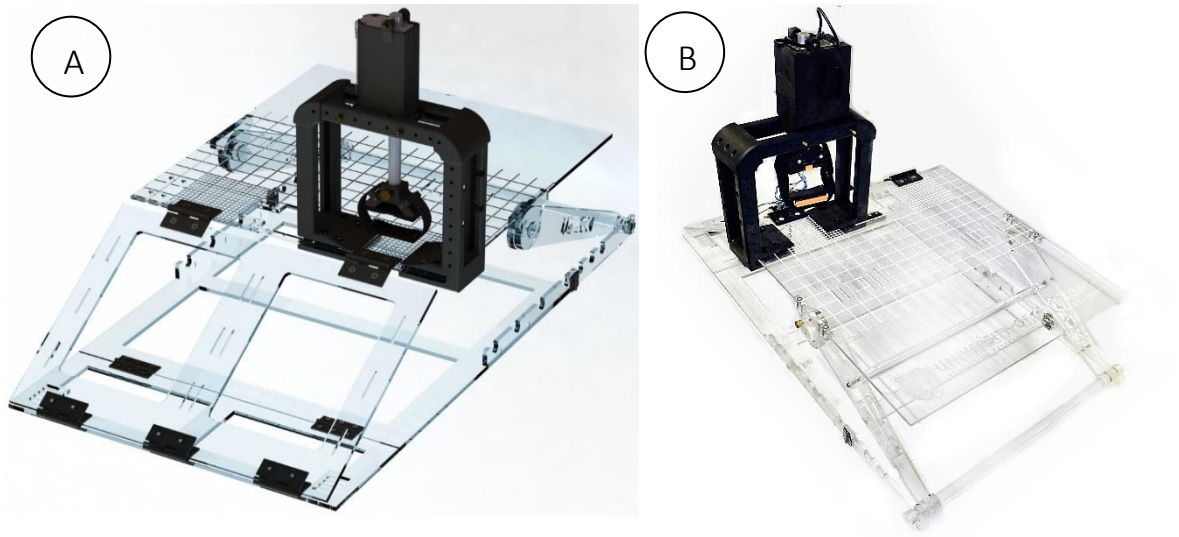

Figure 8.1: The Laxmeter assembly (A rendered (A) and physical depiction (B) of the device).

8.1.5 System Usability

Based on the findings of this study and the requirements for achieving usability i.e. effectiveness, efficiency and satisfaction, the Laxmeter performed acceptably. The device was given a score of 10 according to the usability scale presented in Appendix E. The Laxmeter was able to measure the laxity of the ACL, MCL and LCL at the required knee joint flexion angles. The device was foldable and lightweight providing for convenient storage. The device can be concluded as effective as it achieved majority of the requirements of this study. The device can be considered efficient due to the level of effectiveness achieved with the resources available. The device performed satisfactorily regarding setup and procedure performance.

8.1.6 FMEA review

The failure modes predicted and prioritised according to the FMEA model correlate with the ways in which the Laxmeter failed during the cadaver functional verification trial. Although the FMEA identified the most probable cause of failure, it was understood and assumed that majority of the applied load (during PCL laxity measurement procedures) would be experienced by and translated through the hip joint and onto the X-ray table. However, the load experienced by the heel proved to be significant enough to prove the FMEA right, resulting in the failure of the device to carry out the PCL laxity measurement procedures. The appropriate recommendations would need to be made to ensure that these failure methods are addressed by future iterations of the Laxmeter.

8.2 Recommendations and Future Works

8.2.1 Design

The Laxmeter design would require future modifications for the device to overcome the limitations presented in this study. The significant limitations presented would be the Laxmeter's inability to carry out PCL laxity measurement procedures as well as the Velcro® straps releasing during ACL laxity measurement procedures. The design recommendations are as follows:

- Plexiglas® was selected as the material for the PSS due to its cost effectiveness, light weight, strength and radiolucency. However, alternative materials would improve the structural integrity of the PSS and potentially eliminate the failure of the ULSP due to buckling. A consideration would be carbon fibre reinforced plastic; however, the cost effectiveness of the materials would need to be considered in conjunction with the radiolucency, density and strength.
- Structural modifications could be considered in the case of the ULSP. Ribbing could be added along the length of the panel, stretching from the Fold Assist Panel to the LLSP. This ribbing, however, would need to be accommodated for by the folding mechanism of the PSS.
- The hinges used for the Laxmeter's assembly were large, robust Nylon hinges (due to their radiolucency) used for marine purposes. These hinges, however, were found to be structurally insufficient for the PSS. Therefore, more robust radiolucent hinges would need to be considered. Alternatively, appropriate hinges would need to be designed for the Laxmeter's PSS.
- Although most studies do not stipulate the ankle position during laxity measurement procedures, besides the Lachman test, the ankle position was found to have a significant impact on the laxity measurement result. This was particularly the case for MCL and LCL laxity as the knee joint flexed under the applied load. A study done by Robinson et al. (2006) reported results for ACL laxity with (3.5-4mm) and without (5-7mm) ankle fixation. As a result, the ankle rotation was fixated at approximately 30° externally to avoid inaccurate laxity measurement results. An attachment for fixating the ankle position would need to be developed to improve reproducibility, with the added benefit of allowing for the anterior drawer and Lachman ACL laxity measurement procedures.

- Future iterations would require rapid prototyping and bench testing to ensure the PSS has sufficient structural integrity and that the system can achieve all design outcomes sufficiently.
- An alternative means of fixating and securing the subject to the PSS would require exploration. The Velcro® strapping was considered due to its radiolucency; however, the mechanism is not sufficient for the Laxmeter. A more rigid means of securing the patient would need to be explored.

8.2.2 Procedural

The laxity measurement procedures conducted to validate the efficacy of the Laxmeter are all standard. However, the suggested recommendations would improve the overall result of the study:

- Future work would require more rigorous experimental validation by testing on more cadavers with healthy knee joints, to draw a statistical analysis and statistical validation of the Laxmeter's function. The study would include a test subject inclusion criterion to ensure that the knee joints are healthy. The results presented in this study are insufficient to prove the efficacy of the device, however, the functionality, usability and structural integrity of the device were validated.
- For future works, the laxity measurement stress radiographs would need to be captured and verified by a skilled radiographer and radiographic analyst (radiologist) to reduce the effect of human error.
- Future experimental validation procedures would require clinical trials on participants with healthy knee joints as well as patients with injured and severed ACLs, PCLs, MCLs and LCLs.

References

AposTherapy. (2015). "Knee ligament damage." from http://www.apostherapy.co.uk/en/conditions-we-treat/ligaments-tear.

Arduino. (2017). "Arduino UNO." from http://www.arduino.org/products/boards/arduino-uno.

Ascani, D., C. Mazza, A. D. Lollis, M. Bernardoni and M. Viceconti (2015). "A procedure to estimate the origins and the insertions of the knee." Journal of Biomechanics: 233-237.

Ascani, D., C. Mazza, A. D. Lollis, M. Bernardoni and M. Viceconti (2015). "A procedure to estimate the origins and the insertions of the knee ligaments from computed tomography images." Journal of Biomechanics: 233-237.

Bailey, A. J. and J. P. Mansell (1997). "Do subchondral bone changes exacerbate or precede articular cartilage destruction in osteoarthritis of the elderly?" Gerontology **43**(5): 296-304.

Beldame, J. and S. B. S. Mouchel, J. M. Adam, F. Mouilhade, X. Roussignol, F. Dujardin (2012). "Anterior knee laxity measurement: Comparison of passive stress radiographs Telos and "Lerat", and GNRB arthrometer." Orthopaedics & Traumatology: Surgery & Research: 744-750.

Bendjaballah, M. Z., A. Shirazi-Adl and D. J. Zukor (1997). "Finite element analysis of human knee joint in varus-valgus." Clinical Biomechanics: 139-148.

Berman, B., F. G. Zarb and W. Hall (2012). "3-D printing: The new industrial revolution." Business Horizons: 155-162.

Beukes, G., S. Patnaik and S. Sivarasu (2017). "DEVELOPMENT OF A STRESS RADIOGRAPHY DEVICE TOWARDS MULTI-LIGAMENT LAXITY MEASUREMENTS." Bone & Joint Journal Orthopaedic Proceedings Supplement **99-B** (SUPP 2): 109-109.

Bickley, L. S. and F. R. Prabhu (2003). Bates' Guide to Physical Examination and History Taking. Bates' Guide to Physical Examination and History Taking. Philadelphia, Lippincott Williams & Wilkins**:** 515-516.

Bise, C. (2016) "Physical Therapist's Guide to Anterior Cruciate Ligament (ACL) Tear." Move Forward **Volume**, DOI:

Bollen, S. (2000). "Epidemiology of knee injuries: diagnosis and triage." British Journal of Sports Medicine: 227-228.

Bouguennec, N., G. A. Odri, G. N and P. Colombet (2015). "Comparative reproducibility of TELOS and GNRB for instrumental measurement of anterior tibial translation in normal knees." Orthopaedics & Traumatology: Surgery & Research: 205-209.

Boyer, P., P. Djian, P. Christel, X. Paoletti and R. Degeorges (2004). "[Reliability of the KT-1000 arthrometer (Medmetric) for measuring anterior knee laxity: comparison with Telos in 147 knees]." Revue de chirurgie orthopedique et reparatrice de l'appareil moteur **90**(8): 757-64.

Branch, T. P., H. O. Mayr, J. E. Browne, J. C. Campbell, A. Stoehr and C. A. Jacobs (2010). "Instrumented Examination of Anterior Cruciate Ligament Injuries: Minimizing Flaws of the Manual Clinical Examination." The Journal of Arthroscopic & Related Surgery: 997-1004.

Brantigan, O. C. and A. F. Voshell (1941). "The Mechanics of the Ligaments and Menisci of the Knee Joint." The Journal of Bone & Joint Surgery: 44-66.

Budynas, R. G. and J. K. Nisbett (2011). Shigley's Mechanical Engineering Design. New York, McGraw-Hill.

CCushions. (2017). "Standard X-ray pads." CCushions - Fitted cushions for medical equipment, from http://www.ccushions.com/xray.htm.

Choudhury, I. A. and S. Shirley (2010). "Laser cutting of polymeric materials: An experimental investigation." Optics & Laser Technology: 503-508.

Claes, S., E. Vereecke, M. Maes, J. Victor, P. Verdonk and J. Bellemans (2013). "Anatomy of the anterolateral ligament of the knee." Journal of Anatomy: 321-328.

Collette, M., J. Courville, M. Forton and B. Gagniere (2012). "Objective evaluation of anterior knee laxity; comparison of the KT-1000 and GNRB arthrometers." Knee Surgery, Sports Traumatology, Arthroscopy: 2233-2238.

Converter, T. M. (2017). "From Euro to USD." Retrieved March 19, 2017, 2017, from https://themoneyconverter.com/.

Converter, X. C. (2017, 02 06). USD to ZAR, from http://www.xe.com/currencyconverter/convert/?Amount=4300&From=USD&To=ZAR .

Crane, J. (2017). Dr. Jason Crane. The Correlation between Clinical and Arthroscopic Diagnosis of Meniscal Lesion.

Crawford, R., G. Walley, S. Bridgman and N. Maffulli (2007). "Magnetic resonance imaging versus arthroscopy in the diagnosis of knee pathology, concentrating on meniscal lesions and ACL tears: a systematic review." British Medical Bulletin: 5-23.

Daniel, D. M., L. L. Malcom, G. Losse, M. L. Stone, R. Sachs and R. Burks (1985). "Instrumented measurement of anterior laxity of the knee." J Bone Joint Surg Am 67.

Drake, R. L., A. W. Vogl and A. W. M. Mitchell (2014). Gray's Anatomy for Students. Churchhill Livingstone, Elsevier.

Evonik. (2017). "Properties of Plexiglas(R)." from http://www.plexiglas.de/product/plexiglas/en/about/faq/Pages/properties.aspx#faq_0_2.

Fanelli, G. C., B. F. Giannotti and C. J. Edson (1994). "The posterior cruciate ligament arthroscopic evaluation and treatment." The Journal of Arthroscopic & Related Surgery: 673-688.

FarlexInc. (2017). "Medical Dictionary." The Free Dictionary by Farlex, from http://medical-dictionary.thefreedictionary.com/laxity.

FORSTER, I. W., C. D. WARREN-SMITH and M. TEW (1989). "IS THE KT1000 KNEE LIGAMENT ARTHROMETER RELIABLE?" Journal of Bone & Joint Surgery: 843-847.

Freidberg, R. P. (2016) "UpToDate." Anterior cruciate ligament injury Volume, DOI:

Gartech. (2014). "Semi_Finished Product." Engineering Plastics, from http://www.gartech.co.za/products.html#acry.

Genourob. (2017). "ACL AND PCL ANALYSIS: AUTOMATED LACHMAN TEST." Innovative Laximetry, from http://www.genourob.com/diagnostic-ligaments_lda_the-lda-method-objective-knee-joint-laxity-test_lachman-test-automated.phtml.

Gianotti, S. M., S. W. Marshall, P. A. Hume and L. Bunt (2009). "Incidence of anterior cruciate ligament injury and other knee ligament injuries: A national population-based study." Journal of Science and Medicine in Sport: 622-627.

Gilroy, A. M., B. R. MacPherson and L. M. Ross (2008). Atlas of Anatomy (2nd edition). New York, Thieme.

Gilroy, A. M. M., B. R.; Ross, L. M. (2008). Atlas of Anatomy (2nd edition). New York, Thieme.

GPlastics. (2012). "Cast Nylon." Gemini Plastics, from www.gplastics.com/pdf/cast-nylon-6.pdf.
GrabCAD. (2017). "Sitting Figure." from https://grabcad.com/library/sitting-figure.
Hefzy, F. R. N. D. L. B. E. S. G. R. F. Z. M. S. (1984). "Biomechanical Analysis of Human Ligament Grafts used in Knee-ligament Repairs and Reconstructions." The Journal of Bone and Joint Surgery: 344-352.
Island, U. o. R. (2017). "Anthropometric Data." Introduction to Biomechanics, from http://www.ele.uri.edu/faculty/vetter/BME207/anthropometric-data.pdf.
Jacobsen, K. (1976). "Stress radiographical measurement of the anteroposterior, medial and lateral stability of the knee joint." Acta Orthopaedica: 335-4.
Jacobsen, K. (1977). " Stress Radiographical Measurements of PostTraumatic
Knee Instability: A Clinical Study." Acta Orthopaedica Scandinavica **48**(3): 301-310.
James, E. W., B. T. Williams and R. F. LaPrade (2014). "Stress Radiography for the Diagnosis of Knee Ligament Injuries: A Systematic Review." Clinical Orthopaedics and Related Research: 2644-2657.
Jardin, C., C. Chantelot, H. Migaud and A. Duquennoy (1999). "Low accuracy of the KT-1000 arthrometer versus Telos radiographic measurements to assess knee anterior laxity after ACL graft. Intra and interobserver reproducibility of KT-1000 measurements." Revue de Chirurgie Orthopédique et Réparatrice de l Appareil Moteur: 698-707.
Kakarlapudi, T. K. and D. R. Bickerstaff (2001). "Knee instability - isolated and complex." western journal of medicine: 266-272.
Kincaid, M. (2017). Mark Kincaid Physiotherapy. Physiotherapist in Fourways, Johannesburg.
Kneesafe. (2015). "The most common knee injuries and disorders." Protect Your Knees, from http://kneesafe.com/the-most-common-knee-injuries-and-disorders/.
Kocabey, Y., O. Tetik, W. M. Isbell, Ö. A. Atay and D. L. Johnson (2004). "The value of clinical examination versus magnetic resonance imaging in the diagnosis of meniscal tears and anterior cruciate ligament rupture." The Journal of Arthroscopic & Related Surgery: 696-700.
Kocher, M. S., J. R. Steadman, K. K. Briggs, W. I. Sterett and R. J. Hawkins (2004). "Relationships Between Objective Assessment of Ligament Stability and Subjective Assessment of Symptoms and Function After Anterior Cruciate Ligament Reconstruction." The American Journal of Sports Medicine **32**(3): 629-634.
Kocher, M. S., J. R. Steadman, K. K. Briggs, W. I. Sterett and R. J. Hawkins (2004). "Relationships Between Objective Assessment of Ligament Stability and Subjective Assessment of Symptoms and Function After Anterior Cruciate Ligament Reconstruction." The American Journal of Sports Medicine: 629-634.
Kupper, J. C., B. Loitz-Ramage, D. Corr and J. L. Ronsky (2007). "Measuring knee joint laxity: A review of applicable models and the need for new approaches to minimize variability." Journal of Clinical Biomechanics: 1-13.
LaPrade, R. (2017). Robert LaPrade MD, PhD. KT-1000 Testing.
Leferve, N., Y. Bohu, J. F. Naouri, S. Klouche and S. Herman (2014). "Validity of GNRB® arthrometer compared to Telos™ in the assessment of partial anterior cruciate ligament tears." Knee Surgery, Sports Traumatology, Arthroscopy: 285-290.
Levy, D. B. (2016). Soft Tissue Knee Injury Clinical Presentation. Medscape Logo.
Lewek, M. D., K. S. Rudolph and L. Snyder-Mackler (2004). "Control of Frontal Plane Knee Laxity during Gait in Patients with Medial Compartment Knee Osteoarthritis." Osteoarthritis and cartilage / OARS, Osteoarthritis Research Society **12**(9): 745-51.

Lin, C., J. Ko, C. Chen and W. Chang (2011). The Design and Preliminary Assessment of a new knee ligament arthrometer. 4th International Conference on Biomedical Engineering and Informatics (BMEI), Shanghai, Institute of Electrical and Electronics Engineers.

Liu, X., H. Feng, H. Zhang, L. Hong, X. S. Wang, J. Zhang and J. W. Shen (2013). "Surgical Treatment of Subacute and Chronic Valgus Instability in Multiligament-Injured Knees With Superficial Medial Collateral Ligament Reconstruction Using Achilles Allografts." The American Journal of Sports Medicine **41**(5): 1044-1050.

Liu, X., H. Feng, H. Zhang, L. Hong, X. S. Wang, J. Zhang and J. W. Shen (2013). "Surgical Treatment of Subacute and Chronic Valgus Instability in Multiligament Injured Knees With Superficial Medial Collateral Ligament Reconstruction Using Achilles Allografts." The American Journal of Sports Medicine: 1044-1050.

Lubowitz, J. H., B. J. Bernardini and J. B. Reid, 3rd (2008). "Current concepts review: comprehensive physical examination for instability of the knee." Am J Sports Med **36**(3): 577-94.

Lysholm, J. and Y. Tegner (2009). "Knee injury rating scales." Acta Orthopaedica: 445-453.

Margheritini, F., L. Mancini, C. S. Mauro and P. P. Mariani (2003). "Stress radiography for quantifying posterior cruciate ligament deficiency." The Journal of Arthroscopic & Related Surgery: 706-711.

Markolf, K. L., J. S. Mensch and H. C. Amstutz (1976). "Stiffness and laxity of the knee--the contributions of the supporting structures. A quantitative in vitro study." J Bone Joint Surg Am **58**(5): 583-94.

MayoClinic. (2017). "Symptoms and causes." Knee pain, from http://www.mayoclinic.org/diseases-conditions/knee-pain/symptoms-causes/dxc-20190116.

McDowell, M. A., C. D. Fryar, C. L. Ogden and K. M. Flegal (2008). Anthropometric Reference Data for Children and Adults: United States, 2003-2006. National Health Statistics Reports. Hyattsville, United States of America, U.S. DEPARTMENT OF HEALTH & HUMAN SERVICES: 1-48.

Medical, U. (2015). "Standard X-Ray Table Pad." Universal Medical, from http://www.universalmedicalinc.com/standard-x-ray-table-pad.html.

Medline. (2016). "Standard X-Ray Table Pad by AliMed." Medline, from http://www.medline.com/product/Standard-X-Ray-Table-Pad-by-AliMed/Z05-PF81854;ecomsessionid=Xl4JGzBv+LFO08LJmCZeAg__?_requestid=933946.

MEDmetric. (2011, November 22, 2011). "Hotfrog." MEDmetric(R) Corporation - Product List, from http://www.hotfrog.com/business/ca/san-diego/medmetric/medmetric-corporation-product-list-1135587.

Medsport. (2011). "The Knee Joint & Injury." from http://www.medsport.co.za/the-knee-joint-injury/.

MendMyKnee. (2017). "Cutting Edge Knee Injury Treatments." from http://www.mendmyknee.com/.

Merriam-Webster. (2017). "Medline Plus." Medical Dictionary, from http://c.merriam-webster.com/medlineplus/laxity.

Morgan, B. (2015). SouthAfrica.info. South Africa's Comrades Marathon.

Muller, W. (1996). "Knee ligament injuries." International Orthopaedics: 266-270.

NASA (2008) "3 Anthropometry and Biomechanics." Man-systems integration standards **Volume**, DOI:

News24. (2014, February 16). "The bitter pill of medical costs in SA." from http://www.news24.com/Archives/City-Press/The-bitter-pill-of-medical-costs-in-SA-20150429.
OrthoInfo (2009) "ACL Injury: Does It Require Surgery." OrthoInfo **Volume**, DOI:
Parsons, E. M., A. O. Gee, C. Spiekerman and P. R. Cavanagh (2015). "The biomechanical function of the anterolateral ligament of the knee." The American Journal of Sports Medicine: 669-674.
Pena, E., B. Calvo, M. A. Martinez and M. Doblare (2006). "A three-dimensional finite element analysis of the combines behaviour of ligaments and menisci in the healthu human knee joint." Journal of Biomechanics: 1686-1701.
Pennington, S. (2014). S.A. Fast Facts. South Africa The Good News.
Phisitkul, P., S. L. James, B. R. Wolf and A. Amendola (2006). "MCL Injuries of the Knee: Current Concepts Review." The Iowa Orthopaedic Journal **26**: 77-90.
PhysioPRO. (2017). "Rates." from http://www.physiopro.co.za/contact-us/rates/.
Plexiglass(R). (2013). "Properties of Plexiglas(R)." Evonik, from http://www.plexiglas.de/sites/lists/PM/DocumentsAP/211-1-PLEXIGLAS-GS-XT-en.pdf.
Quadrant. (2017). "Ertalyte® PET-P." from http://www.quadrantplastics.com/za-en/products/engineering-plastics/engineering-80-160-c/ertalyte-R-pet-p.html.
Roach, K. E. and T. P. Miles (1991). "Normal Hip and Knee Active Range of Motion: The Relationship to Age." Journal of the American Physical Therapy Association: 656-665.
Robert, H., S. Nouveau, S. Gageot and B. Gagniere (2009). "A new knee arthrometer, the GNRB: experience in ACL complete and partial tears." Orthopaedics & Traumatology: Surgery & Research: 171-176.
Robinson, J. R., A. M. Bull, R. R. Thomas and A. A. Amis (2006). "The role of the medial collateral ligament and posteromedial capsule in controlling knee laxity." Am J Sports Med **34**(11): 1815-23.
Rose, N. E. and S. M. Gold (1996). "A comparison of accuracy between clinical examination and magnetic resonance imaging in the diagnosis of meniscal and anterior cruciate ligament tears." The Journal of Arthroscopic & Related Surgery: 398-405.
RScomponets. (2017). "SKF 500N CAHB-10 Electric Linear Actuator, 24V dc, 100mm stroke." Electric Linear Actuators, from http://za.rs-online.com/web/p/electric-linear-actuators/7643471/.
SASCOC. (2016). "Team South Africa named for the 2016 Rio Olympics." SASCOC, from http://www.sascoc.co.za/2016/07/14/team-south-africa-named-for-the-2016-rio-olympics/.
Savarese, E., S. Bisicchia, R. Romeo and A. Amendola (2011). "Role of high tibial osteotomy in chronic injuries of posterior cruciate ligament and posterolateral corner." Journal of Orthopaedics and Traumatology **12**(1): 1-17.
Sbihi, A., J.-P. Franceschi, P. Christel, P. Colombet, P. Djian and G. Bellier (2004). "Reconstruction du ligament croisé antérieur par greffe de tendons de la patte d'oie à un ou à deux faisceaux." Revue de Chirurgie Orthopédique et Réparatrice de l'Appareil Moteur: 643-650.
Scheuba, P. D. G. (2009) "telosmedical." Austin & Associates, Inc Operating instructions telos Stress Device GA lll/E **Volume**, DOI:
Sivarasu, S. and S. Patnaik (2014a). "Novel Device for Measuring Knee Laxity at Various Flexion Angles—Laxmeter." Journal of Medical Devices: 020938-1-2.

Sivarasu, S. and S. Patnaik (2014b). Design and prototype development of a novel low cost stress radiographic device - laxmeter (an Indo-Africa invention). Appropriate Healthcare Technologies for Low Resource Settings, London, Institute of Electrical and Electronics Engineers (IEEE).

SKF. (2013). "CAHB-10 operating manual." Retrieved 06 March, 2017, from http://www.skf.com/group/knowledge-centre/media-library/index.html#tcm:12-30013.

Souryal, T. O. (2015) "Texas Sports Medicine and Orthopaedic Group." ACL Injury, ACL Tear, ACL Surgery Volume, DOI:

Staubli, H. and R. Jakob (1991). "Anterior knee motion analysis. Measurement simultaneous radiography." The American Journal of Sports Medicine: 172-177.

STMicroelectronics. (2000). "Dual Full-Bridge Driver." SparkFun, from https://www.sparkfun.com/datasheets/Robotics/L298_H_Bridge.pdf.

Takeda, Y., J. W. Xerogeanes, G. A. Livesay, F. H. Fu and S. L. Woo (1994). "Biomechanical function of the human anterior cruciate ligament." Arthroscopy **10**(2): 140-7.

Tegner, Y. and J. Lysholm (1985). "Rating Systems in the Evaluation of Knee Ligament Injuries." Clinical orthopaeidics and related research: 43-49.

Thomas, S., M. Pullagura, E. Robinson, A. Cohen and P. Banaszkiewicz (2007). "The value of magnetic resonance imaging in our current management of ACL and meniscal injuries." Knee Surgery, Sports Traumatology, Arthroscopy: 533-536.

Timmerman, L. A., M. L. Schwartz and J. R. Andrews (1994). "Preoperative Evaluation of the Ulnar Collateral Ligament by Magnetic Resonance Imaging and Computed Tomography Arthrography." The American Journal of Sports Medicine: 26-32.

ToolBox, E. (2017). "Modulus of Elasticity or Young's Modulus - and Tensile Modulus for common Materials." The Engineering ToolBox, from http://www.engineeringtoolbox.com/young-modulus-d_417.html.

Tsai, A. G., V. Musahl, H. Steckel, K. M. Bell, T. Zantop, J. J. Irrgang and F. H. Fu (2008). "Rotational knee laxity: Reliability of a simple measurement device in vivo." BMC Musculoskeletal Disorders **9**(1): 35.

UCORS. (2011). "The GNRB: computerized analysis robot of lesions of the Crusader Ligament Anterior." from http://www.chirurgieorthopedie-ucors.fr/2010/01/25/le-gnrb-robot-d%E2%80%99analyse-informatisee-des-lesions-du-ligament-croise-anterieur/.

Vauhnik, R., M. C. Morrissey, M. P. Perme, F. Sevsek and D. Rugelj (2014). "Inter-rater reliability of the GNRB® knee arthrometer." The Knee: 541-543.

Ventola, C. L. (2014). "Medical Applications for 3D Printing: current and projected uses." Pharmacy and Therapeutics: 704-711.

Wiertsema, S. H., H. J. A. v. Hooff, L. A. A. Migchelsen and M. P. M. Steultjens (2008). "Reliability of the KT1000 arthrometer and the Lachman test in patients with an ACL rupture." The Knee: 107-110.

Woo, S. L., R. E. Debski, J. D. Withrow and M. A. Janaushek (1999). "Biomechanics of knee ligaments." Am J Sports Med **27**(4): 533-43.

Woon, C. and M. Hughes (2015). Orthobullets. Ligaments.

Appendix A

Bilateral Support Structure

The Bilateral Support Structure concept was inspired by the Laxmeter's bilateral imaging feature and would potentially be a viable solution for the LAS support structure (Sivarasu & Patnaik, 2014). The LAS Bilateral Support Structure would span across the width of the Laxmeter with a mid-support in the centre of the structure. The load applicator would attach to the superior and lateral supports of the structure, thereby allowing for cruciate and collateral laxity measurements. Figure illustrates the concept (at the initial ideation stage) attached to the LLSP, prior to the incorporation of the material dependant - and general design - considerations.

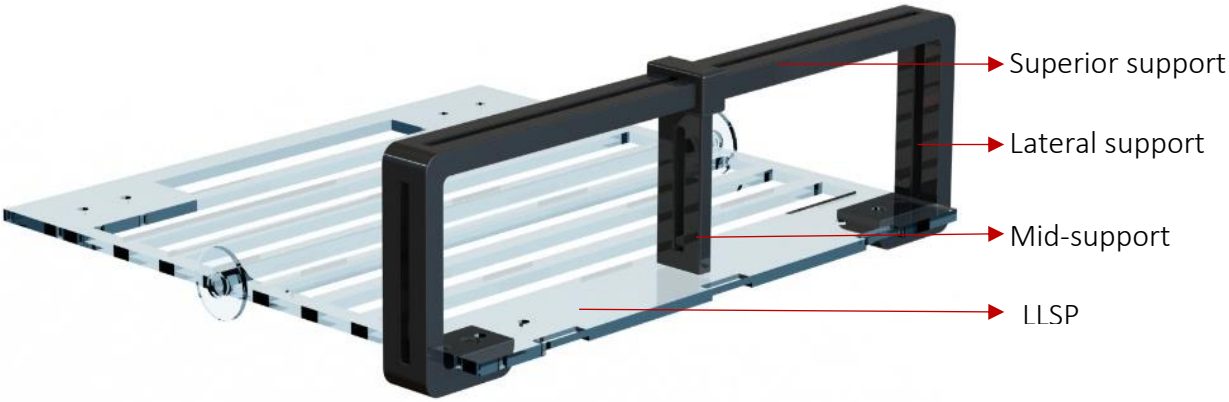

Figure A: The bilateral LAS support structure attached to the LLSP of the existing Laxmeter Prototype

The image illustrates the bilateral LAS support structure in the ideation phase. The structure would span the width of the Laxmeter and be fitted to the lower leg panel by means of pins or bolts. The load applicator would be attached to the lateral and superior supports of the Bilateral Support Structure so as to induce AP and ML lower leg translation.

The Bilateral Support Structure would complement the bilateral imaging and ML laxity measurement capabilities of the existing Laxmeter Prototype. Theoretically, the concept would require the operator to slide the support structure onto the LLSP and fix it into position by means of bolts or pins. The operator would manually attach the load applicator to the structure to achieve AP and ML lower leg translation. In addition, two load applicators could potentially be attached to both lateral support structures and induce proximal lower leg translation to the injured limb as well as the healthy limb, simultaneously. This would allow for real-time comparison of injured-healthy limb translation for MCL and LCL laxity measurements only. This concept, however, would require further ideation and development for it to be a viable option for the support structure of the LAS.

Appendix B

Arduino Specifications

ARDUINO MICROCONTROLLER	
Microcontroller	ATmega328
Architecture	AVR
Operating Voltage	5 V
Flash memory	32 KB of which 0.5 KB used by bootloader
SRAM	2 KB
Clock Speed	16 MHz
Analog I/O Pins	6
EEPROM	1 KB
DC Current per I/O Pins	40 mA on I/O Pins; 50 mA on 3,3 V Pin

GENERAL	
Input Voltage	7-12 V
Digital I/O Pins	20 (of wich 6 provide PWM output)
PWM Output	6
PCB Size	53.4 x 68.6 mm
Weight	25 g
Product Code	A000066 (TH); A000073 (SMD)

Appendix C

Drawings

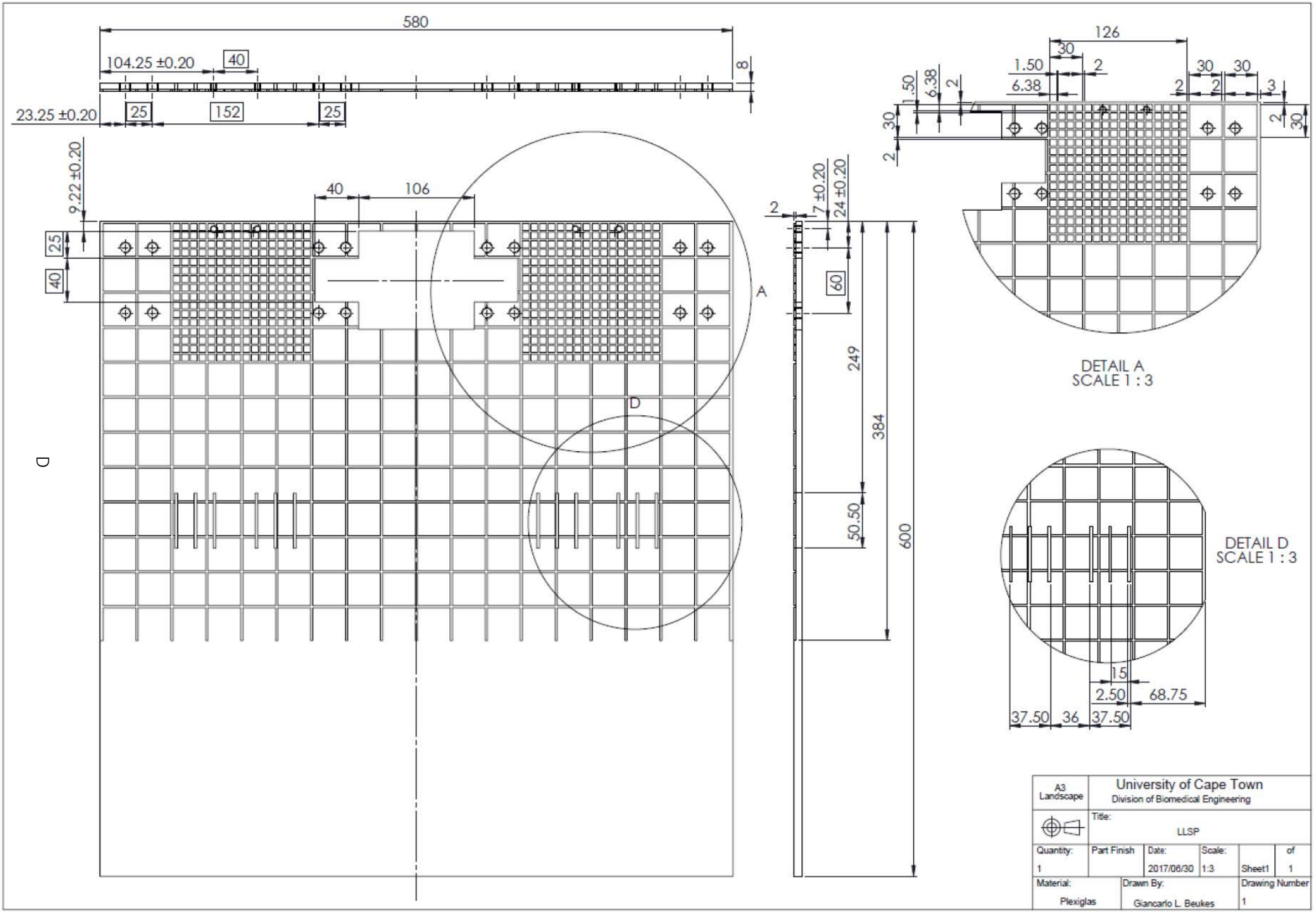

A3 Landscape	University of Cape Town Division of Biomedical Engineering				
	Title: LLSP				
Quantity: 1	Part Finish	Date: 2017/06/30	Scale: 1:3	Sheet1	of 1
Material: Plexiglas	Drawn By: Giancarlo L. Beukes			Drawing Number 1	

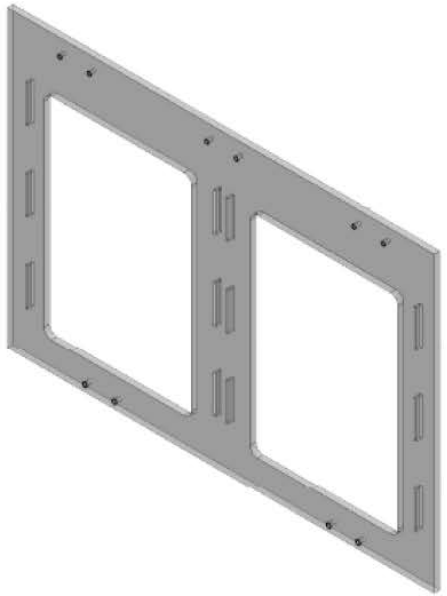

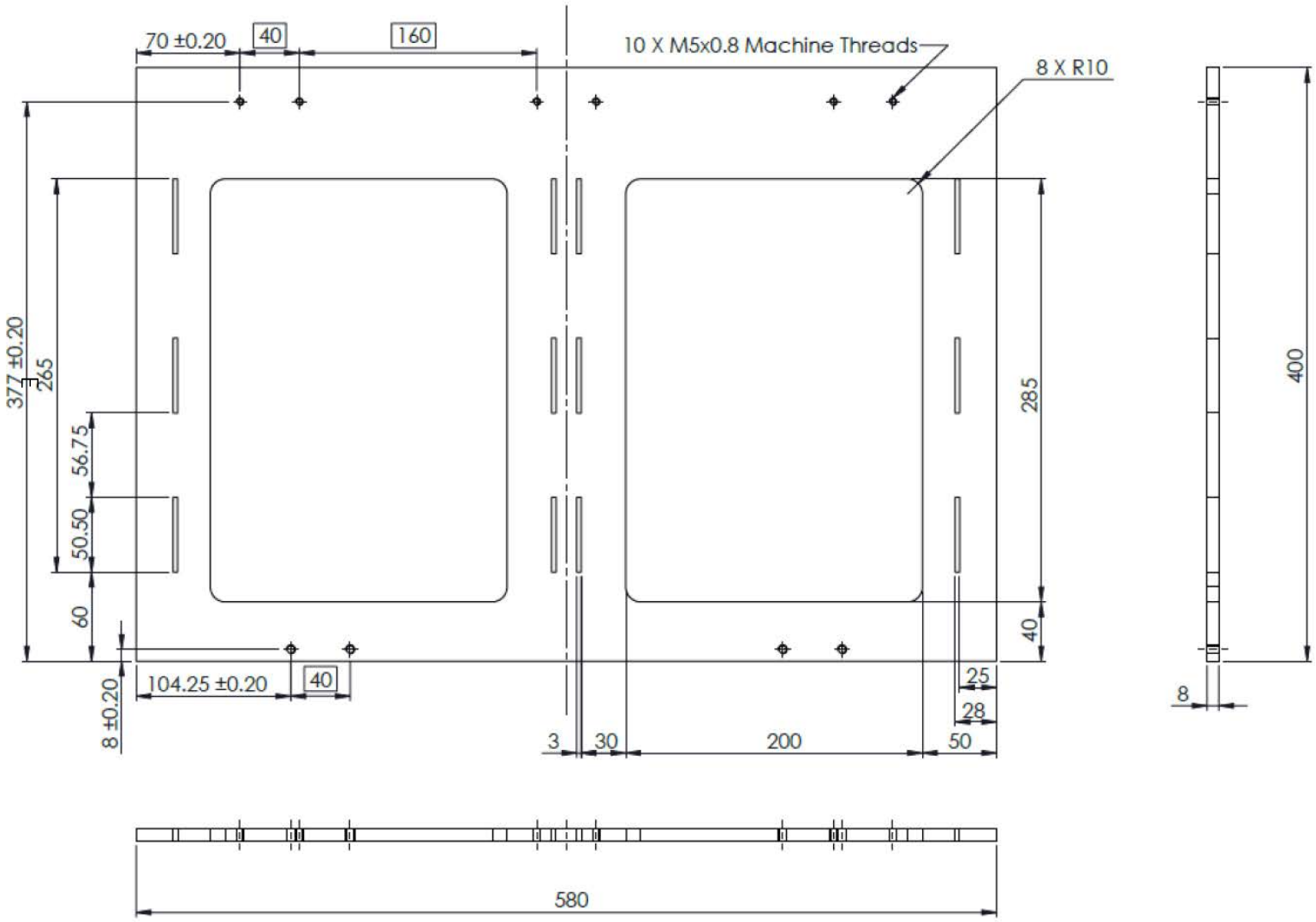

A3 Landscape	University of Cape Town Division of Biomedical Engineering				
	Title: ULSP				
Quantity: 1	Part Finish	Date: 2017/06/30	Scale: 1:5	Sheet1	of 1
Material: Plexiglas	Drawn By: Giancarlo L. Beukes			Drawing Number 2	

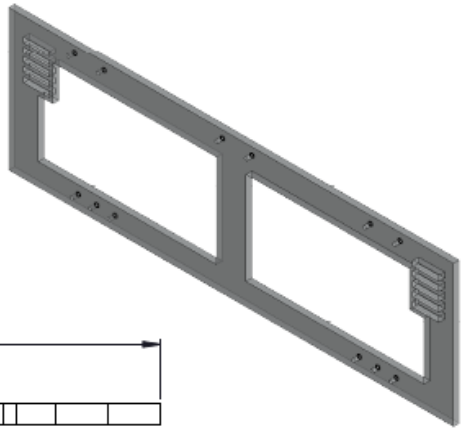

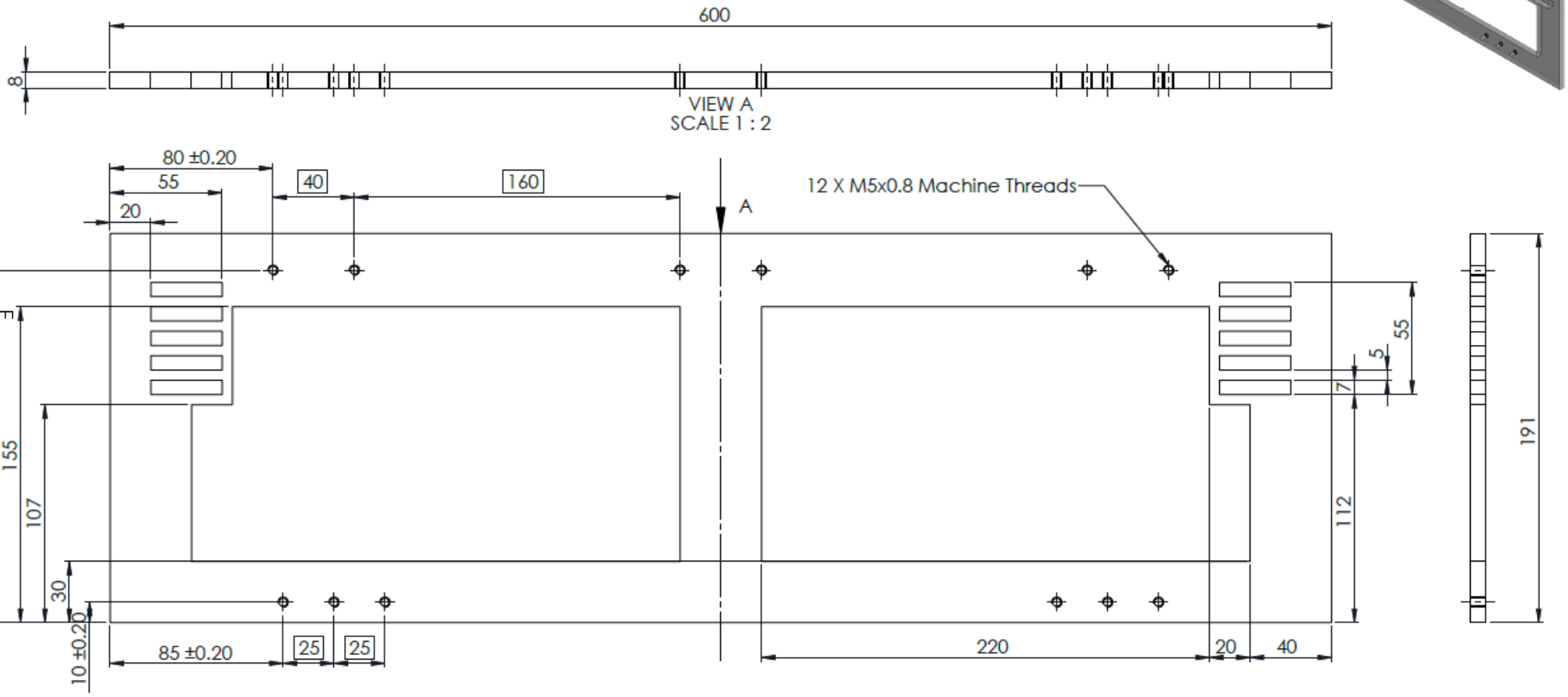

A3 Landscape	University of Cape Town Division of Biomedical Engineering				
	Title: LLSP Hinge Arch				
Quantity: 1	Part Finish	Date: 2017/06/30	Scale: 1:2	Sheet1	of 1
Material: Plexiglas	Drawn By: Giancarlo L. Beukes			Drawing Number 3	

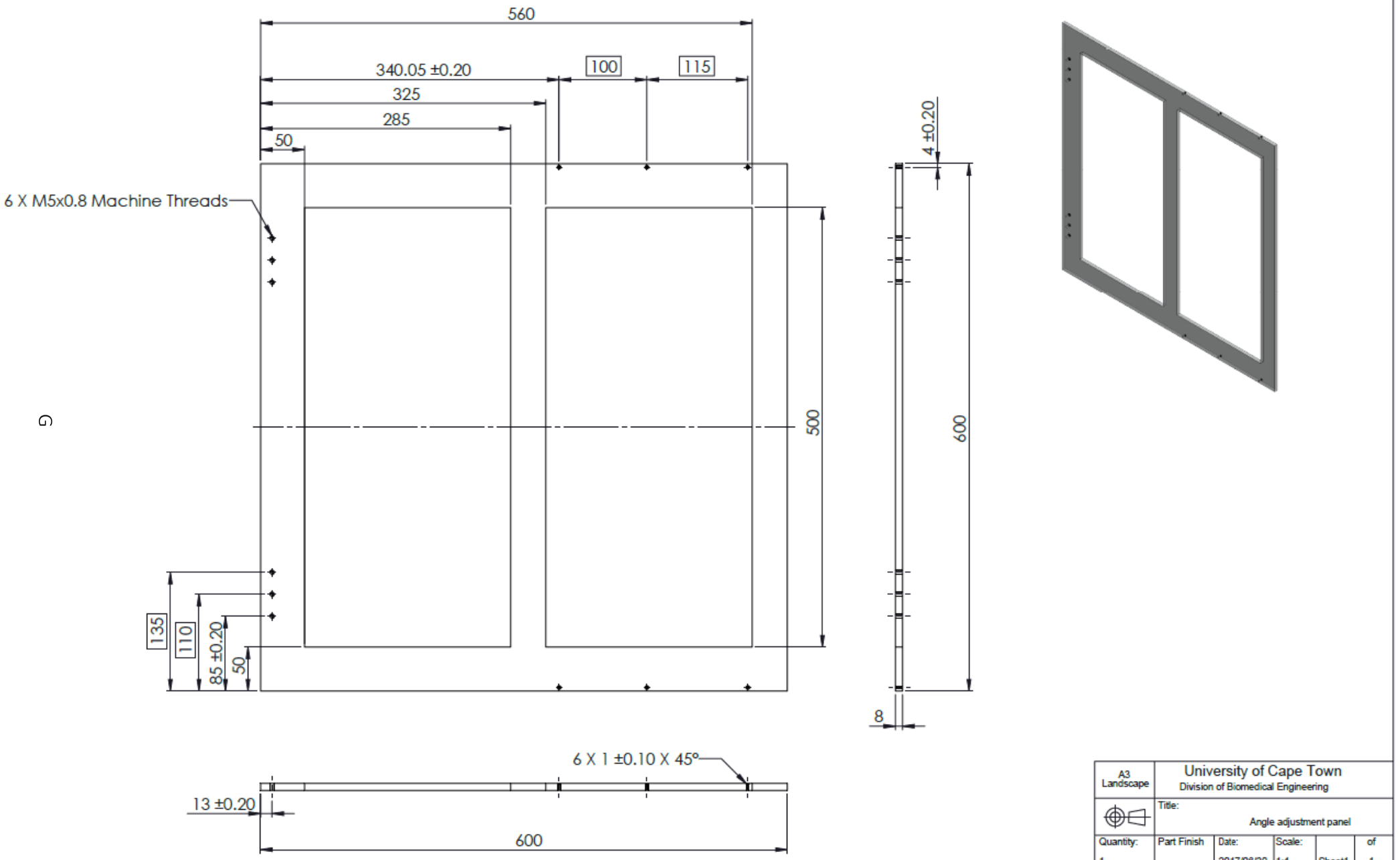

A3 Landscape	University of Cape Town Division of Biomedical Engineering				
	Title: Angle adjustment panel				
Quantity: 1	Part Finish	Date: 2017/06/30	Scale: 1:4	Sheet1	of 1
Material: Plexiglas	Drawn By: Giancarlo L. Beukes			Drawing Number 4	

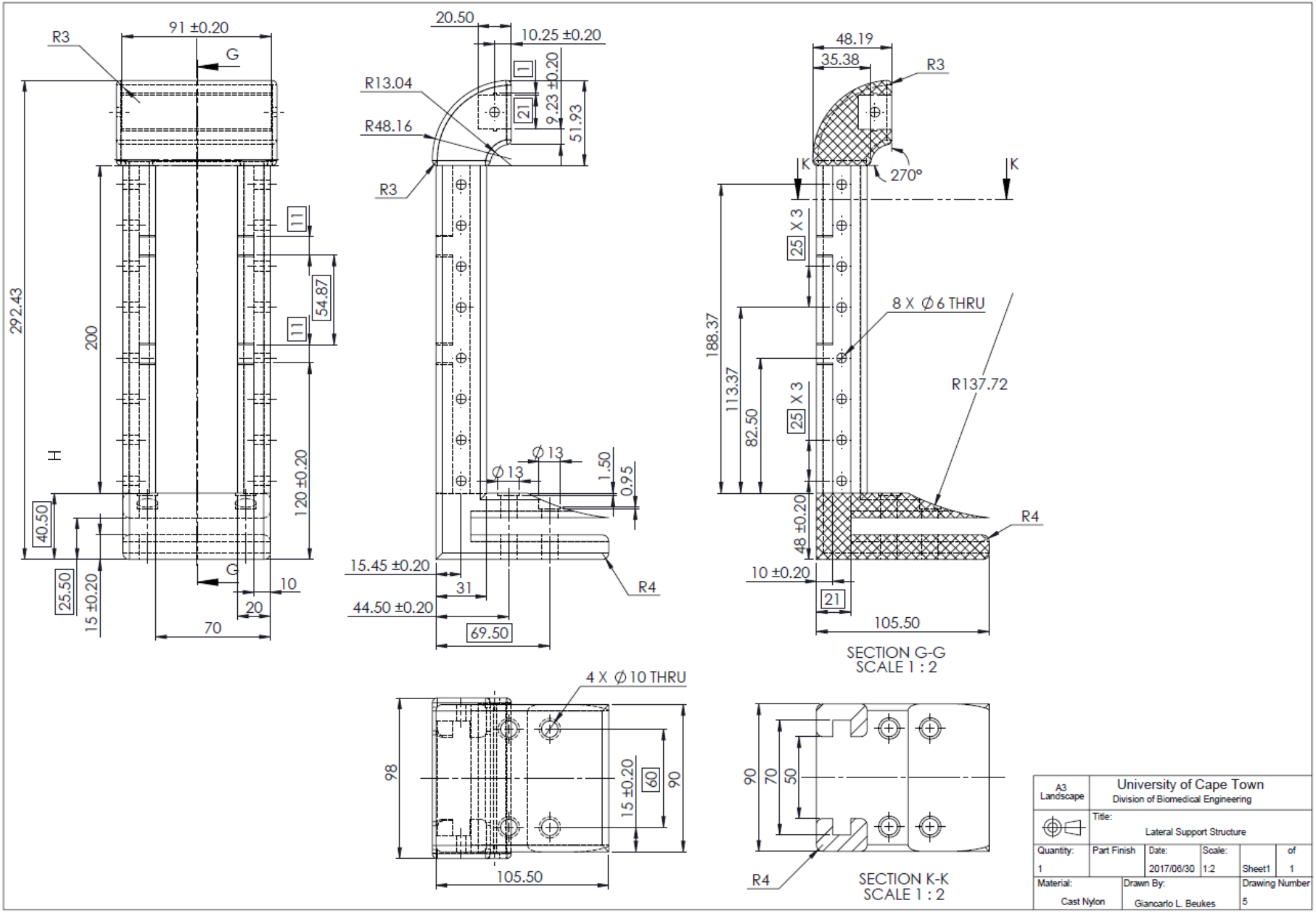
R3
91 ±0.20
G
292.43
200
H
11
54.87
11
120 ±0.20
40.50
25.50
15 ±0.20
G
10
20
70
20.50
10.25 ±0.20
1
21
9.23 ±0.20
51.93
R13.04
R48.16
R3
Ø 13
Ø 13
1.50
0.95
15.45 ±0.20
31
44.50 ±0.20
69.50
R4
48.19
35.38
R3
K
270°
K
25 X 3
8 X Ø 6 THRU
188.37
113.37
82.50
25 X 3
R137.72
48 ±0.20
R4
10 ±0.20
21
105.50
SECTION G-G
SCALE 1 : 2
4 X Ø 10 THRU
98
15 ±0.20
60
90
105.50
90
70
50
R4
SECTION K-K
SCALE 1 : 2
A3 Landscape
University of Cape Town
Division of Biomedical Engineering
Title:
Lateral Support Structure
Quantity:
1
Part Finish
Date:
2017/06/30
Scale:
1:2
Sheet1
of
1
Material:
Cast Nylon
Drawn By:
Giancarlo L. Beukes
Drawing Number
5

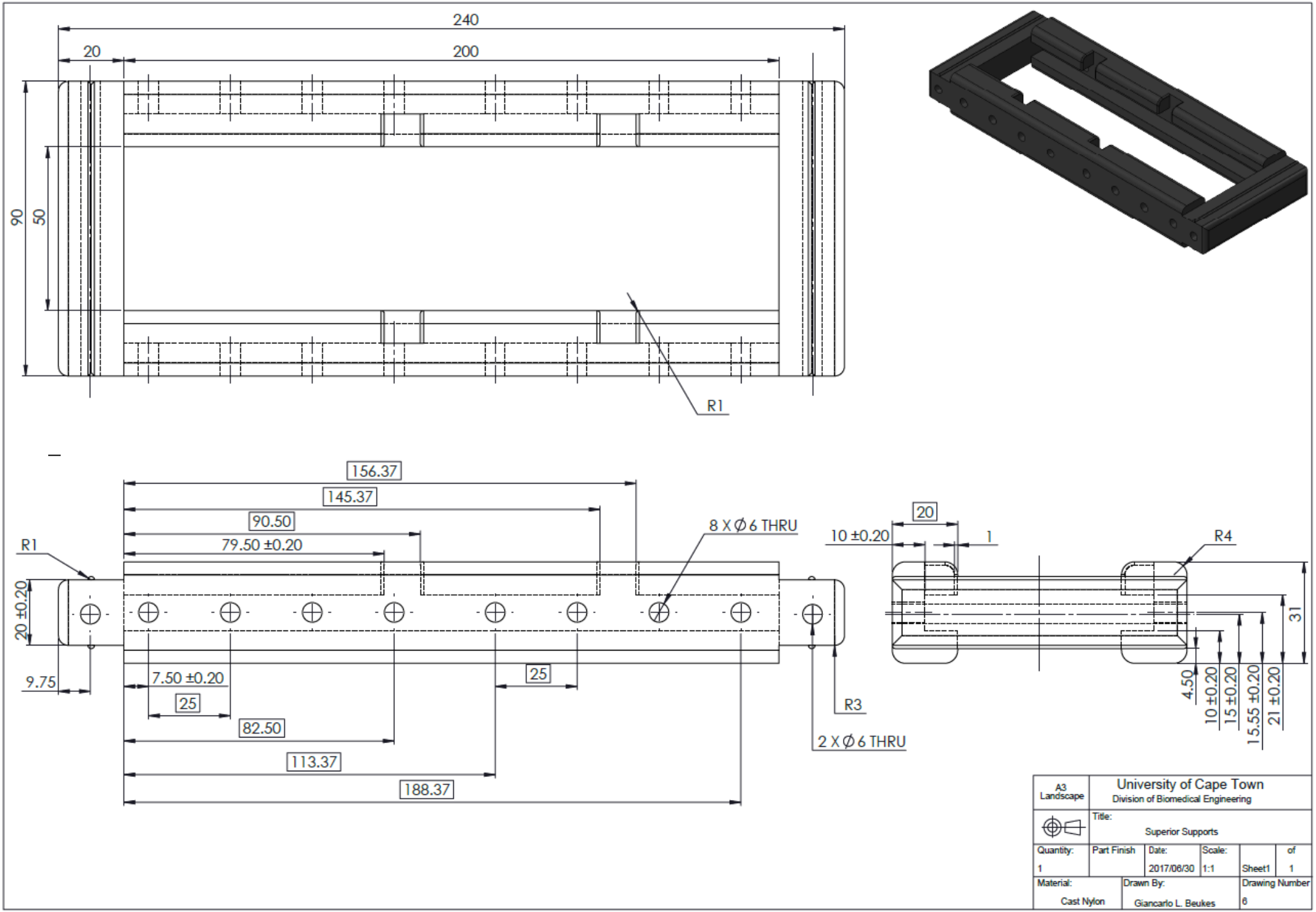

A3 Landscape	University of Cape Town Division of Biomedical Engineering				
	Title: Superior Supports				
Quantity: 1	Part Finish	Date: 2017/06/30	Scale: 1:1	Sheet1	of 1
Material: Cast Nylon	Drawn By: Giancarlo L. Beukes			Drawing Number 6	

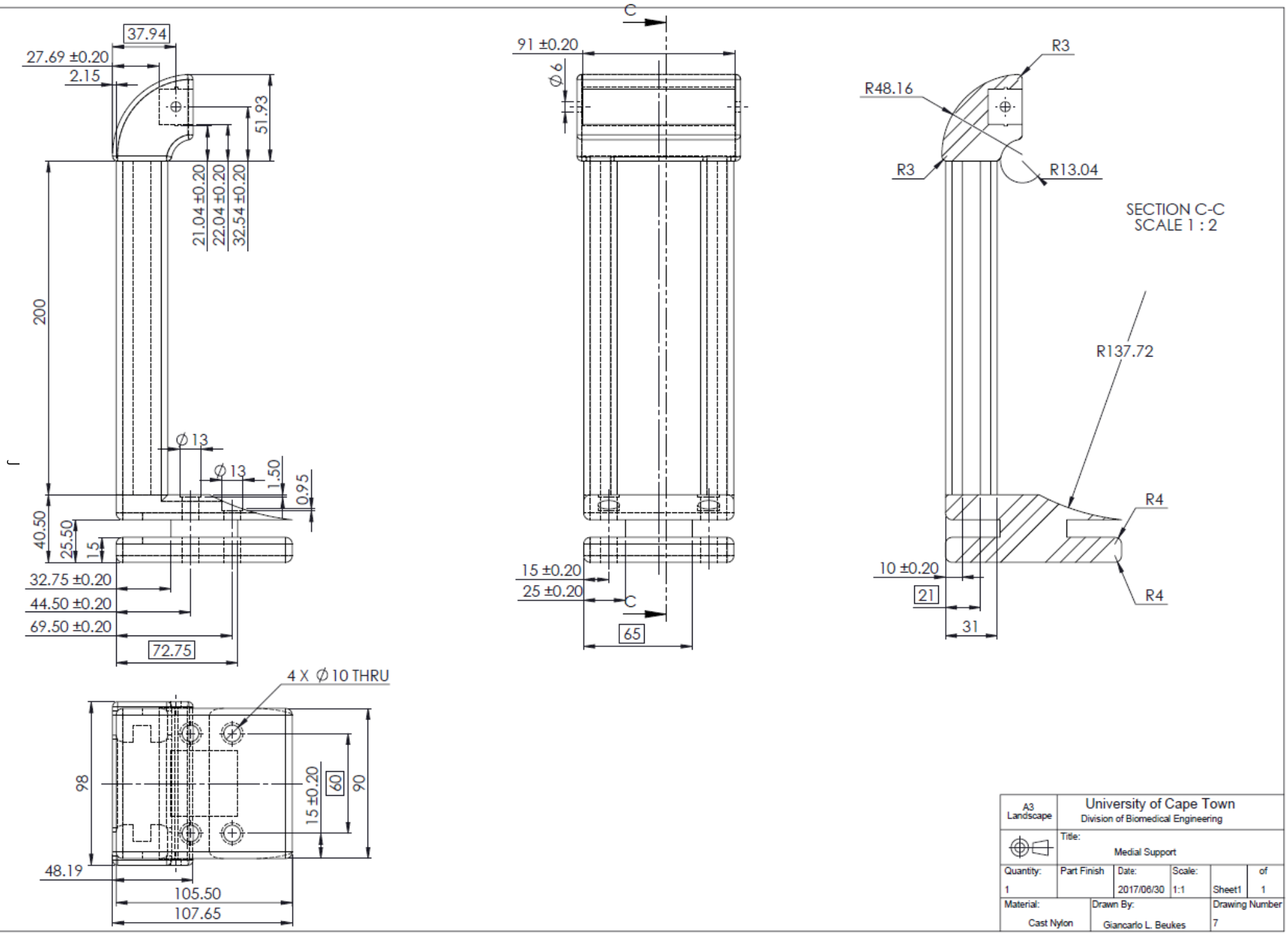
37.94
27.69 ±0.20
2.15
51.93
21.04 ±0.20
22.04 ±0.20
32.54 ±0.20
200
Ø13
Ø13
1.50
0.95
40.50
25.50
15
32.75 ±0.20
44.50 ±0.20
69.50 ±0.20
72.75
4 X Ø10 THRU
98
15 ±0.20
60
90
48.19
105.50
107.65
C
91 ±0.20
Ø6
15 ±0.20
25 ±0.20
C
65
R3
R48.16
R3
R13.04
SECTION C-C
SCALE 1 : 2
R137.72
R4
10 ±0.20
21
31
R4
A3
Landscape
University of Cape Town
Division of Biomedical Engineering
Title:
Medial Support
Quantity:
1
Part Finish
Date:
2017/06/30
Scale:
1:1
Sheet1
of
1
Material:
Cast Nylon
Drawn By:
Giancarlo L. Beukes
Drawing Number
7

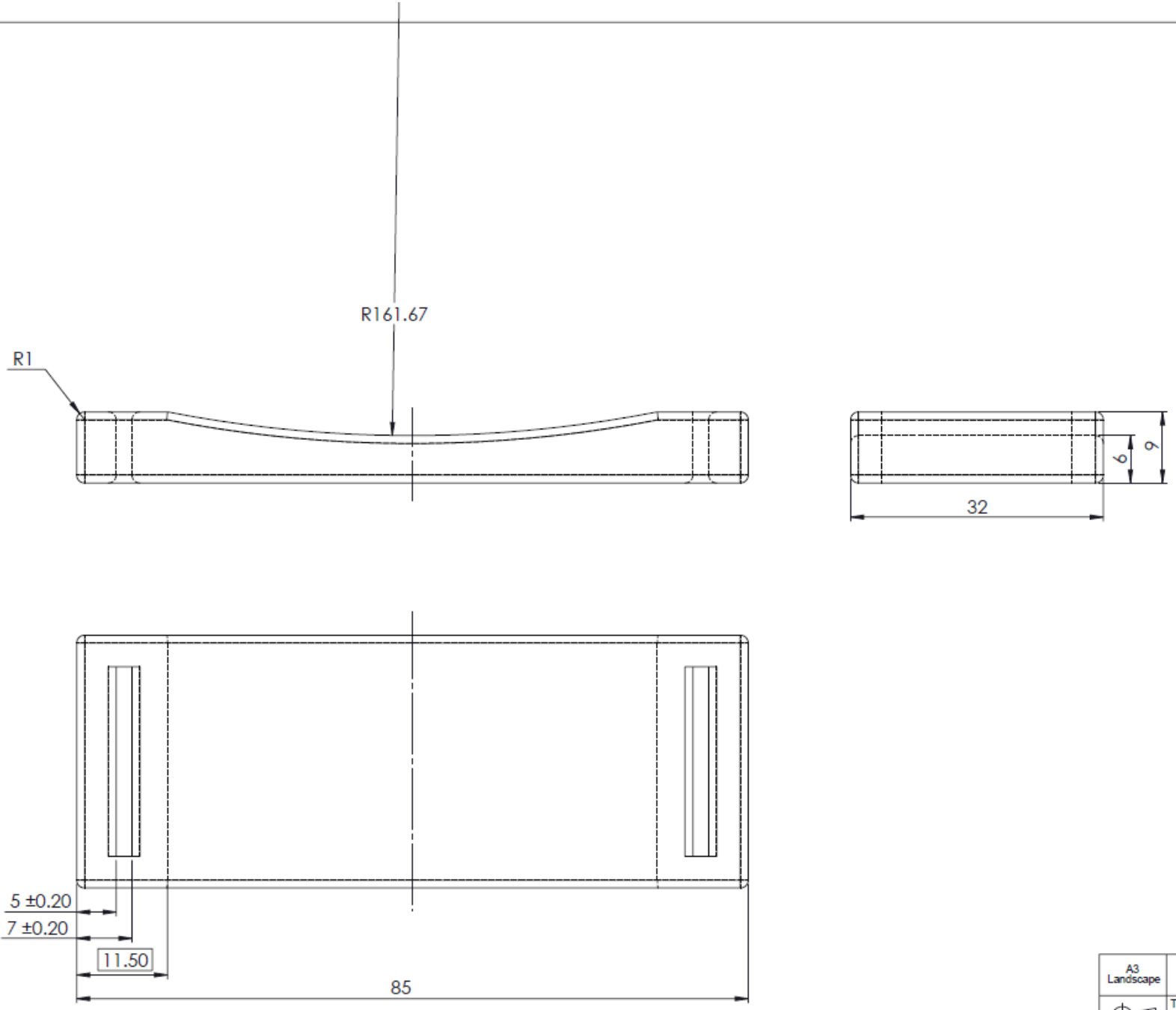

A3 Landscape	University of Cape Town Division of Biomedical Engineering				
	Title: Anterior-lateral FSP				
Quantity: 1	Part Finish	Date: 2017/06/30	Scale: 1:1	Sheet1	of 1
Material: Ertalyte	Drawn By: Giancarlo L. Beukes			Drawing Number 8	

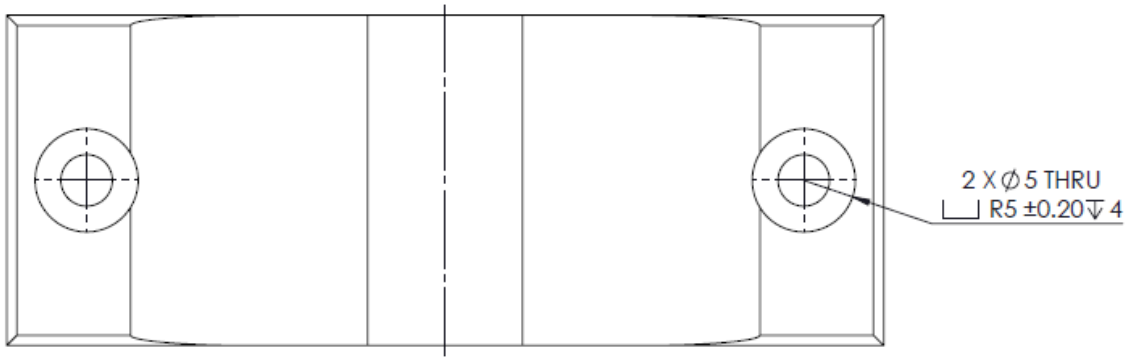

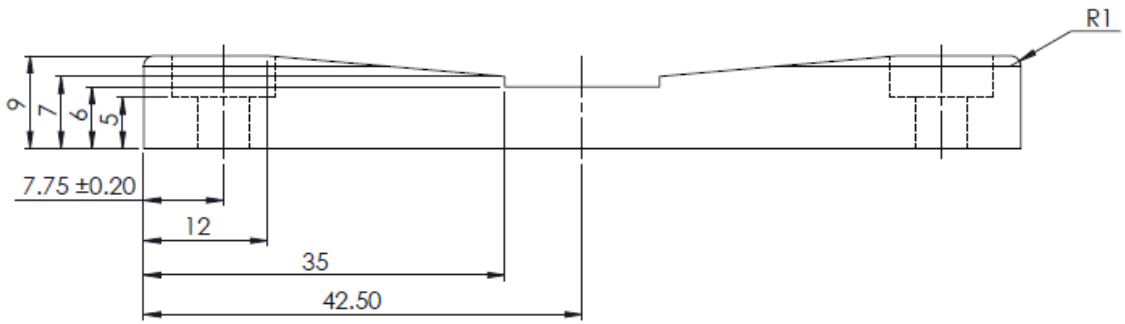

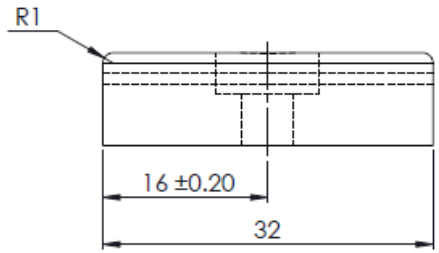

A3 Landscape	University of Cape Town Division of Biomedical Engineering				
	Title: Posterior-medial FSP				
Quantity: 1	Part Finish	Date: 2017/06/30	Scale: 2:1	Sheet1	of 1
Material: Ertalyte	Drawn By: Giancarlo L. Beukes			Drawing Number 9	

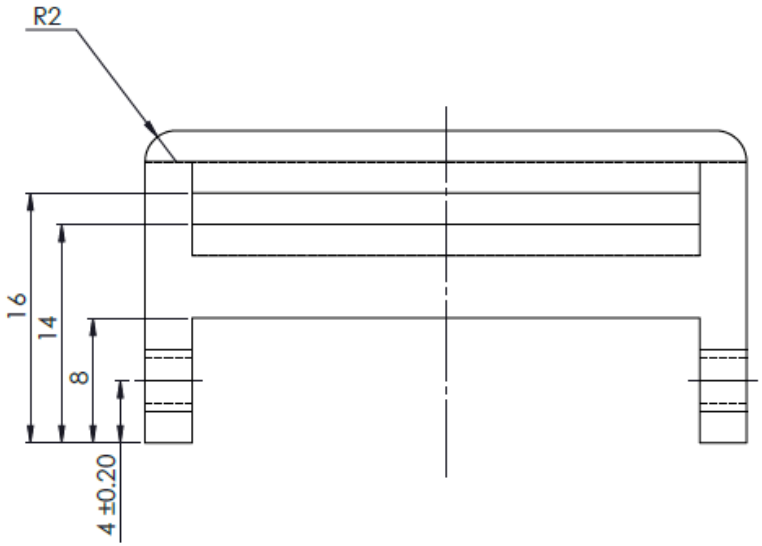

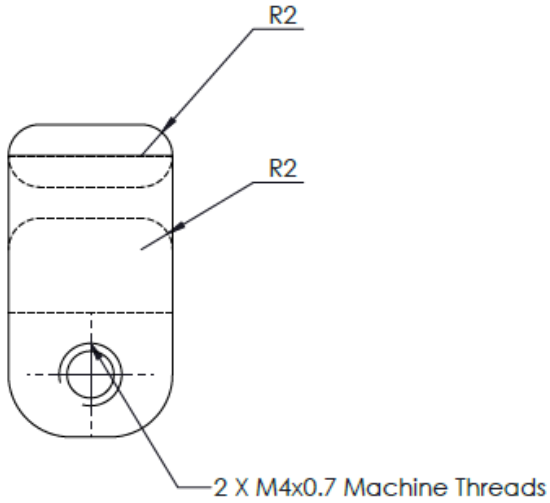

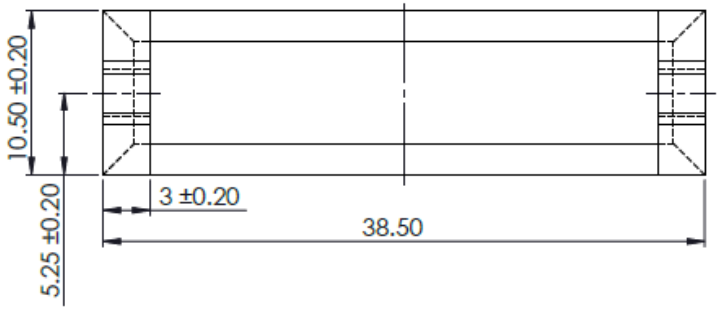

A3 Landscape	University of Cape Town Division of Biomedical Engineering				
	Title: Posterior-medial FSP attachment				
Quantity: 2	Part Finish	Date: 2017/06/30	Scale: 3:1	Sheet1	of 1
Material: Cast Nylon	Drawn By: Giancarlo L. Beukes			Drawing Number 10	

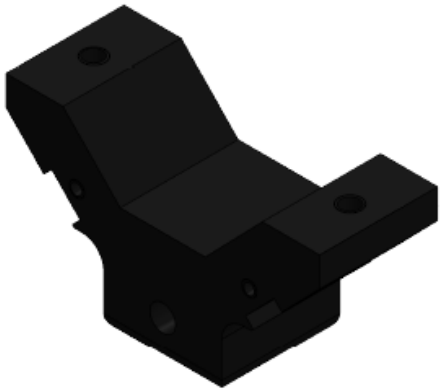

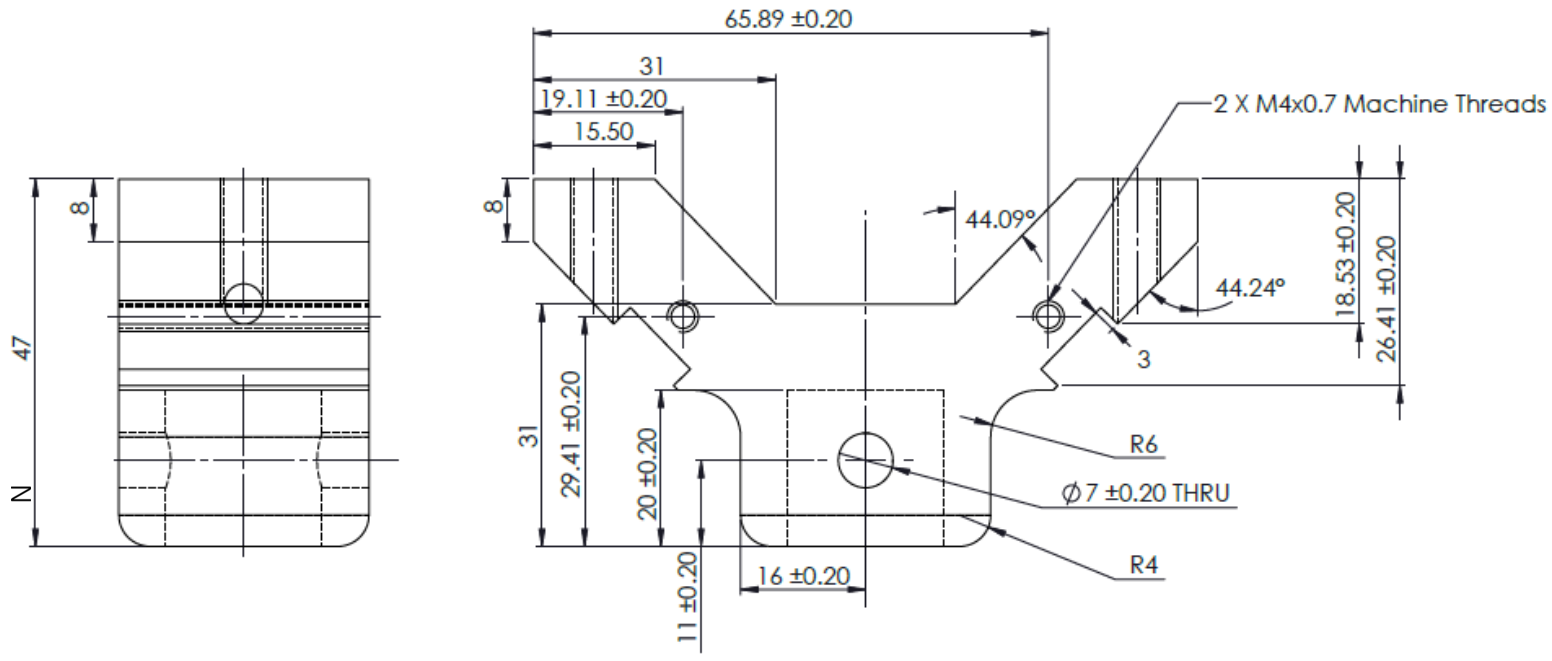

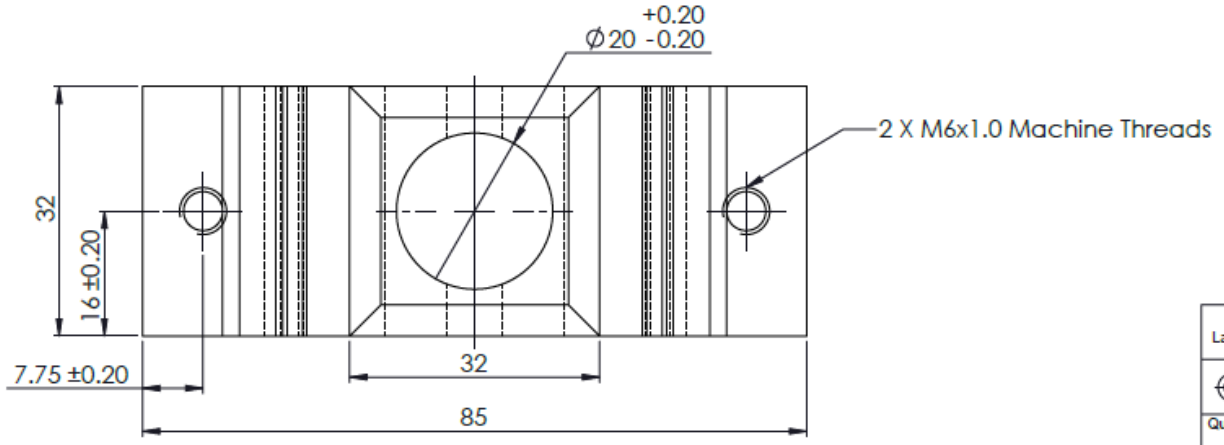

A3 Landscape	University of Cape Town Division of Biomedical Engineering				
	Title: Posterior-Medial FSP adaptor				
Quantity: 1	Part Finish	Date: 2017/06/30	Scale: 1.5:1	Sheet1	of 1
Material: Cast Nylon	Drawn By: Giancarlo L. Beukes			Drawing Number 11	

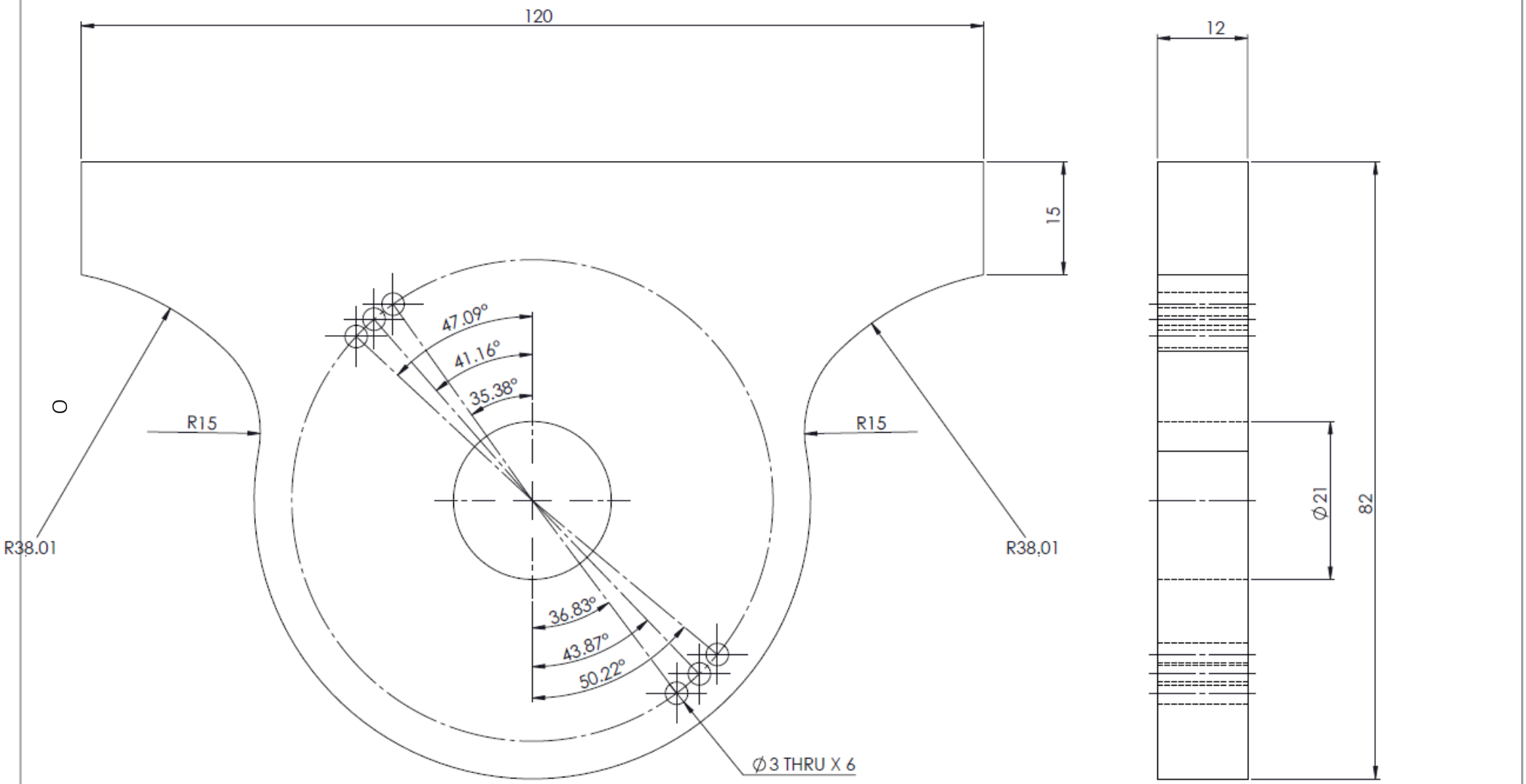

A3 Landscape	University of Cape Town Division of Biomedical Engineering				
	Title: LLSP Hinge Arch				
Quantity: 2	Part Finish	Date: 2017/06/30	Scale: 2:1	Sheet1	of 1
Material: Plexiglas	Drawn By: Giancarlo L. Beukes			Drawing Number 12	

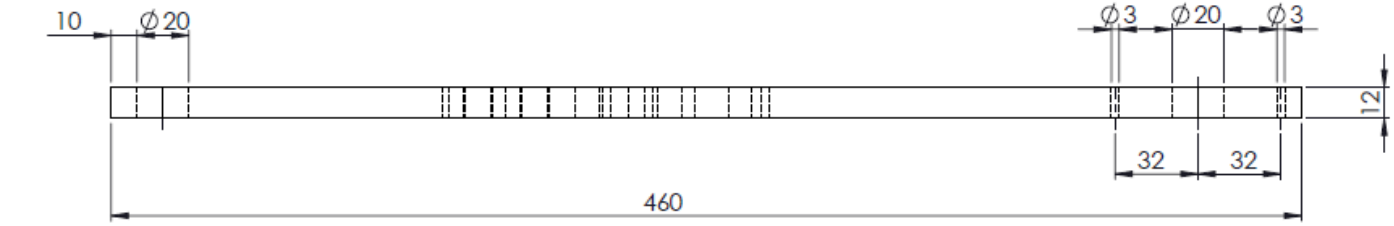

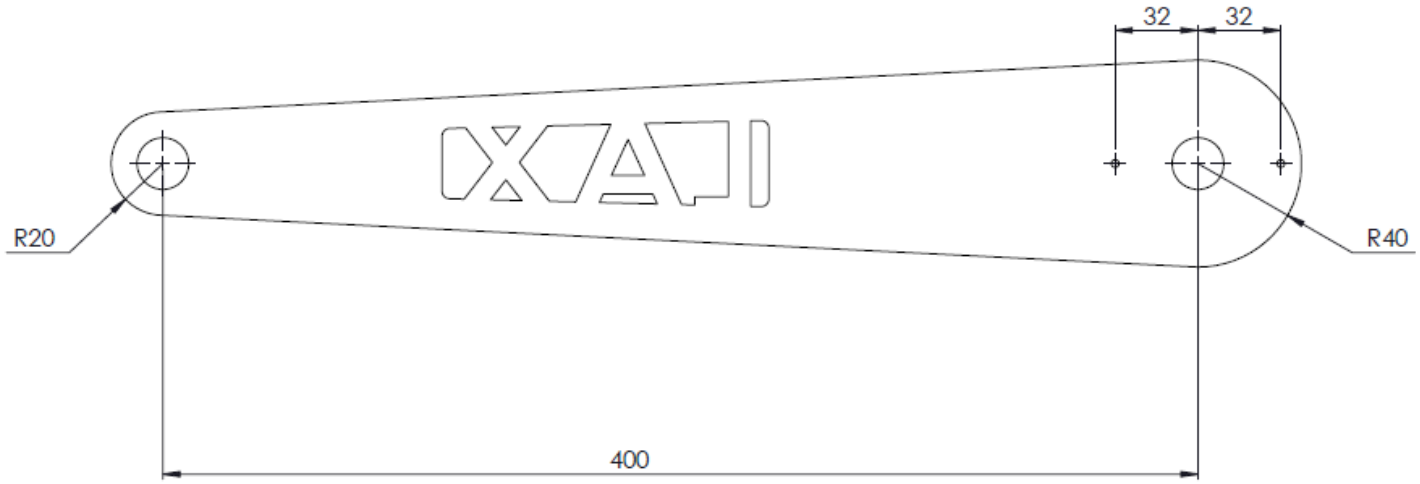

P

A3 Landscape	University of Cape Town Division of Biomedical Engineering				
	Title: LLSP Hinge Arch				
Quantity: 2	Part Finish	Date: 2017/06/30	Scale: 1:2	Sheet1	of 1
Material: Plexiglas	Drawn By: Giancarlo L. Beukes			Drawing Number 13	

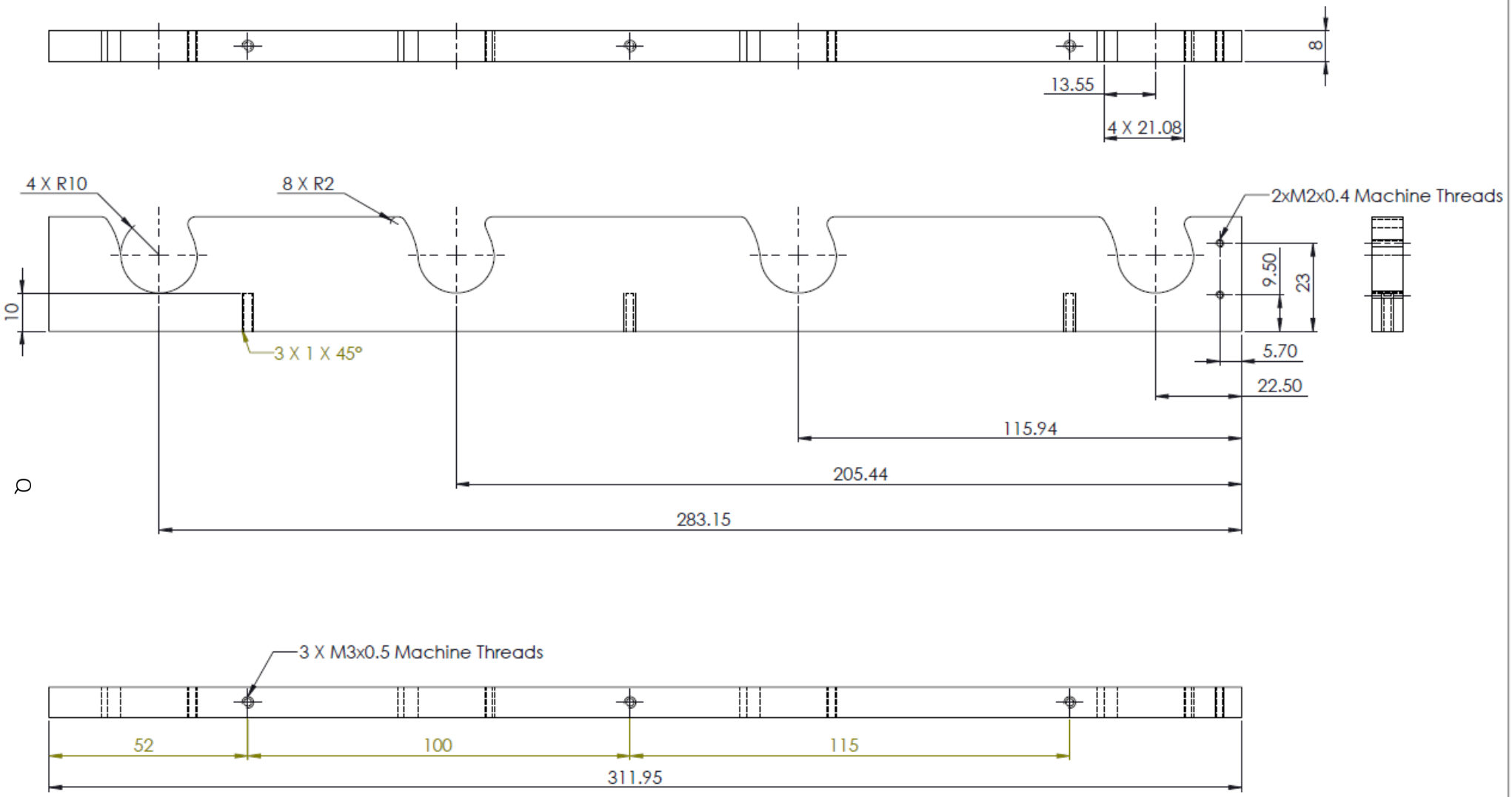

A3 Landscape	University of Cape Town Division of Biomedical Engineering				
	Title: Fixed slot				
Quantity: 2	Part Finish	Date: 2017/06/30	Scale: 1:1	Sheet1	of 1
Material: Plexiglas	Drawn By: Giancarlo L. Beukes			Drawing Number 14	

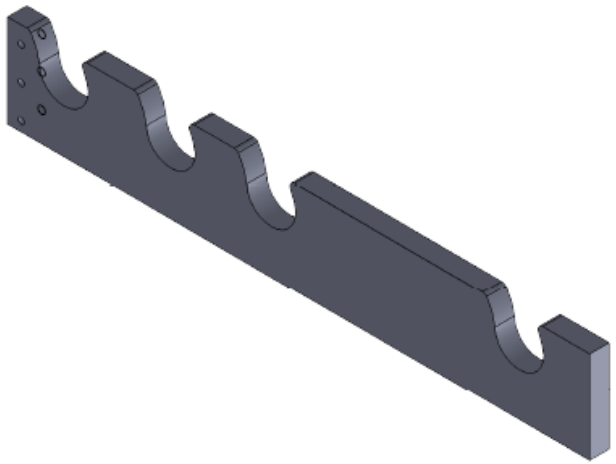

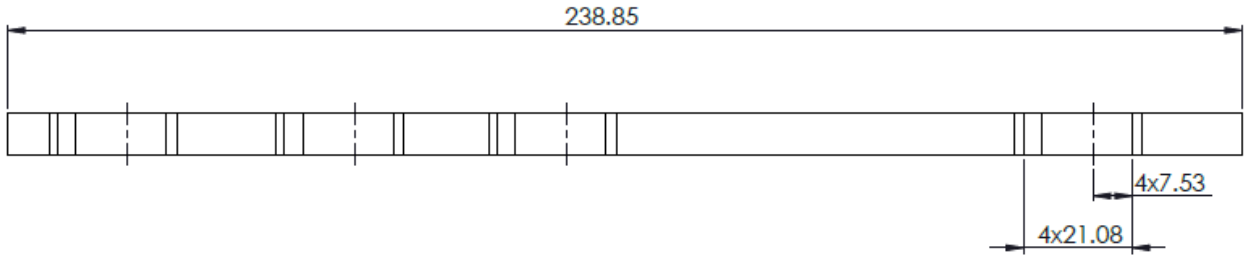

R

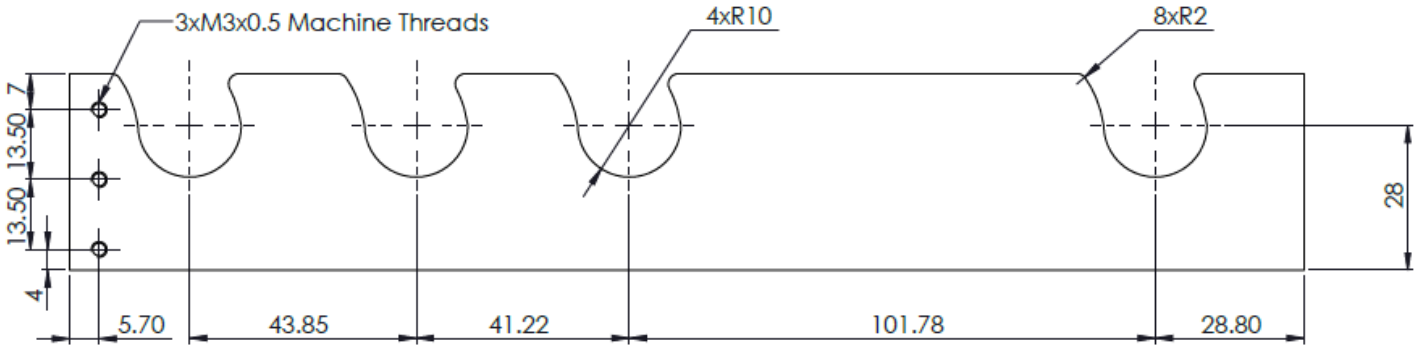

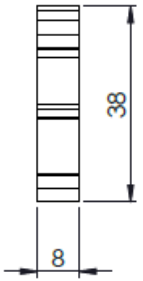

A3 Landscape	University of Cape Town Division of Biomedical Engineering				
	Title: Hinging Slot 2				
Quantity: 2	Part Finish	Date: 2017/06/30	Scale: 1:1	Sheet1	of 1
Material: Plexiglas	Drawn By: Giancarlo L. Beukes			Drawing Number 15	

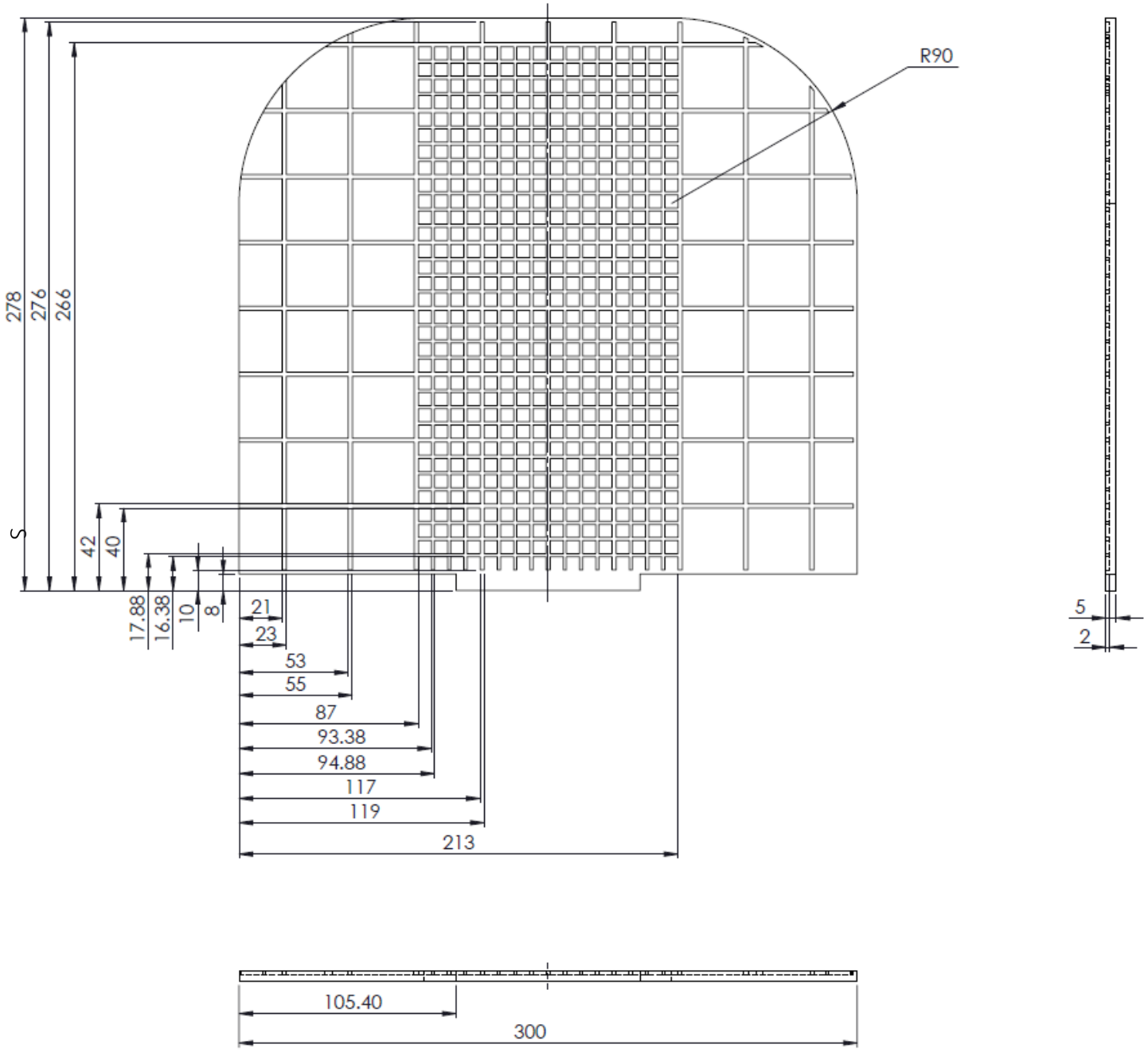

A3 Landscape	University of Cape Town Division of Biomedical Engineering				
	Title: AP translation Tracking Scale				
Quantity: 1	Part Finish	Date: 2017/06/30	Scale: 1:2	Sheet1	of 1
Material: Plexiglas	Drawn By: Giancarlo L. Beukes			Drawing Number 16	

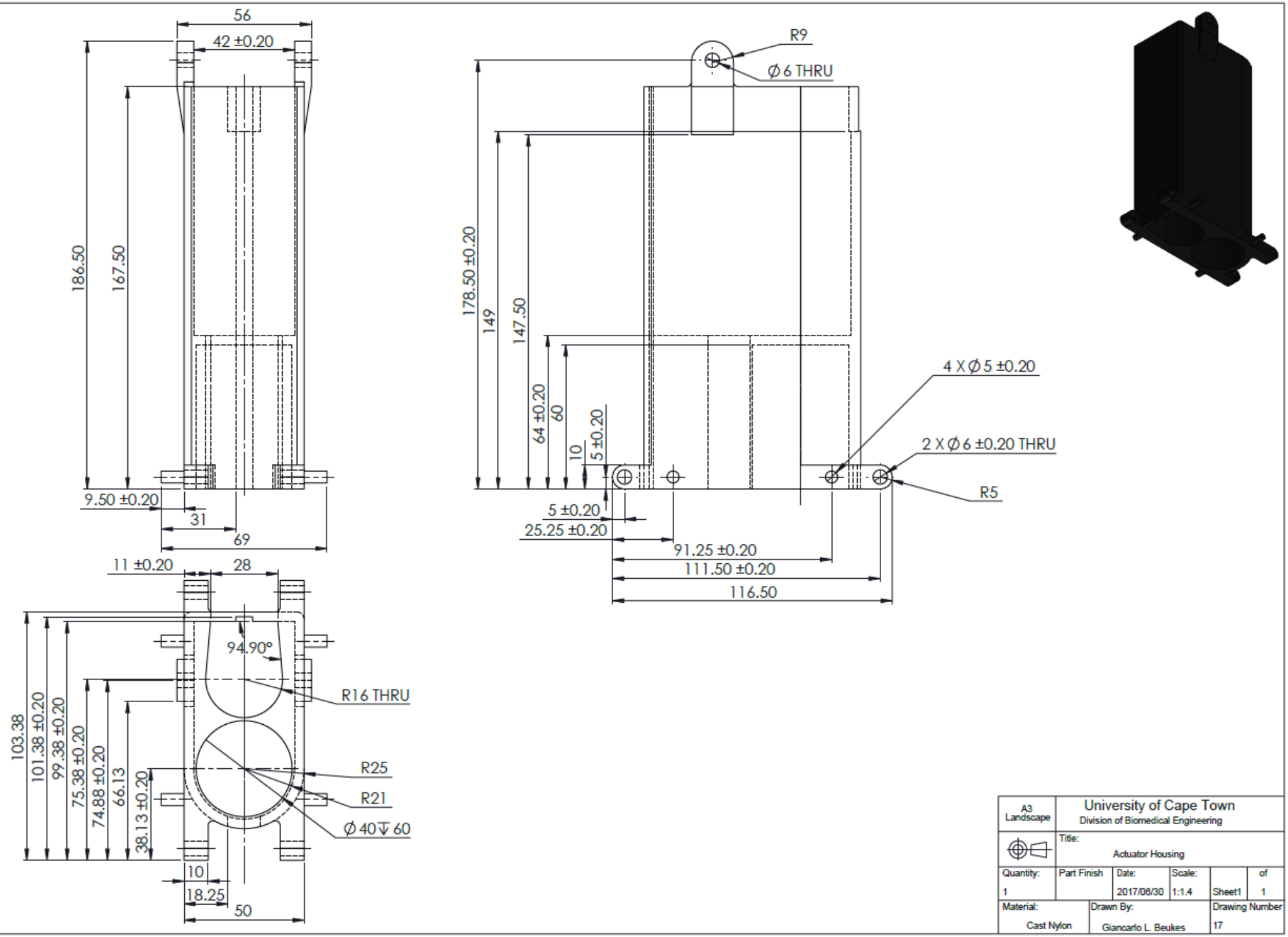
56
42 ±0.20
186.50
167.50
9.50 ±0.20
31
69
R9
Ø 6 THRU
178.50 ±0.20
149
147.50
64 ±0.20
60
10
5 ±0.20
4 X Ø 5 ±0.20
2 X Ø 6 ±0.20 THRU
R5
5 ±0.20
25.25 ±0.20
91.25 ±0.20
111.50 ±0.20
116.50
11 ±0.20
28
94.90°
R16 THRU
103.38
101.38 ±0.20
99.38 ±0.20
75.38 ±0.20
74.88 ±0.20
66.13
38.13 ±0.20
R25
R21
Ø 40 ↧ 60
10
18.25
50
A3 Landscape
University of Cape Town
Division of Biomedical Engineering
Title:
Actuator Housing
Quantity:
1
Part Finish
Date:
2017/06/30
Scale:
1:1.4
Sheet1
of
1
Material:
Cast Nylon
Drawn By:
Giancarlo L. Beukes
Drawing Number
17

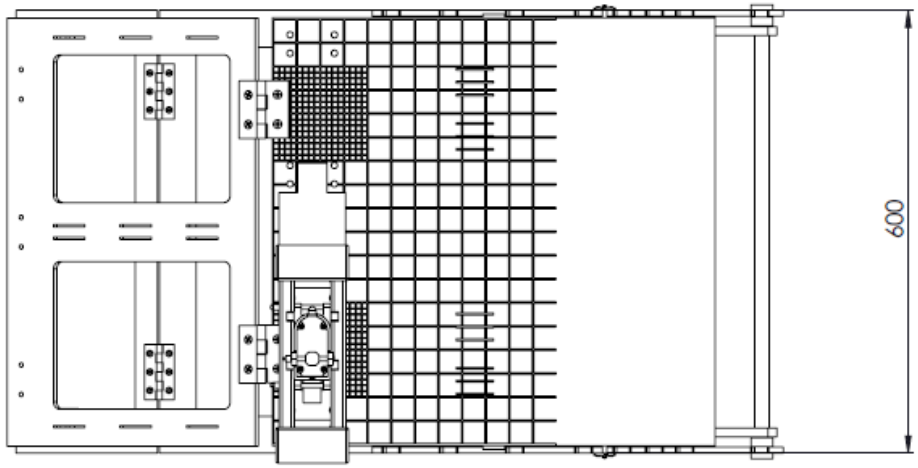

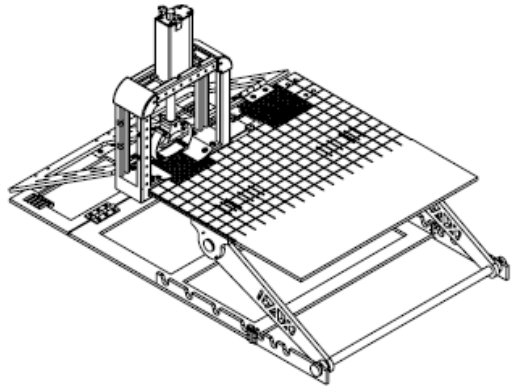

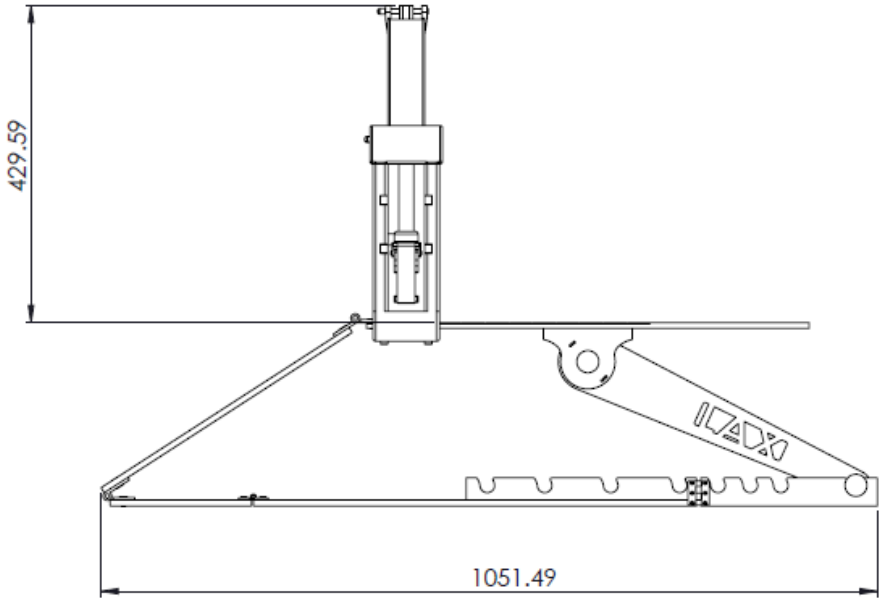

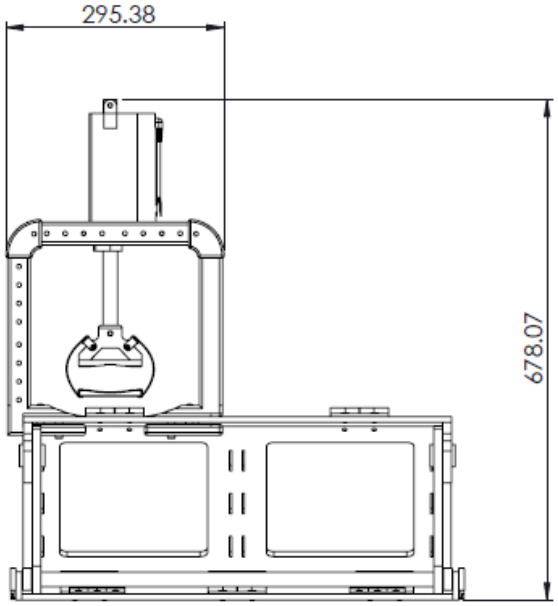

A3 Landscape	University of Cape Town Division of Biomedical Engineering			
	Title: Laxmeter Assembly			
Assembly Drawing	Scale: 1:7	Date: 2017/06/30	Sheet 1	of 2
	Drawn By: Giancarlo L. Beukes		Drawing Number 18	

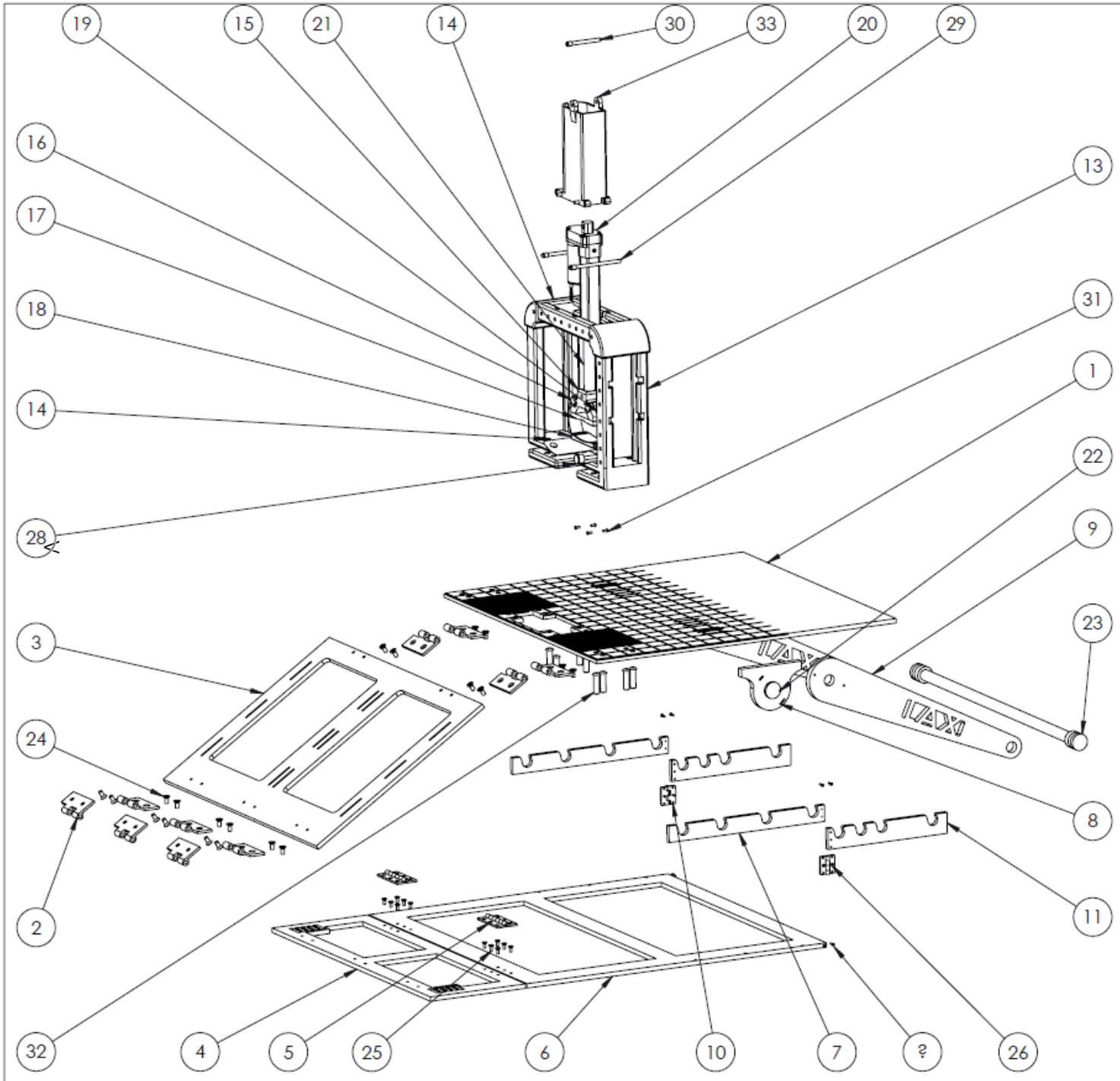

ITEM NO.	PART NUMBER	MATERIAL	QTY.
1	LLSP	Plexiglas	1
2	Large Hinge 1	Nylon	10
3	ULSP	Plexiglas	1
4	Fold assist panel	Plexiglas	1
5	Small hinge	Nylon	4
6	Angle adjustment panel	Plexiglas	1
7	Slot 1	Plexiglas	2
8	pivot part	Plexiglas	2
9	Parallel Arm	Plexiglas	2
10	tiny hinge	Nylon	4
11	Slot 2	Plexiglas	2
12	Superior LAS support	Nylon	1
13	Lateral LAS support	Nylon	1
14	Medial LAS support	Nylon	1
15	Posterior-medial FSP adaptor	Nylon	1
16	Anterior-lateral FSP adaptor	Nylon	2
17	Posterior-medial FSP	Ertalyte	1
18	Anterior-lateral FSP	Ertalyte	1
19	velcro straps	Velcro	2
20	Linear Actuator	Stainless steel	1
21	CAHB10 shaft	Stainless steel	1
22	Top pin	Plexiglas	2
23	long rod	Plexiglas	1
24	flat head screw_am	Nylon	20
25	flat head screw_am	Nylon	12
26	flat head screw_am	Nylon	11
27	flat head screw_am	Nylon	1
28	FAS pin	Brass	1
29	Large pin	Brass	2
30	Actuator pin	Brass	1
31	socket button head cap screw_am	Nylon	4
32	Large bolt for LAS mounting	Nylon	8
33	Carriage housing v3	Nylon	1

A3 Landscape	University of Cape Town Division of Biomedical Engineering			
	Title: Laxmeter Assembly			
Assembly Drawing	Scale: 1:7	Date: 2017/06/30	Sheet 2	of 2
	Drawn By: Giancarlo L. Beukes		Drawing Number 19	

Appendix D

Ethics Approval Letter

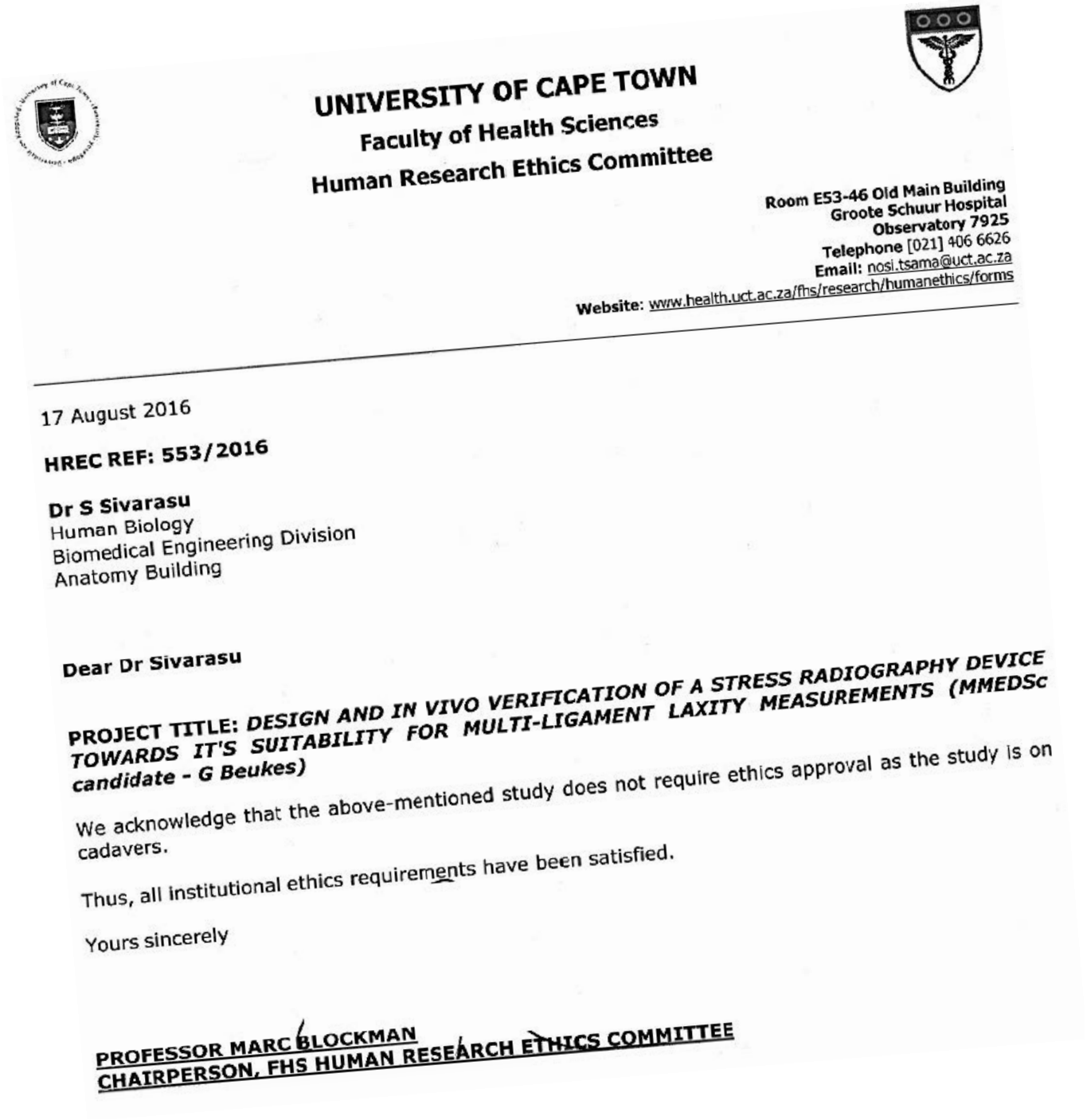

UNIVERSITY OF CAPE TOWN
Faculty of Health Sciences
Human Research Ethics Committee

Room E53-46 Old Main Building
Groote Schuur Hospital
Observatory 7925
Telephone [021] 406 6626
Email: nosi.tsama@uct.ac.za
Website: www.health.uct.ac.za/fhs/research/humanethics/forms

17 August 2016

HREC REF: 553/2016

Dr S Sivarasu
Human Biology
Biomedical Engineering Division
Anatomy Building

Dear Dr Sivarasu

PROJECT TITLE: ***DESIGN AND IN VIVO VERIFICATION OF A STRESS RADIOGRAPHY DEVICE TOWARDS IT'S SUITABILITY FOR MULTI-LIGAMENT LAXITY MEASUREMENTS (MMEDSc candidate - G Beukes)***

We acknowledge that the above-mentioned study does not require ethics approval as the study is on cadavers.

Thus, all institutional ethics requirements have been satisfied.

Yours sincerely

PROFESSOR MARC BLOCKMAN
CHAIRPERSON, FHS HUMAN RESEARCH ETHICS COMMITTEE

Appendix E

Usability Analysis

The usability of the system was evaluated by considering the effectiveness (E_1), efficiency (E_2) and satisfaction (S_2) of the device and its performance. The following scales were used to rate the E_1, E_2, and S_2 values. Thereafter, a summation of the E_1, E_2, and S_2 values was carried to produce a usability score to assess the system usability.

Effectiveness rating scale

Score	*Effectiveness (E_1)*
0	Ineffectiveness
1	
2	
3	
4	
5	Meets expectation

Efficiency rating scale

Score	*Efficiency (E_2)*
0	Inefficiency
1	
2	
3	
4	
5	Meets expectation

Satisfaction rating scale

Score	*Satisfaction (S_2)*
0	Dissatisfactory
1	
2	
3	
4	
5	Meets expectation

Overall usability scale

Score ($E_1 + E_2 + S_2$)	*Usability – Assessment term*
0-5	Failure
6-10	Acceptable
11-15	Meets expectation